Electronic Supplementary Material (ESI) for Organic Chemistry Frontiers.

Supporting Information

Nucleophilic aromatic substitution approach to phosphanyl-substituted diboraanthracenes: biphilic compounds with tunable electron affinities

Tao Jin,[a] Michael Bolte,[a] Hans-Wolfram Lerner,[a] Matthias Wagner [a]*

[a]Institut für Anorganische Chemie, Goethe-Universität Frankfurt
Max-von-Laue-Strasse 7, 60438 Frankfurt (Main) (Germany)
E-mail: Matthias.Wagner@chemie.uni-frankfurt.de

Table of contents:

1. General experimental procedures

If not stated otherwise, all reactions and manipulations were carried out under an atmosphere of dry nitrogen using Schlenk techniques or in an inert-atmosphere glovebox. *n*-Pentane, *n*-Hexane, C_6H_6, and THF were distilled from Na/benzophenone prior to use. CH_2Cl_2 and Me_3SiCl were distilled from CaH_2. NMR solvents were stored over molecular sieves under argon. BBr_3 was stored over Hg under argon. Commercial S_8 was recrystallized from CS_2 prior to use; commercial MeOTf (abcr), and Ph_3P (Sigma-Aldrich) were used as received. The starting materials **Ph$_2$PSiMe$_3$**,[S1] **B**, **C**, [S2] and **D**[S3] were prepared according to literature procedures.

NMR spectra were recorded at 298 K using the following spectrometers: Bruker DPX-250, Avance-300, or Avance-500. Chemical shift values are referenced to (residual) solvent signals ($^1H/^{13}C\{^1H\}$; $CDCl_3$: δ = 7.26/77.16 ppm, CD_2Cl_2: δ = 5.32/53.84 ppm) or external $BF_3{\cdot}Et_2O$ (^{11}B: 0.00 ppm) and $CFCl_3$ ($^{19}F\{^1H\}$): 0.00 ppm). Abbreviations: s = singlet, d = doublet, t = triplet, m = multiplet, dd = doublet of doublets, br. = broad, n.o. = not observed. Resonances of C atoms attached to B atoms were typically broadened and sometimes not observed due to the quadrupolar relaxation of boron. ^{11}B resonances of triarylborane compounds were typically very broad ($h_{½}$ > 1000 Hz) and only observed in highly concentrated samples. Resonance assignments were aided by ^{HH}COSY, ^{H,C}HSQC, ^{H,C}HMBC, and ^{F,C}HSQC spectra.

UV/Vis absorption spectra were recorded at room temperature by using a *Varian* Cary 50 Scan or a *Varian* Cary 60 Scan UV/Vis spectrophotometer. Photoluminescence (PL) spectra were recorded at room temperature by using a *Jasco* FP-8300 spectrofluorometer equipped with a calibrated *Jasco* ILF-835 100 mm diameter integrating sphere and analyzed using the *Jasco* FWQE-880 software. For PL quantum yield (Φ_{PL}) measurements, each sample was carefully degassed with argon using an injection needle and a septum-capped cuvette. Under these conditions the Φ_{PL} of the fluorescence standard 9,10-diphenylanthracene was determined as 97% (lit.: 97%). [S4,S5] For all Φ_{PL} measurements, at least three samples of different concentrations were used (range between 10^{-5} and 10^{-7} mol L^{-1}). Due to self-absorption, slightly lower Φ_{PL} values were observed at higher concentrations. This effect was corrected by applying a method reported by *Bardeen et al.*, which slightly improved the Φ_{PL} values (4% at most). [S6]

Cyclic voltammetry (CV) measurements were performed in a glovebox at room temperature in a one-chamber, three-electrode cell using an *EG&G* Princeton Applied Research 263A potentiostat. A Pt-disk electrode (2.00 mm diameter) was used as the working electrode with a Pt-wire counter electrode and an Ag-wire reference electrode, which was coated with AgCl by immersion into HCl/HNO_3 (3:1). Prior to measurements, the solvent CH_2Cl_2 was dried with CaH_2 and degassed by three freeze-pump-thaw cycles. $[nBu_4N][PF_6]$ (Sigma-Aldrich; used as received) was employed as the supporting electrolyte (0.1 mol L^{-1}). All potential values were referenced against the FcH/FcH^+ redox couple (FcH = ferrocene; $E_{1/2}$ = 0 V). Scan rates were varied between 100 and 400 mV s^{-1}.

High-resolution mass spectra were measured in positive mode using a *Thermo Fisher Scientific* MALDI LTQ Orbitrap XL spectrometer and 2,5-dihydroxybenzoic acid or α-cyano-4-hydroxycinnamic acid as the matrix.

Melting points were measured on an *OptiMelt MPA 100* instrument from *Stanford Research Systems* in sealed glass capillaries.

2. Nomenclature and blank control of an ^{11}B NMR spectrum

2.1. Nomenclature

Assignment of NMR signals: To maintain consistency with previous publications, the NMR signals were assigned according to the numbering scheme below (shown for an all-carbon framework).

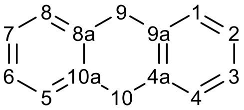

Substituents are numbered as indicated below (shown for an all-carbon framework).

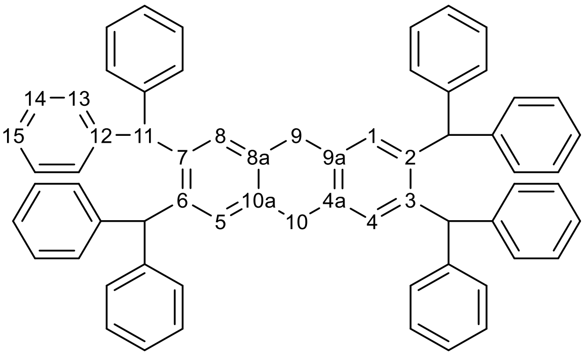

2.2 Blank control of an ^{11}B NMR spectrum

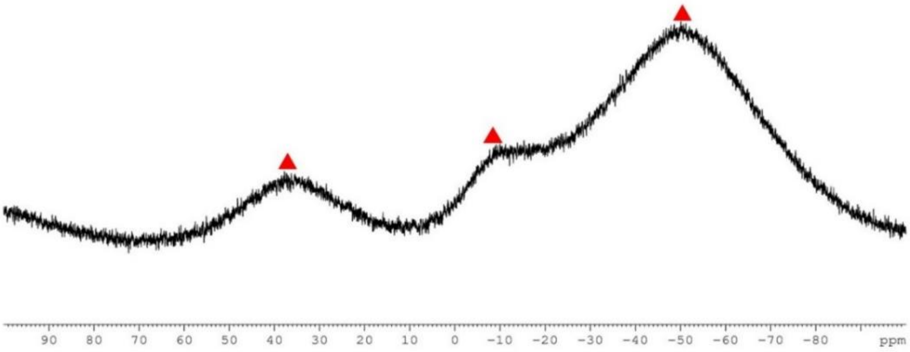

Note: To ensure that the ^{11}B NMR signals of the investigated substances are correctly identified, we measured an ^{11}B NMR spectrum of the NMR tube containing only CD_2Cl_2 without a sample compound.
(▲ : borosilicate glass resonance)

3. Syntheses, purification methods, and analytical data

3.1 Synthesis of 1:

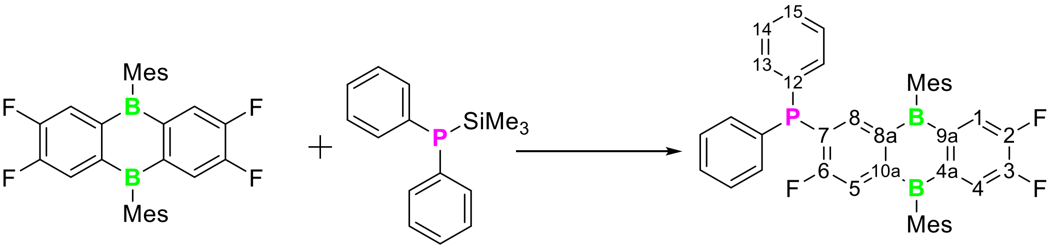

B **Ph$_2$PSiMe$_3$** **1**

A thick-walled glass ampoule was charged with **B** (500 mg, 1.03 mmol) and **Ph$_2$PSiMe$_3$** (267 mg, 1.03 mmol). C_6H_6 (5 mL) was added as the solvent. The ampoule was flame-sealed under vacuum and subsequently heated to 160 °C in an oven for 3 d. The pale brown solution obtained was cooled to room temperature. The ampoule was opened to ambient atmosphere and its content was transferred to a flask. All volatiles were removed in vacuo. Afterwards, the residual crude product was purified by column chromatography (5 cm silica gel, cyclohexane) to obtain the yellow-colored solid product **1**. Yield: 305 mg, 46%. Single crystals suitable for X-ray diffraction were grown in a glovebox by slow evaporation of a solution of **1** in *n*-hexane and CH_2Cl_2 (1:1).

^{1}H NMR (500.2 MHz, CDCl$_3$): δ = 7.41-7.36 (m, 2H; H-1,4), 7.31-7.28 (m, 2H; H-15), 7.25-7.19 (m, 9H; H-5,13,14), 6.93 (s, 2H; Mes-C*H*-*m*), 6.88 (dd, ^3J(H,P), ^4J(H,F) = 7.5, 4.8 Hz, 1H; H-8), 6.69 (s, 2H; Mes-C*H*-*m*), 2.39 (s, 3H; Mes-CH_3-*p*), 2.36 (s, 3H; Mes-CH_3-*p*), 2.05 (s, 6H; Mes-CH_3-*o*), 1.83 (s, 6H; Mes-CH_3-*o*)
^{13}C{^{1}H} NMR(125.8 MHz, CDCl$_3$): δ = 167.9 (dd, ^1J(C,F) = 257.2 Hz, ^2J(C,P) = 14.9 Hz; C-6), 154.2 (dd, ^1J(C,F) = 259.1 Hz, ^2J(C,F) = 11.8 Hz; C-2 or 3), 153.9 (dd, ^1J(C,F) = 258.5 Hz, ^2J(C,F) = 11.8 Hz; C-2 or 3), 148.4 (br.; C-10a), 146.3 (m; C-8), 143.6 (br.; C-4a or 9a), 143.4 (br.; C-4a or 9a), 140.6 (br.; C-8a), 139.1 (br.; Mes-C-*i*), 138.9 (br.; Mes-C-*i*), 137.9 (Mes-C-*o*), 137.8 (Mes-C-*p*), 137.3 (Mes-C-*o*), 136.9 (Mes-C-*p*), 134.5 (d, ^1J(C,P) = 9.9 Hz; C-12), 133.8 (d, ^2J(C,P) = 20.6 Hz; C-13), 131.4 (m; C-7), 129.3 (C-15), 128.7 (d, ^3J(C,P) = 7.6 Hz; C-14), 127.9 (d, ^2J(C,F) = 13.5 Hz; C-1 or 4), 127.7 (d, ^2J(C,F) = 13.5 Hz; C-1 or 4), 127.4 (Mes-*C*H-*m*), 127.2 (Mes-*C*H-*m*), 124.6 (d, ^2J(C,F) = 19.7 Hz; C-5), 22.8 (Mes-*C*H$_3$-*o*), 22.5 (Mes-*C*H$_3$-*o*), 21.4 (Mes-*C*H$_3$-*p*), 21.4 (Mes-*C*H$_3$-*p*)
^{11}B NMR (96.3 MHz, CDCl$_3$): δ = 69.6 (very br.)
^{19}F{^{1}H} NMR (282.3 MHz, CDCl$_3$): δ = −95.6 (d, ^3J(F,P) = 44.9 Hz, 1F; F-6), −130.8 (d, ^3J(F,F) = 20.1 Hz, 1F; F-2 or 3), −131.5 (d, ^3J(F,F) = 20.1 Hz, 1F; F-2 or 3)
^{31}P{^{1}H} NMR (121.5 MHz, CDCl$_3$): δ = −17.9 (d, ^3J(P,F) = 44.9 Hz)
UV/Vis (CH$_2$Cl$_2$): λ_{max} (ε) = 257 (42700), 274 (sh), 360 (5700), 405 (sh) nm (M^{-1} cm^{-1})
Cyclic voltammetry (CH$_2$Cl$_2$, [*n*-Bu$_4$N][PF$_6$] 0.1 M, 200 mV s^{-1}, vs. FcH/FcH$^+$): $E_{1/2}$ = −1.63 V
Melting Point: 276–279 °C
HRMS: Calculated *m*/*z* for $[C_{42}H_{36}B_2F_3P_1+H]^+$: 651.27656, found: 651.27797

3.2 Synthesis of 2:

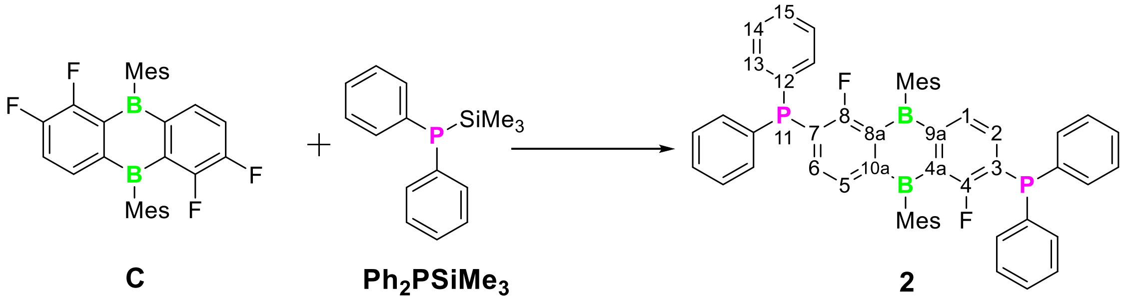

C **Ph$_2$PSiMe$_3$** **2**

A thick-walled glass ampoule was charged with **B** (486 mg, 1 mmol) and **Ph$_2$PSiMe$_3$** (3.89 g, 15 mmol). C_6H_6 (10 mL) was added as the solvent. The ampoule was flame-sealed under vacuum and subsequently heated to 180 °C in an oven for 2 d. The brown solution obtained was cooled to room temperature. The ampoule was opened in the glovebox and its content was transferred to a Schlenk flask. All volatiles were removed at room temperature in vacuo. Afterwards, unconsumed starting material **Ph$_2$PSiMe$_3$** was recovered by distillation from the mixture under full vacuum (10^{-3} torr) at 130 °C for 0.5 h. The solid residue was washed with *n*-pentane (20 mL); the yellow-colored product **2** was isolated by filtration. Yield: 787 mg, 96%. Single crystals suitable for X-ray diffraction were grown under ambient atmosphere by slow evaporation of a solution of **2** in *n*-hexane and CH_2Cl_2 (1:1).

^{1}H NMR (500.2 MHz, CD$_2$Cl$_2$): δ = 7.38-7.32 (m, 12H; H-14,15), 7.29-7.26 (m, 8H; H-13), 7.20 (d, ^3J(H,H) = 7.4 Hz, 2H; H-1,5), 6.84-6.80 (m, 2H; H-2,6), 6.78 (s, 4H; Mes-C*H*-*m*), 2.27 (s, 6H; Mes-CH_3-*p*), 2.01 (s, 12H; Mes-CH_3-*o*)
^{13}C{^{1}H} NMR (125.8 MHz, CD$_2$Cl$_2$): δ = 170.6 (dd, ^1J(C,F) = 260.3 Hz, ^2J(C,P) = 14.4 Hz; C-4,8), 147.8 (br.; C-9a,10a), 142.9 (br.; Mes-C-*i*), 140.4 (m; C-2,6), 136.9 (Mes-C-*o*), 136.6 (Mes-C-*p*), 135.4 (C-1,5), 135.2 (d, ^1J(C,P) = 10.6 Hz; C-12), 134.3 (d, ^2J(C,P) = 20.8 Hz; C-13), 133.3 (m; C-3,7), 129.8 (C-15), 129.1 (d, ^3J(C,P) = 7.5 Hz; C-14,4a,8a), 127.1 (Mes-*C*H-*m*), 22.3 (Mes-*C*H$_3$-*o*), 21.3 (Mes-*C*H$_3$-*p*)
Note: According to ^{HC}HSQC and ^{HC}HMBC experiments, the ^{13}C NMR signals of C-4a,8a overlap with that of C-14.
^{11}B NMR (96.3 MHz, CD$_2$Cl$_2$): δ = 66.0 (very br.)
^{19}F{1H} NMR (282.3 MHz, CD$_2$Cl$_2$): δ = –87.7 (d, ^3J(F,P) = 58.2 Hz, 2F; F-4,8)
^{31}P{^{1}H} NMR (202.5 MHz, CD$_2$Cl$_2$): δ = –16.3 (d, ^3J(P,F) = 58.2 Hz, 2P; P-3,7)
UV/Vis (CH$_2$Cl$_2$): λ_{max} (ε) = 247 (43200), 290 (37500), 395 nm (16100 M^{-1} cm^{-1})
Cyclic voltammetry (CH$_2$Cl$_2$, [*n*-Bu$_4$N][PF$_6$] 0.1 M, 200 mV s^{-1}, vs. FcH/FcH$^+$): $E_{1/2}$ = –1.58 V
Melting Point: >300 °C
HRMS: Calculated *m*/*z* for $[C_{54}H_{46}B_2F_2P_2+H]^+$: 817.33017, found: 817.33187

3.3 Synthesis of 3:

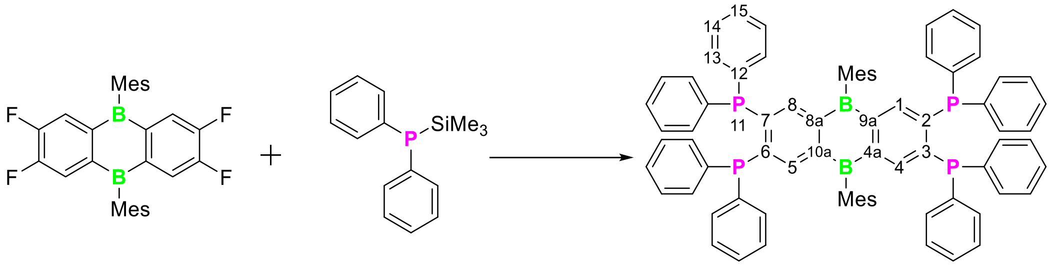

B **Ph_2PSiMe_3** **3**

A thick-walled glass ampoule was charged with **B** (500 mg, 1.03 mmol) and **Ph_2PSiMe_3** (4.0 g, 15.5 mmol). C_6H_6 (10 mL) was added as the solvent. The ampoule was flame-sealed under vacuum and subsequently heated to 180 °C in an oven for 3 d. The brown solution obtained was cooled to room temperature. The ampoule was opened in the glovebox and its content was transferred to a Schlenk flask. All volatiles were removed at room temperature in vacuo. Afterwards, unconsumed starting material **Ph_2PSiMe_3** was recovered by distillation from the mixture under full vacuum (10^{-3} torr) at 130 °C for 0.5 h. The residual solid washed with *n*-hexane (4 x 10 mL) under ambient atmosphere; the red-colored product **3** was isolated by filtration. Yield: 1.16 g, 98%. Single crystals suitable for X-ray diffraction were grown in a sealed NMR tube by slowly decreasing the temperature of the **3** solution in C_6D_6 from 180 °C to room temperature in the oven.

^{1}H NMR (500.2 MHz, $CDCl_3$): δ = 7.14-7.09 (m, 12H; H-1,4,5,8,15), 7.06-7.03 (m, 16H; H-14), 7.01-6.98 (m, 16H; H-13), 6.44 (s, 4H; Mes-C*H*-*m*), 2.27 (s, 6H; Mes-CH_3-*p*), 1.60 (s, 12H; Mes-CH_3-*o*)
^{13}C{^{1}H} NMR (125.8 MHz, $CDCl_3$): δ = 149.6 (m; C-2,3,6,7), 144.1 (m; C-1,4,5,8,4a,8a,9a,10a), 138.8 (br.; Mes-C-*i*), 136.7 (Mes-C-*o*), 136.4 (m; C-12), 135.7 (Mes-C-*p*), 133.9 (m; C-13), 128.4 (C-15), 128.2 (m; C-14), 126.7 (Mes-*C*H-*m*), 22.5 (Mes-*C*H_3-*o*), 21.3 (Mes-*C*H_3-*p*)
Note: According to ^{HC}HSQC and ^{HC}HMBC experiments, the ^{13}C NMR signals of C-1,4,5,8 overlap with those of C-4a,8a,9a,10a.
^{11}B NMR (161 MHz, $CDCl_3$): δ = n.o.
^{31}P{^{1}H} NMR (121.5 MHz, $CDCl_3$): δ = −14.4
UV/Vis (CH_2Cl_2): λ_{max} (ε) = 258 (77600), 293 (78100), 330 (sh), 381 (sh), 484 (sh) nm (M^{-1} cm^{-1})
Cyclic voltammetry (CH_2Cl_2, [*n*-Bu_4N][PF_6] 0.1 M, 200 mV s^{-1}, vs. FcH/FcH$^+$): $E_{1/2}$ = −1.70 V
Melting Point: >300 °C
HRMS: Calculated *m*/*z* for [$C_{78}H_{66}B_2P_4$+H]$^+$: 1149.43739, found: 1149.43903

3.4 Synthesis of 4:

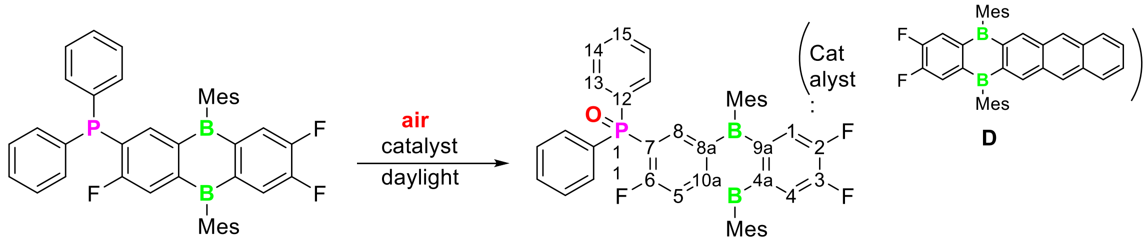

1 **4**

A round-bottom flask was charged with a stirring bar, **1** (300 mg, 461 µmol), **D** (50 mg, 91 µmol), and CH_2Cl_2 (100 mL). The solution was stirred under air and daylight for 12 h, whereupon an oxidation reaction took place (no oxidation was observed under similar conditions in the dark or in daylight without the photocatalyst **D**). The progress of the reaction was monitored by ^{31}P NMR spectroscopy, and the conversion was considered complete when the signal of **1** at $\delta = -17.9$ had vanished, leaving only a new signal at $\delta = 25.4$. The solvent was removed in vacuo. The solid residue was re-dissolved in *n*-hexane (20 mL), and the solution was slowly concentrated to a volume of approximately 3 mL under vacuum, whereupon the yellow-colored product **4** precipitated, which was isolated by filtration. Yield: 193 mg, 63%.

^1H NMR (500.2 MHz, $CDCl_3$): δ = 7.66-7.62 (m, 4H; H-13), 7.59-7.55 (m, 1H; H-8), 7.53-7.50 (m, 2H; H-15), 7.45-7.39 (m, 6H; H-1,4,14), 7.30-7.28 (m, 1H; H-5), 6.92 (s, 2H; Mes-C*H*-*m*), 6.75 (s, 2H; Mes-C*H*-*m*), 2.38 (s, 3H; Mes-CH_3-*p*), 2.34 (s, 3H; Mes-CH_3-*p*), 2.03 (s, 6H; Mes-CH_3-*o*), 1.90 (s, 6H; Mes-CH_3-*o*)
$^{13}C\{^1H\}$ NMR (125.8 MHz, $CDCl_3$): δ = 167.6 (d, ^1J(C,F) = 262.7 Hz; C-6), 154.5 (dd, ^1J(C,F) = 260.2 Hz, ^2J(C,F) = 12.1 Hz; C-2 or 3), 154.1 (dd, ^1J(C,F) = 259.1 Hz, ^2J(C,F) = 11.8 Hz; C-2 or 3), 152.2 (br.; C-10a), 146.2 (m; C-8), 143.6 (br.; C-4a or 9a), 143.0 (br.; C-4a or 9a), 140.6 (br.; C-8a), 138.6 (br.; Mes-C-*i*), 138.4 (br.; Mes-C-*i*), 138.1 (Mes-C-*p*), 137.8 (Mes-C-*o*), 137.4 (Mes-C-*p*), 137.3 (Mes-C-*o*), 132.3 (d, ^4J(C,P) = 2.6 Hz; C-15), 131.7 (d, ^2J(C,P) = 10.2 Hz; C-13), 131.4 (d, ^1J(C,P) = 108.2 Hz; C-12), 128.7 (d, ^3J(C,P) = 12.7 Hz; C-14), 128.4 (d, ^2J(C,F) = 13.3 Hz; C-1 or 4), 128.1 (d, ^2J(C,F) = 13.7 Hz; C-1 or 4), 127.6 (Mes-*C*H-*m*), 127.5 (Mes-*C*H-*m*), 125.7 (dd, ^2J(C,F) = 19.6 Hz, ^3J(C,P) = 4.3 Hz; C-5), 125.3 (dd, ^1J(C,P) = ≈90 Hz, ^2J(C,F) = 17.4 Hz; C-7), 22.8 (Mes-CH_3-*o*), 22.7 (Mes-CH_3-*o*), 21.4 (Mes-CH_3-*p*), 21.4 (Mes-CH_3-*p*)
Note: According to ^{HC}HSQC and ^{HC}HMBC experiments, half of ^{13}C NMR signal of C-7 overlaps with that of C-5.
^{11}B NMR (96.3 MHz, $CDCl_3$): δ = 67.1 (very br.)
$^{19}F\{^1H\}$ NMR (282.3 MHz, $CDCl_3$): δ = −92.1 (s, 1F; F-6), −129.6 (d, ^3J(F,F) = 20.1 Hz, 1F; F-2 or 3), −130.7 (d, ^3J(F,F) = 20.1 Hz, 1F; F-2 or 3)
$^{31}P\{^1H\}$ NMR (121.5 MHz, $CDCl_3$): δ = 25.4 (d, ^3J(P,F) = 1.6 Hz)
UV/Vis (CH_2Cl_2): λ_{max} (ε) = 266 (86000), 328 (sh), 338 nm (6800 M^{-1} cm^{-1})
Fluorescence (CH_2Cl_2, λ_{ex} = 265 nm): λ_{max} = 528 nm; Φ_{PL} = 46 %
Fluorescence (C_6H_6, λ_{ex} = 340 nm): λ_{max} = 516 nm; Φ_{PL} = 37 %
Fluorescence (THF, λ_{ex} = 340 nm): λ_{max} = 543 nm; Φ_{PL} = 18 %
Cyclic voltammetry (CH_2Cl_2, [*n*-Bu_4N][PF_6] 0.1 M, 200 mV s^{-1}, vs. FcH/FcH^+): $E_{1/2} = -1.52$ V
Melting Point: 282–284 °C
HRMS: Calculated *m*/*z* for $[C_{42}H_{36}B_2F_3O_1P_1+H]^+$: 667.27147, found: 667.27266

3.5 Synthesis of 5:

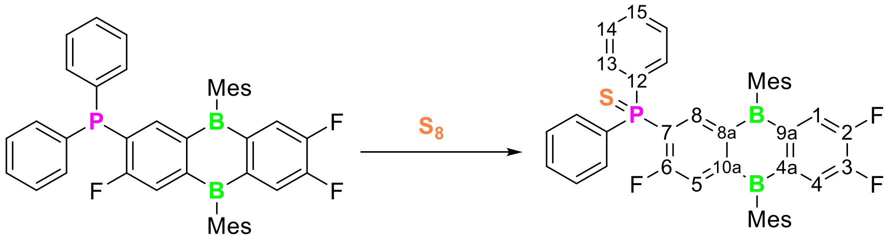

1 **5**

A thick-walled glass ampoule was charged with **1** (100 mg, 154 µmol), S_8 (7 mg, 27 µmol), and C_6H_6 (5 mL). The ampoule was flame-sealed under vacuum and subsequently heated to 100 °C in an oven overnight. The orange solution obtained was cooled to room temperature. The ampoule was opened under ambient atmosphere and its content was transferred to a Schlenk flask. All volatiles were removed under vacuum and the solid residue was washed with *n*-pentane (5 mL); the pale yellow product of **5** was isolated by filtration. Yield: 82 mg, 79%.

^{1}H NMR (500.2 MHz, $CDCl_3$): δ = 7.74-7.70 (m, 4H; H-13), 7.49-7.33 (m, 9H; H-1,4,8,14,15), 7.28 (m, 1H; H-5), 6.92 (s, 2H; Mes-C*H*-*m*), 6.74 (s, 2H; Mes-C*H*-*m*), 2.38 (s, 3H; Mes-CH_3-*p*), 2.36 (s, 3H; Mes-CH_3-*p*), 2.04 (s, 6H; Mes-CH_3-*o*), 1.89 (s, 6H; Mes-CH_3-*o*)

^{13}C{^{1}H} NMR (125.8 MHz, $CDCl_3$): δ = 167.2 (d, ^1J(C,F) = 264.3 Hz; C-6), 154.4 (dd, ^1J(C,F) = 260.5 Hz, ^2J(C,F) = 12.1 Hz; C-2 or 3), 154.1 (dd, ^1J(C,F) = 259.4 Hz, ^2J(C,F) = 12.1 Hz; C-2 or 3), 151.7 (br.; C-10a), 145.8 (m; C-8), 143.6 (br.; C-4a or 9a), 143.1 (br.; C-4a or 9a), 140.6 (br.; C-8a), 138.6 (br.; Mes-C-*i*), 138.3 (br.; Mes-C-*i*), 138.1 (Mes-C-*p*), 137.8 (Mes-C-*o*), 137.3 (Mes-C-*p*), 137.3 (Mes-C-*o*), 131.9 (d, ^4J(C,P) = 3.1 Hz; C-15), 131.8 (d, ^2J(C,P) = 11.0 Hz; C-13), 131.4 (d, ^1J(C,P) = 87.9 Hz; C-12), 128.6 (d, ^3J(C,P) = 13.0 Hz; C-14), 128.4 (d, ^2J(C,F) = 13.7 Hz; C-1 or 4), 128.1 (d, ^2J(C,F) = 13.7 Hz; C-1 or 4), 127.6 (Mes-*C*H-*m*), 127.4 (Mes-*C*H-*m*), 126.5 (dd, ^1J(C,P) = 89.3 Hz, ^2J(C,F) = 15.6 Hz; C-7), 126.0 (dd, ^2J(C,F) = 19.3 Hz, ^3J(C,P) = 4.4 Hz; C-5), 22.8 (Mes-*C*H_3-*o*), 22.7 (Mes-*C*H_3-*o*), 21.4 (Mes-*C*H_3-*p*), 21.4 (Mes-*C*H_3-*p*)

^{11}B NMR (96.3 MHz, $CDCl_3$): δ = 69.8 (very br.)

^{19}F{^{1}H} NMR (282.3 MHz, $CDCl_3$): δ = −90.7 (d, ^3J(F,P) = 2.6 Hz, 1F; F-6), −129.7 (d, ^3J(F,F) = 20.1 Hz, 1F; F-2 or 3), −130.6 (d, ^3J(F,F) = 20.1 Hz, 1F; F-2 or 3)

^{31}P{^{1}H} NMR (121.5 MHz, $CDCl_3$): δ = 37.8 (d, ^3J (P,F) = 2.6 Hz)

UV/Vis (CH_2Cl_2): λ_{max} (ε) = 265 (89300), 343 nm (8200 M^{-1} cm^{-1})

Cyclic voltammetry (CH_2Cl_2, [*n*-Bu_4N][PF_6] 0.1 M, 200 mV s^{-1}, vs. FcH/FcH$^+$): $E_{1/2}$ = −1.43 V

Melting Point: 294–296 °C

HRMS: Calculated *m*/*z* for $[C_{42}H_{36}B_2F_3P_1S_1+H]^+$: 683.24863, found: 683.24978

3.6 Synthesis of [**6**]OTf:

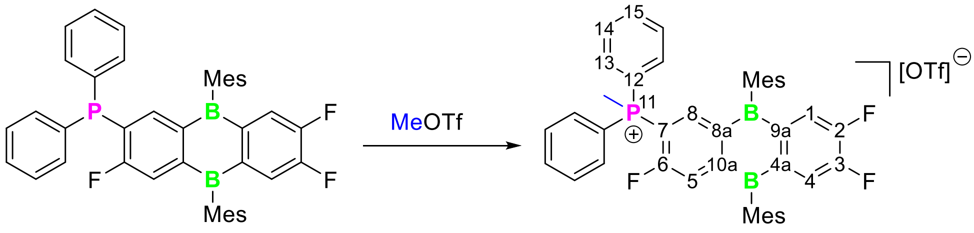

1 [**6**]OTf

A Schlenk flask was charged with a stirring bar, **1** (500 mg, 769 µmol), and CH_2Cl_2 (20 mL). Neat MeOTf (190 mg, 1.16 mmol) was added at room temperature via syringe. The solution was stirred under nitrogen overnight. All volatiles were removed under vacuum and the solid residue was washed with cooled *n*-pentane (15 mL); the bright yellow-colored product [**6**]OTf was isolated by filtration. Yield: 590 mg, 94%.

^{1}H NMR (500.2 MHz, CD_2Cl_2): δ = 7.83-7.80 (m, 2H; H-15), 7.65-7.62 (m, 4H; H-14), 7.58-7.47 (m, 7H; H-1,4,5,13), 7.02-6.98 (m, 1H; H-8), 6.97 (s, 2H; Mes-C*H*-*m*), 6.73 (s, 2H; Mes-C*H*-*m*), 2.90 (d, ^2J(H,P) = 13.8 Hz, 3H; PC*H*3), 2.39 (s, 3H; Mes-C*H*3-*p*), 2.35 (s, 3H; Mes-C*H*3-*p*), 2.05 (s, 6H; Mes-C*H*3-*o*), 1.85 (s, 6H; Mes-C*H*3-*o*)

^{13}C{^{1}H} NMR (125.8 MHz, CD_2Cl_2): δ = 168.0 (d, ^1J(C,F) = 263.4 Hz; C-6), 156.0 (br.; C-10a), 155.0 (dd, ^1J(C,F) = 261.2 Hz, ^2J(C,F) = 12.1 Hz; C-2 or 3), 154.7 (dd, ^1J(C,F) = 259.5 Hz, ^2J(C,F) = 12.1 Hz; C-2 or 3), 146.2 (d, ^2J(C,P) or ^3J(C,F) = 6.3 Hz; C-8), 143.3 (br.; C-8a, 4a or 9a), 142.3 (br.; C-4a or 9a), 139.0 (Mes-C-*p*), 138.2 (Mes-C-*p*), 138.1 (Mes-C-*o*), 137.9 (br.; Mes-C-*i*), 137.6 (Mes-C-*o*) 137.6 (br.; Mes-C-*i*), 136.0 (d, ^4J(C,P) = 3.1 Hz; C-15), 133.1 (d, ^2J(C,P) = 11.0 Hz; C-13), 131.0 (d, ^3J(C,P) = 13.3 Hz; C-14), 129.4 (d, ^2J(C,F) = 13.8 Hz; C-1 or 4), 129.0 (d, ^2J(C,F) = 13.8 Hz; C-1 or 4), 128.0 (Mes-*C*H-*m*), 127.7(Mes-*C*H-*m*), 126.2 (dd, ^2J(C,F) = 17.9 Hz, ^3J(C,P) = 4.9 Hz; C-5), 121.3 (q, ^1J(C,F) = 321.2 Hz; CF_3), 117.3 (d, ^1J(C,P) = 90.8 Hz; C-12), 112.2 (dd, ^1J(C,P) = 86.6 Hz, ^2J(C,F) = 16.5 Hz; C-7), 22.8 (Mes-*C*H3-*o*), 22.6 (Mes-*C*H3-*o*), 21.4 (Mes-*C*H3-*p*), 21.4 (Mes-*C*H3-*p*), 9.4 (dd, ^1J(C,P) = 57.3 Hz, ^4J(C,F) = 3.7 Hz; P*C*H3)

Note: According to an ^{HC}HMBC experiment, the ^{13}C NMR signal of C-2 or 3 overlaps with that of C-10a, the signal of C-8a overlaps with that of C-4a or 9a, and the signal of Mes-C-*o* overlaps with that of Mes-C-*i*.

^{11}B NMR (160.5 MHz, CD_2Cl_2): δ = 66.4 (very br.)

^{19}F{^{1}H} NMR (282.3 MHz, CD_2Cl_3): δ = −78.3 (s, 3F; CF_3), −91.0 (d, ^3J(F,P) = 2.9 Hz, 1F; F-6), −127.9 (d, ^3J(F,F) = 20.1 Hz, 1F; F-2 or 3), −128.8 (d, ^3J(F,F) = 20.1 Hz, 1F; F-2 or 3)

^{31}P{^{1}H} NMR (121.5 MHz, CD_2Cl_2): δ = 20.8 (d, ^3J(P,F) = 2.9 Hz)

UV/Vis (CH_2Cl_2): λ_{max} (ε) = 267 (49100), 338 nm (4400 M^{-1} cm^{-1})

Fluorescence (CH_2Cl_2, λ_{ex} = 267 nm): λ_{max} = 574 nm; Φ_{PL} = 11 %.

Fluorescence ($CHCl_3$, λ_{ex} = 267 nm): λ_{max} = 560 nm; Φ_{PL} = 7 %.

Cyclic voltammetry (CH_2Cl_2, [*n*-Bu_4N][PF_6] 0.1 M, 200 mV s^{-1}, vs. FcH/FcH$^+$): $E_{1/2}$ = −1.24 V

Melting Point: decomposition at elevated temperatures

HRMS: Calculated *m*/*z* for $[C_{43}H_{39}B_2F_3P_1]^+$: 665.29221, found: 665.29307

3.7 Synthesis of 7:

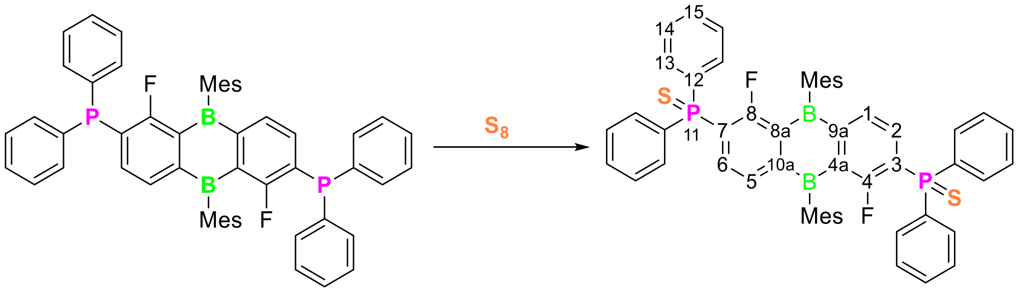

2 **7**

A thick-walled glass ampoule was charged with **2** (150 mg, 184 µmol) and S_8 (17 mg, 66 µmol). C_6H_6 (5 mL) was added as the solvent. The ampoule was flame-sealed under vacuum and subsequently heated to 100 °C in an oven overnight. The orange solution obtained was cooled to room temperature. The ampoule was opened under ambient atmosphere and its content was transferred to a flask. All volatiles were removed under vacuum and the residual solid was washed with *n*-pentane (5mL); the orange-colored product **7** was isolated by filtration. Yield: 123 mg, 76%.

^{1}H NMR (500.2 MHz, CD_2Cl_2): δ = 7.76-7.69 (m, 10H; H-2,6,13), 7.54-7.51 (m, 4H; H-15), 7.45-7.42 (m, 8H; H-14), 7.39 (dd, ^3J(H,H) = 7.5 Hz, ^4J(H,P) = 1.8 Hz, 2H; H-1,5), 6.79 (s, 4H; Mes-C*H*-*m*), 2.29 (s, 6H; Mes-CH_3-*p*), 1.94 (s, 12H; Mes-CH_3-*o*)

^{13}C{^{1}H} NMR (125.8 MHz, CD_2Cl_2): δ = 169.8 (d, ^1J(C,F) = 267.1 Hz; C-4,8), 151.4 (br.; C-9a,10a), 141.7 (dd, ^2J(C,P) = 7.9 Hz, ^3J(C,F) = 4.0 Hz; C-2,6, Mes-C-*i*), 137.5 (Mes-C-*p*), 136.6 (Mes-C-*o*), 135.3 (m; C-1,5), 132.3 (d, ^1J(C,P) = 88.3 Hz; C-12), 132.3 (d, ^4J(C,P) = 3.0 Hz; C-15), 132.0 (d, ^2J(C,P) = 11.0 Hz; C-13), 130.4(*)(br.; C-4a,8a), 129.0 (d, ^3J(C,P) = 13.0 Hz; C-14), 127.4 (Mes-*C*H-*m*), 127.3 (dd, ^1J(C,P)= 77.7 Hz, ^2J(C,F)= 21.3 Hz; C-3,7), 22.4 (Mes-*C*H_3-*o*), 21.3 (Mes-*C*H_3-*p*)

Note: (*) The ^{13}C NMR signal of C-4a,8a was unequivocally detected in an ^{H,C}HMBC spectrum. According to ^{HC}HSQC and ^{HC}HMBC experiments, the ^{13}C NMR signals of C-2,6 overlap with that of Mes-C-*i*.

^{11}B NMR (96.3 MHz, CD_2Cl_2): δ = 68.0 (very br.)

^{19}F{^{1}H} NMR (282.3 MHz, CD_2Cl_2): δ = −81.5 (d, ^3J(F,P) = 2.5 Hz, 2F)

^{31}P{^{1}H} NMR (121.5 MHz, CD_2Cl_2): δ = 38.7 (d, ^3J(P,F) = 2.5 Hz, 2P)

UV/Vis (CH_2Cl_2): λ_{max} (ε) = 260 (58900), 374 (16200 M^{-1} cm^{-1}), 430 nm (sh).

Cyclic voltammetry (CH_2Cl_2, [*n*-Bu_4N][PF_6] 0.1 M, 200 mV s^{-1}, vs. FcH/FcH$^+$): $E_{1/2}$ = −1.33 V

Melting Point: >300 °C

HRMS: Calculated *m*/*z* for [$C_{54}H_{46}B_2F_2P_2S_2$+H]$^+$: 881.27431, found: 881.27569

3.8 Synthesis of 8:

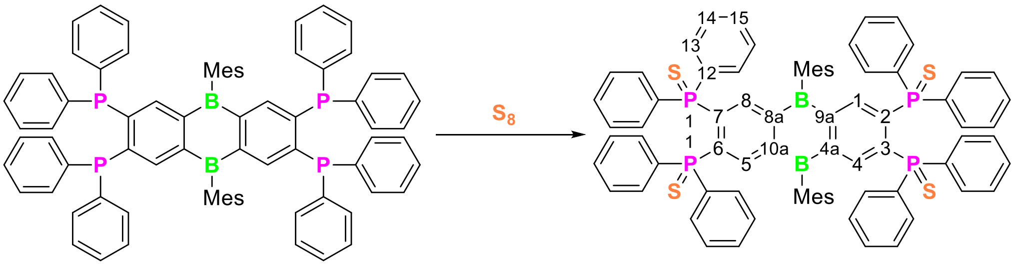

3 **8**

A thick-walled glass ampoule was charged with **2** (150 mg, 131 µmol) and S_8 (25 mg, 98 µmol). C_6H_6 (10 mL) was added as the solvent. The ampoule was flame-sealed under vacuum and subsequently heated to 100 °C in an oven overnight. The orange solution obtained was cooled to room temperature. The ampoule was opened in a glovebox and its content was transferred to a Schlenk flask. All volatiles were removed in vacuo. The solid residue was re-dissolved in a mixture of *n*-hexane and CH_2Cl_2 (4 : 1, 20 mL), and the solution was concentrated to a volume of approximately 3 mL under vacuum, whereupon the orange-colored product **8** precipitated and could be isolated by filtration. Yield: 130 mg, 78%. Single crystals of **8** suitable for X-ray diffraction were grown by slowly cooling a solution of **8** in C_6D_6 from 100 °C to room temperature.

^{1}H NMR (500.2 MHz, CD_2Cl_2): δ = 7.41-7.33 (m, 28H; H-1,4,5,8,13,15), 7.23-7.20 (m, 16H; H-14), 6.43 (s, 4H; Mes-C*H*-*m*), 2.32 (s, 6H; Mes-CH_3-*p*), 1.56 (s, 12H; Mes-CH_3-*o*)

^{13}C{^{1}H} NMR (125.8 MHz, CD_2Cl_2): δ = 146.6 (m; C-1,4,5,8), 145.3 (br.; C-4a,8a,9a,10a), 143.4 (dd, ^1J(C,P), ^2J(C,P) = 77.1, 8.1 Hz; C-2,3,6,7), 137.2 (Mes-C-*p*), 136.7 (Mes-C-*o*, Mes-C-*i*), 134.9 (d, ^1J(C,P) = 88.0 Hz; C-12), 132.0 (m; C-13), 131.4 (C-15), 128.4 (m; C-14), 127.7 (Mes-*C*H-*m*), 22.4 (Mes-*C*H_3-*o*), 21.4 (Mes-*C*H_3-*p*)

Note: According to ^{HC}HSQC and ^{HC}HMBC experiments, the ^{13}C NMR signal of Mes-C-*o* overlaps with that of Mes-C-*i*.

^{11}B NMR (96.3 MHz, CD_2Cl_2): n.o.

^{31}P{^{1}H} NMR (121.5 MHz, CD_2Cl_2): δ = 46.5

UV/Vis (CH_2Cl_2): λ_{max} (ε) = 262 (121000), 298 (sh), 371 (19000 M^{-1} cm^{-1}), 463 nm (sh)

Cyclic voltammetry (CH_2Cl_2, [*n*-Bu_4N][PF_6] 0.1 M, 200 mV s^{-1}, vs. FcH/FcH$^+$): $E_{1/2}$ = −1.23 V

Melting Point: >300 °C

HRMS: Calculated *m*/*z* for [$C_{78}H_{66}B_2P_4S_4$+H]$^+$: 1277.32567, found: 1277.32588

3.9 Synthesis of [**10**](OTf)$_2$:

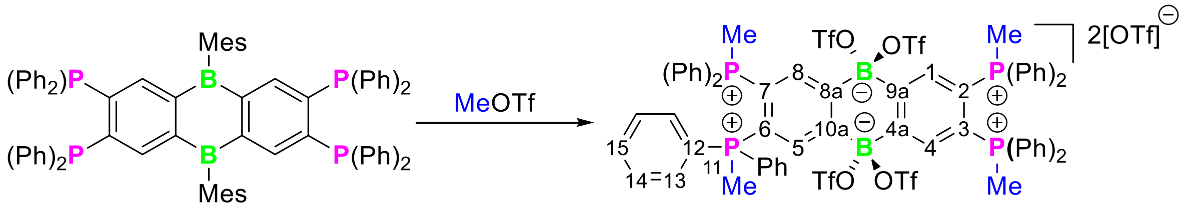

3

[**10**](OTf)$_2$

A thick-walled glass ampoule was charged with **3** (200 mg, 174 µmol) and CH_2Cl_2 (5 mL). Neat MeOTf (172 mg, 1.05 mmol) was added at room temperature via syringe. The ampoule was flame-sealed under vacuum and subsequently heated to 130 °C in an oven for 1.5 d. The pink solution obtained was cooled to room temperature. The ampoule was opened in a glovebox and its content was transferred to a Schlenk flask. All volatiles were removed in vacuo. The solid residue was washed with CH_2Cl_2 (5 mL); the colorless product [**10**](OTf)$_2$ could be isolated by filtration. Yield: 146 mg, 45%. Single crystals of [**10**](OTf)$_2$ suitable for X-ray diffraction were grown by storing a CD_2Cl_2 solution of [**10**](OTf)$_2$ in a flame-sealed NMR tube at 2 °C in the fridge.

^{1}H NMR (500.2 MHz, CD_2Cl_2): δ = 8.20 (m, 4H; H-1,4,5,8), 7.84-7.81 (m, 8H; H-15), 7.67-7.65 (m, 16H; H-14), 7.52-7.48 (m, 16H; H-13), 2.40 (d, ^2J(H,P) =12.2 Hz, 6H; PCH_3)
^{13}C{^{1}H} NMR (125.8 MHz, CD_2Cl_2): δ = 153.5 (br.; C-4a,8a,9a,10a), 146.4 (m; C-1,4,5,8), 136.3 (C-15), 133.5 (m; C-13), 131.4 (m; C-14), 119.9 (dd, ^1J(C,P) = 83.6, ^2J(C,P) = 9.0 Hz; C-2,3,6,7) 119.2 (d, ^1J(C,P) = 89.7 Hz; C-12), 118.5 (q, ^1J(C,F) = 318.6 Hz; CF_3), 12.5 (d, ^1J(C,P) = 55.8 Hz; PCH_3)
^{11}B NMR (96.3 MHz, CD_2Cl_2): n.o.
^{19}F NMR (282.3 MHz, CD_2Cl_2): δ = –78.0 (12F; BOTf), –78.8 (6F; [OTf]$^-$)
^{31}P{^{1}H} NMR (202.5 MHz, CD_2Cl_2): δ = 25.4
Melting Point: 280–282 °C

4. Plots of ^{1}H, ^{13}C{^{1}H}, ^{11}B, ^{19}F{^{1}H}, and ^{31}P{^{1}H} spectra

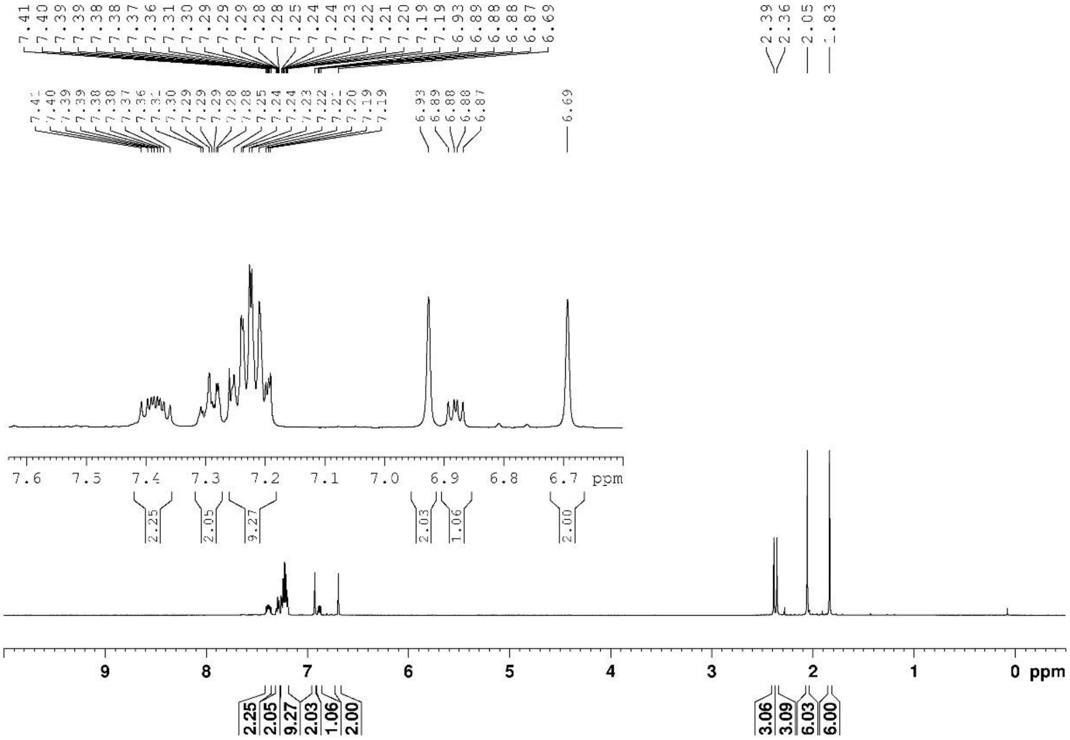

Figure S1: ^{1}H NMR spectrum of **1** (CDCl$_3$, 500.2 MHz).

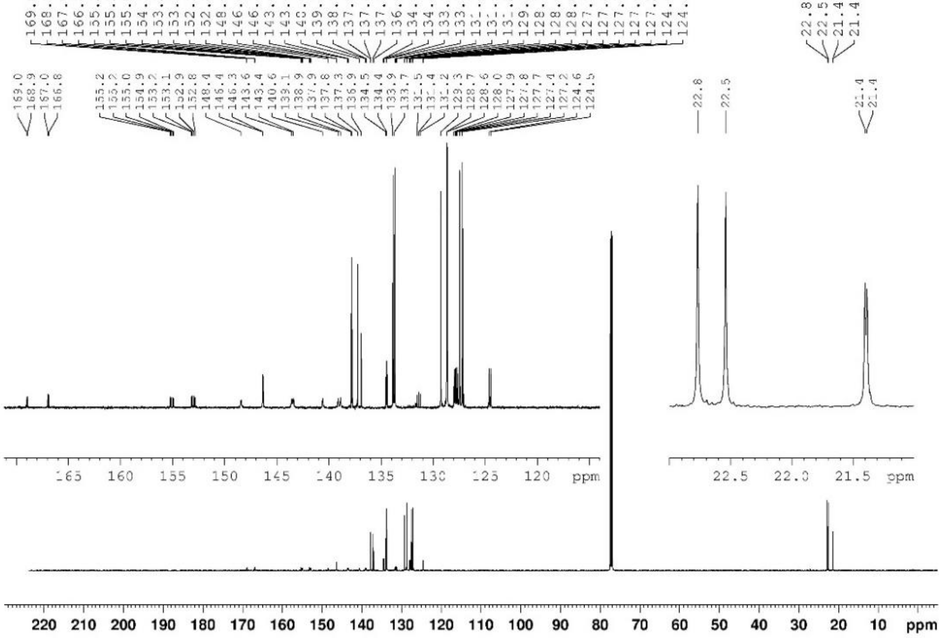

Figure S2: ^{13}C{^{1}H} NMR spectrum of **1** (CDCl$_3$, 125.8 MHz).

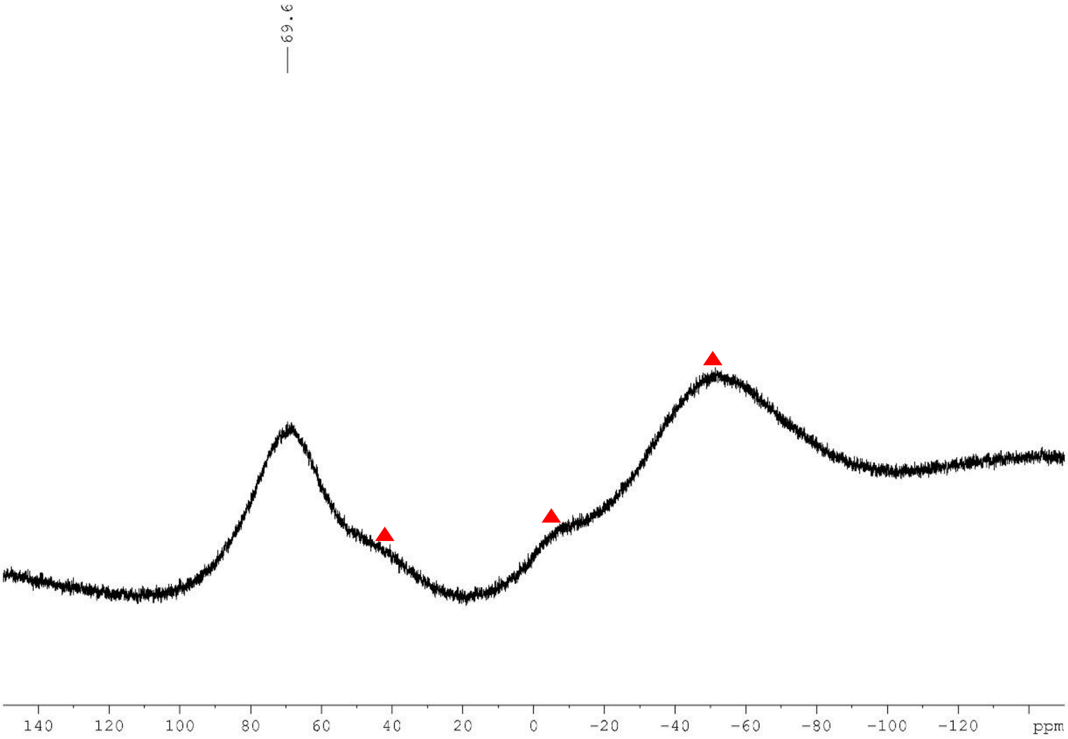

Figure S3: ^{11}B NMR spectrum of **1** (CDCl$_3$, 96.3 MHz; ▲: borosilicate glass resonance).

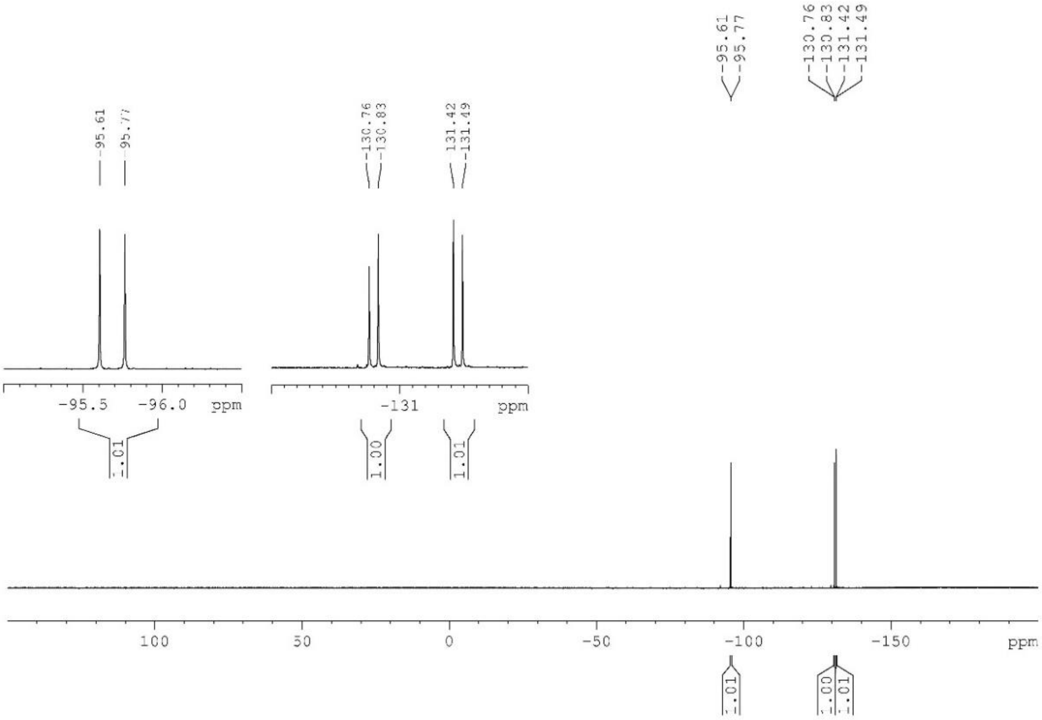

Figure S4: ^{19}F{^{1}H} NMR spectrum of **1** (CDCl$_3$, 282.3 MHz).

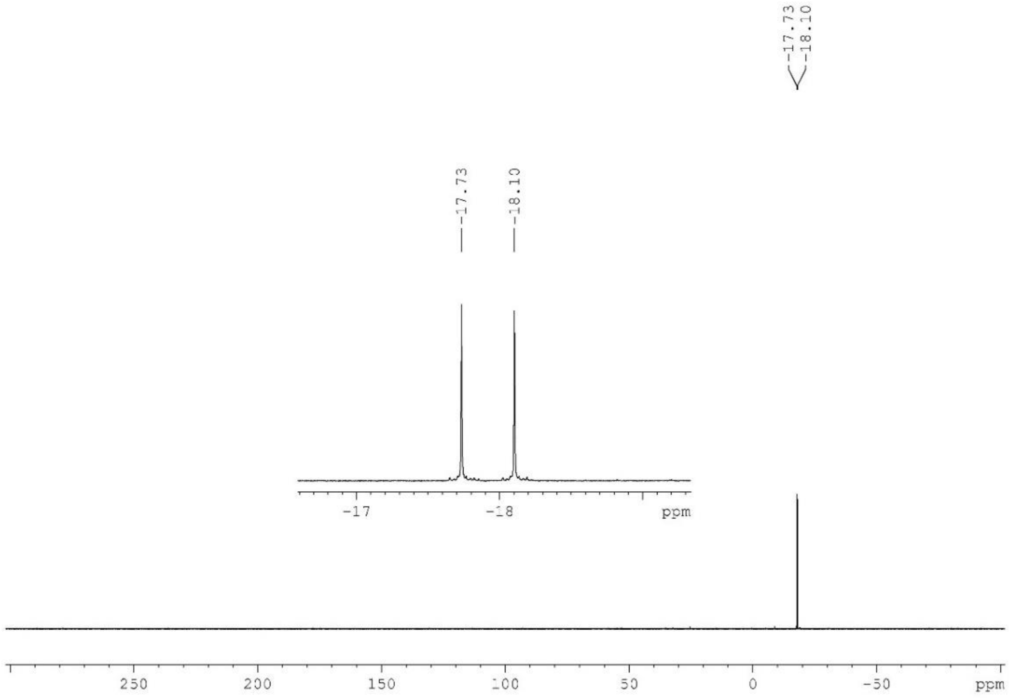

Figure S5: $^{31}P\{^1H\}$ NMR spectrum of **1** ($CDCl_3$, 121.5 MHz).

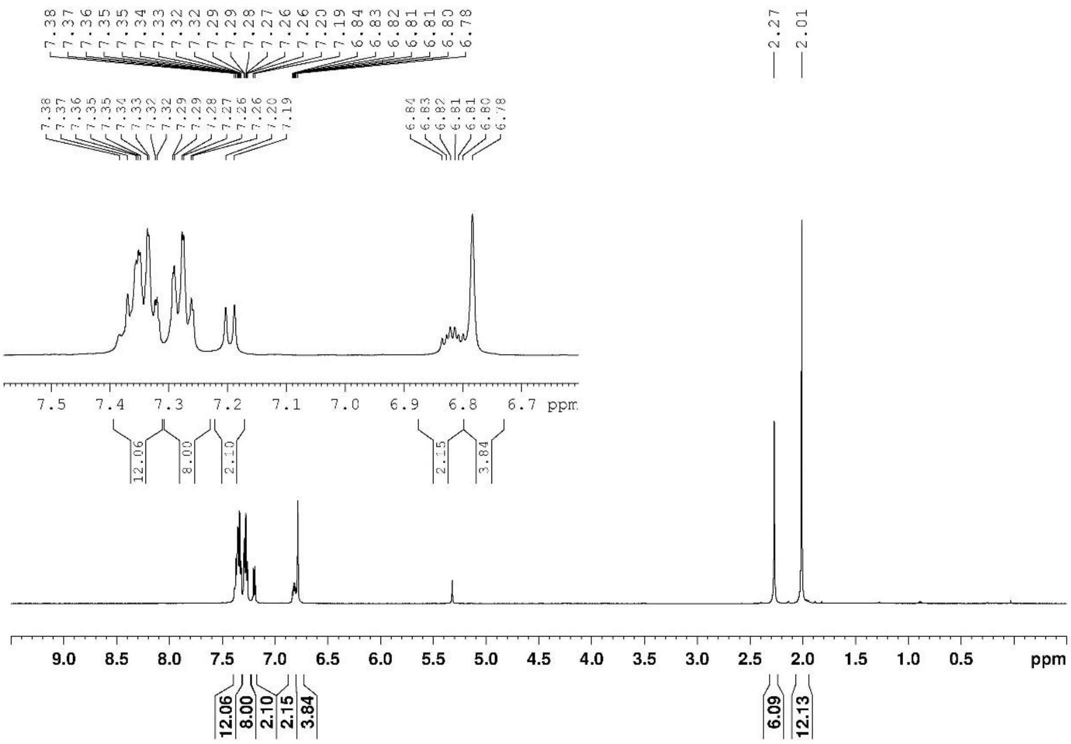

Figure S6: ^{1}H NMR spectrum of **2** (CD_2Cl_2, 500.2 MHz).

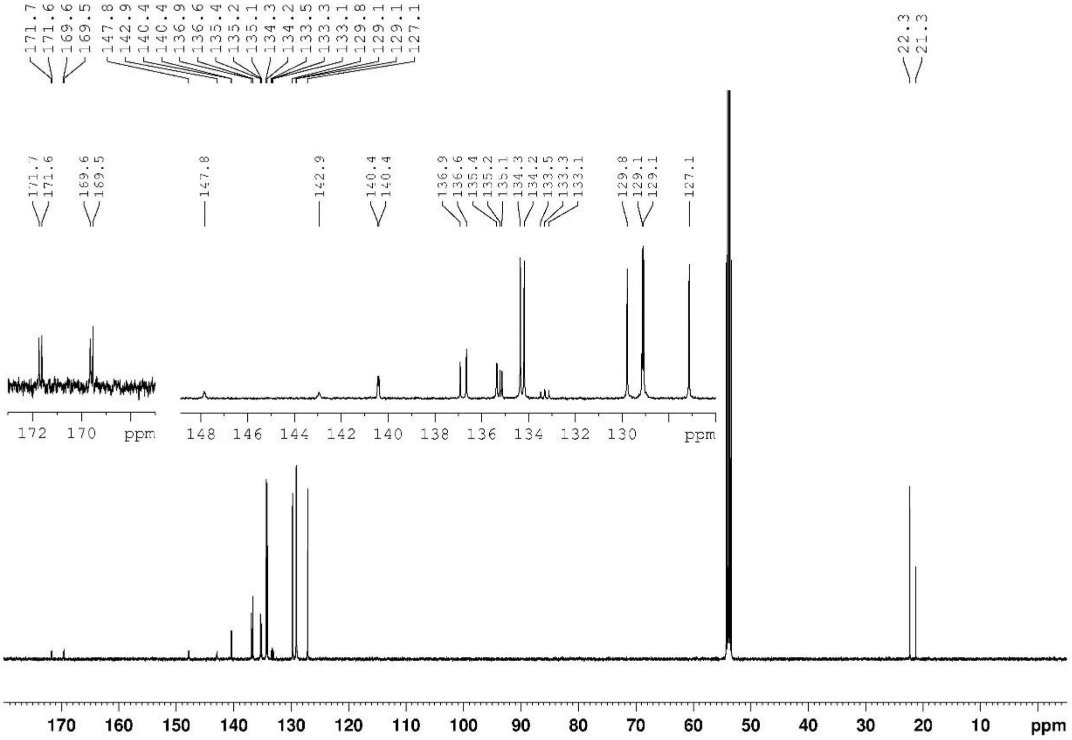

Figure S7: $^{13}C\{^1H\}$ NMR spectrum of **2** (CD_2Cl_2, 125.8 MHz).

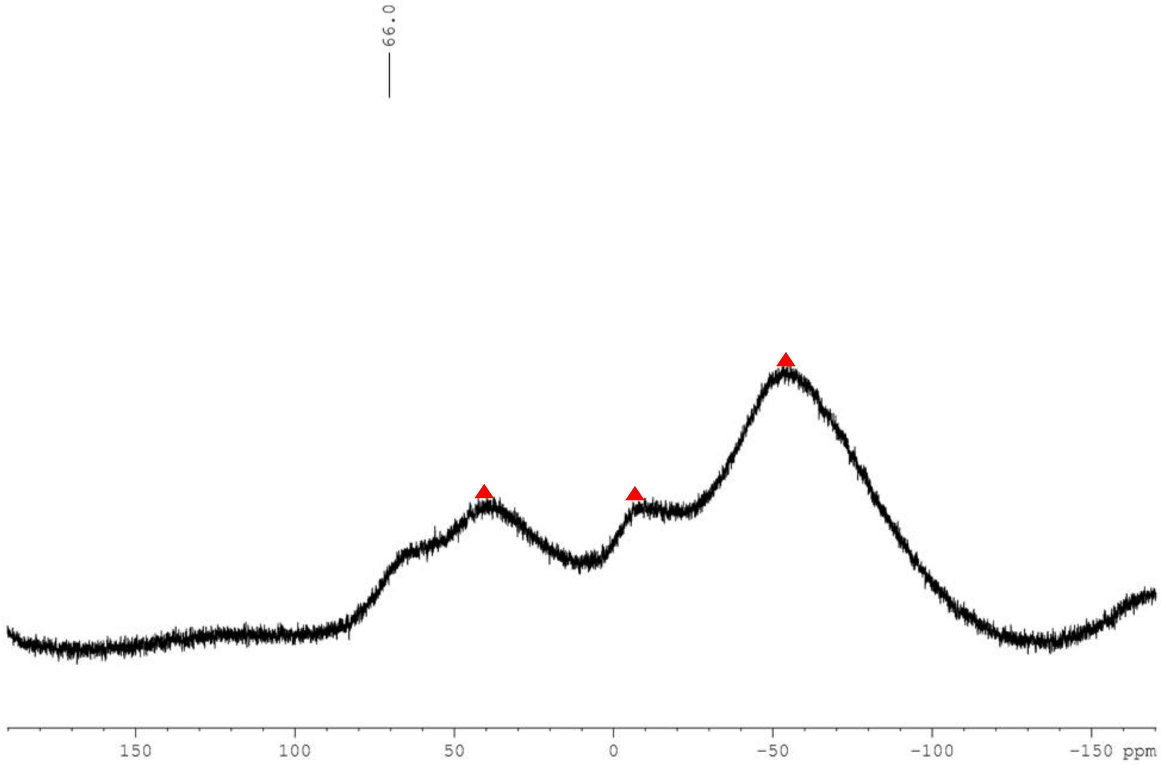

Figure S8: ^{11}B NMR spectrum of **2** (CD_2Cl_2, 96.3 MHz; ▲: borosilicate glass resonance).

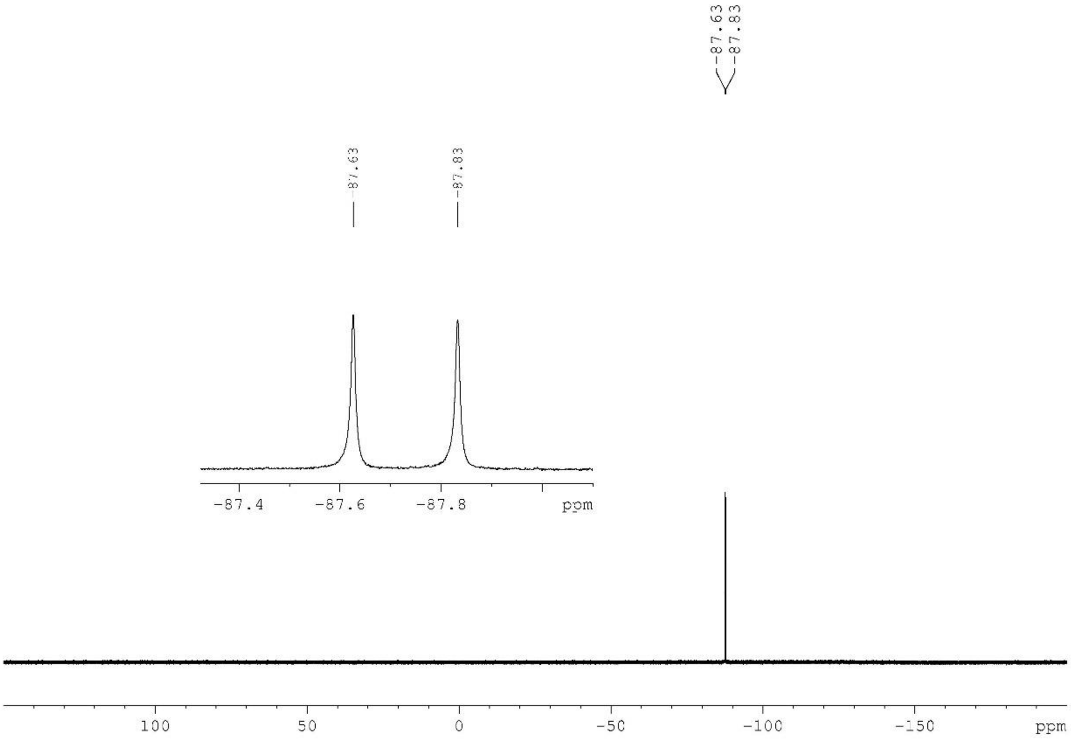

Figure S9: $^{19}F\{^1H\}$ NMR spectrum of **2** (CD_2Cl_2, 282.3 MHz).

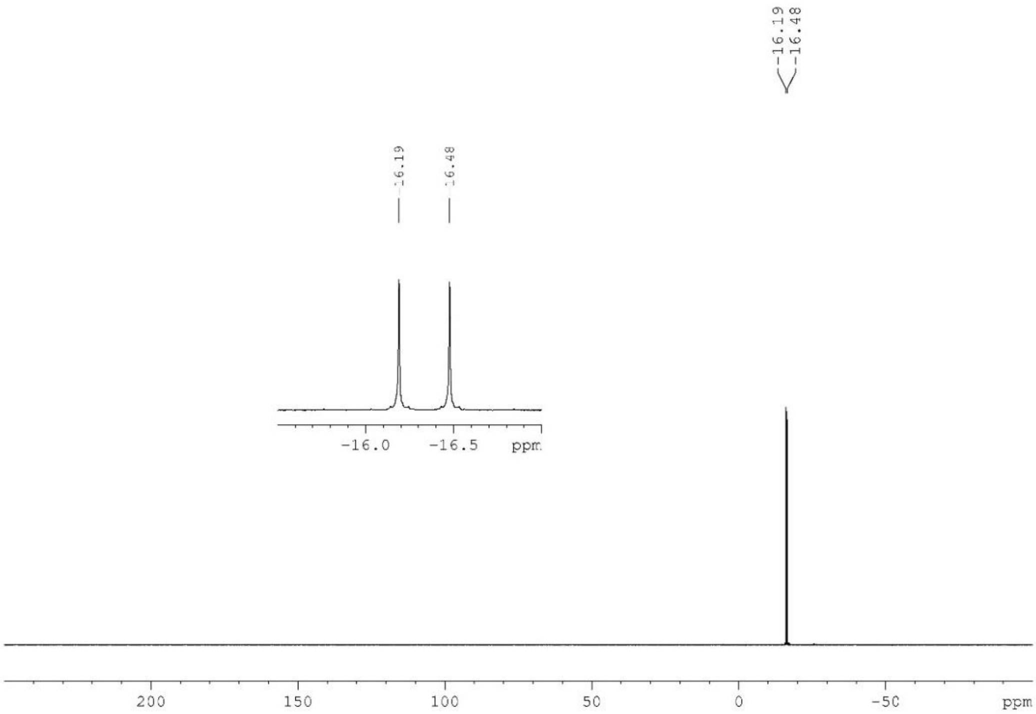

Figure S10: $^{31}P\{^1H\}$ NMR spectrum of **2** (CD_2Cl_2, 202.5 MHz).

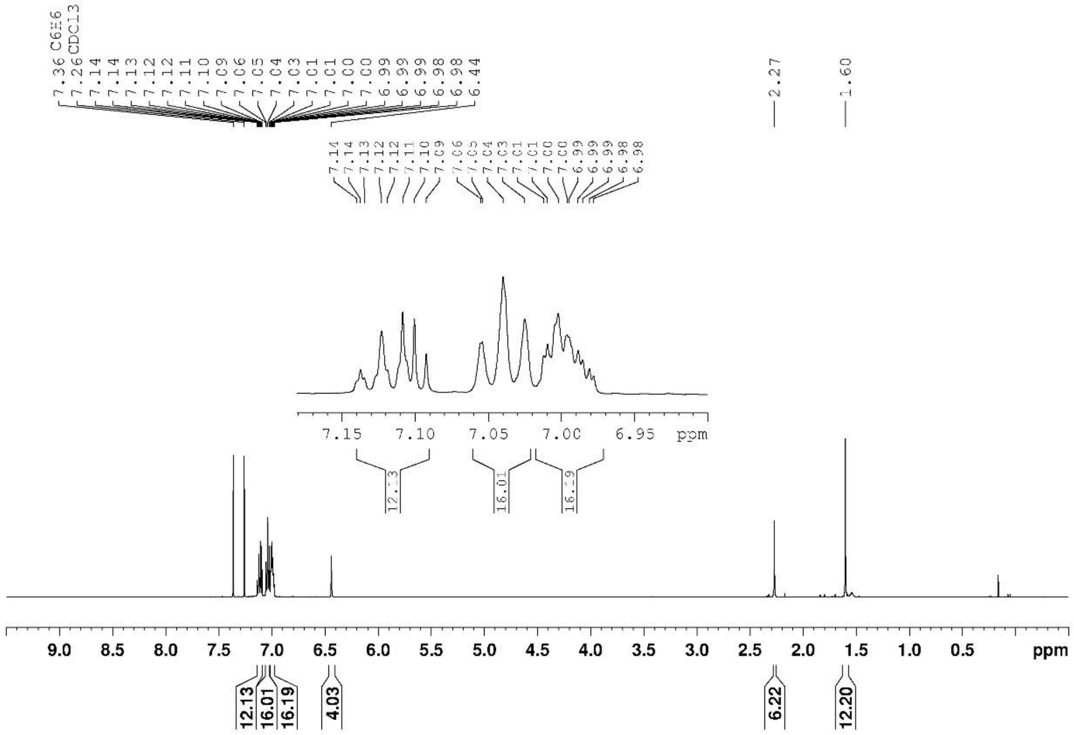

Figure S11: ^{1}H NMR spectrum of **3** (CDCl$_3$, 500.2 MHz).

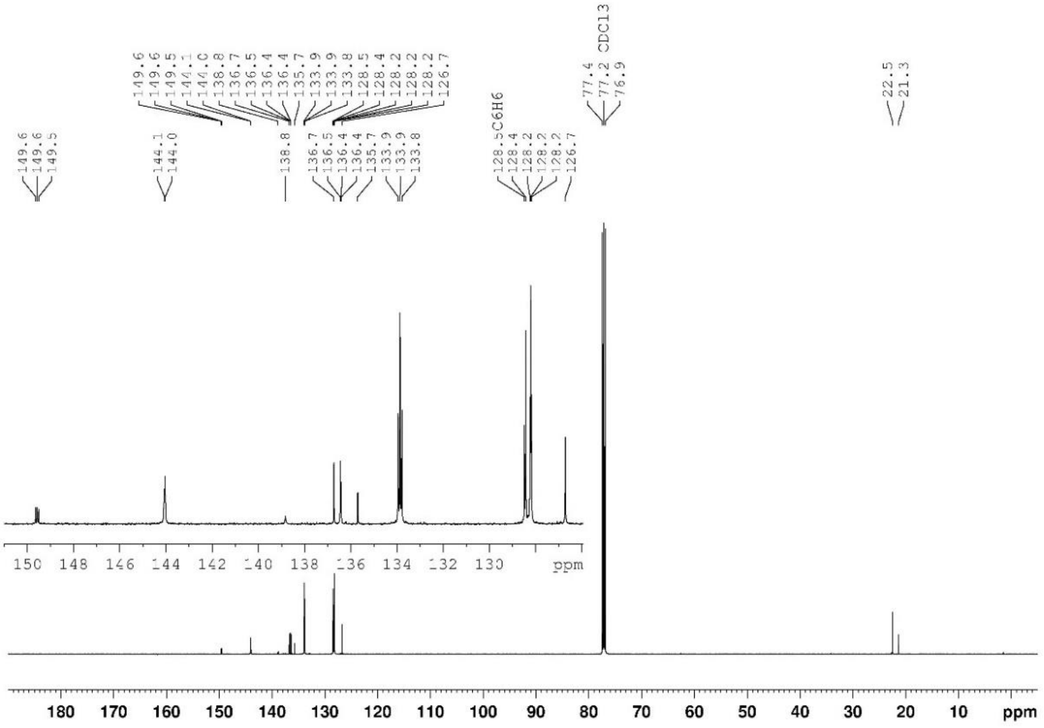

Figure S12: ^{13}C{^{1}H} NMR spectrum of **3** (CDCl$_3$, 125.8 MHz).

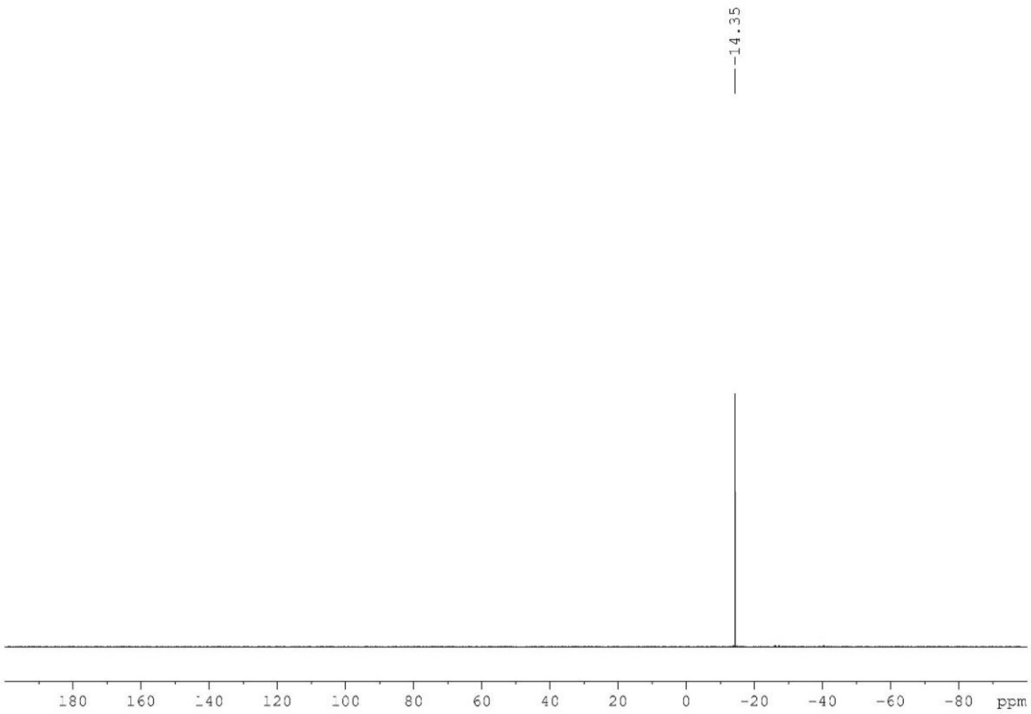

Figure S13: $^{31}P\{^1H\}$ NMR spectrum of **3** ($CDCl_3$, 121.5 MHz).

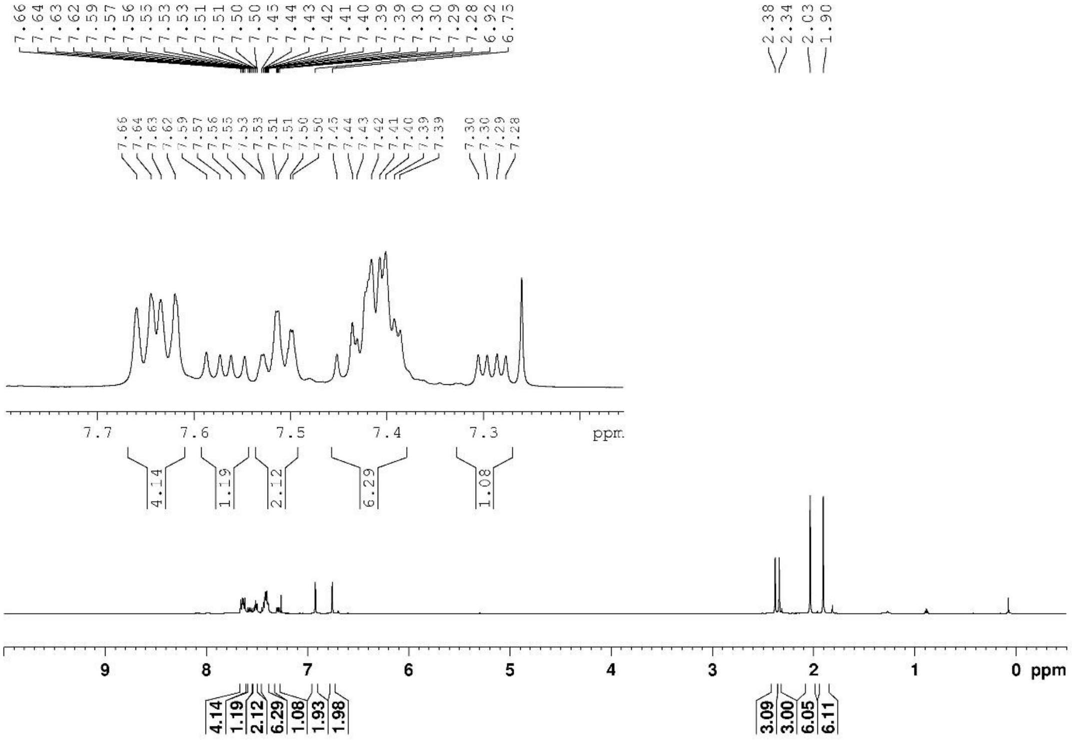

Figure S14: ^{1}H NMR spectrum of **4** (CDCl$_3$, 500.2 MHz).

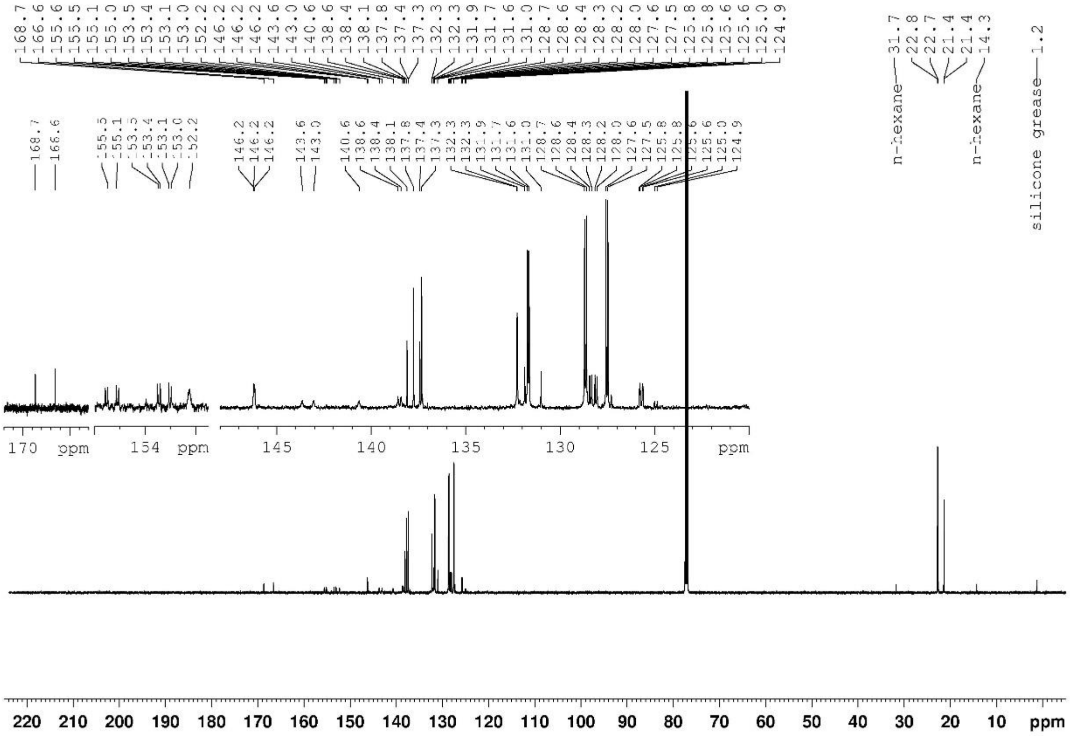

Figure S15: ^{13}C{^{1}H} NMR spectrum of **4** (CDCl$_3$, 125.8 MHz).

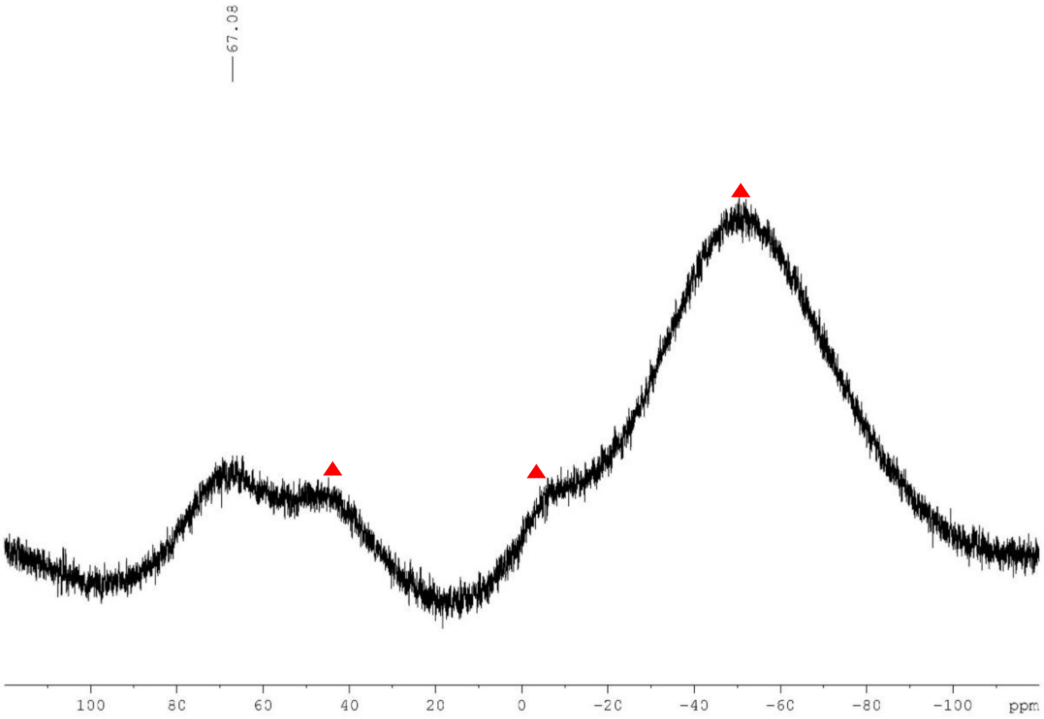

Figure S16: ^{11}B NMR spectrum of **4** ($CDCl_3$, 96.3 MHz; ▲: borosilicate glass resonance).

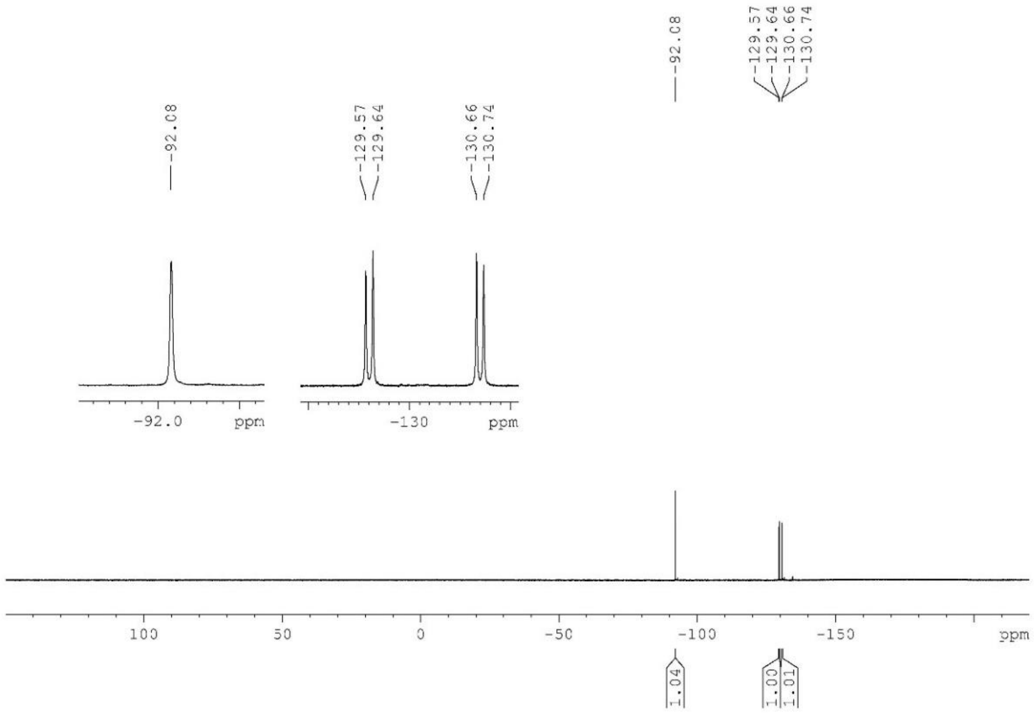

Figure S17: ^{19}F{^{1}H} NMR spectrum of **4** ($CDCl_3$, 282.3 MHz).

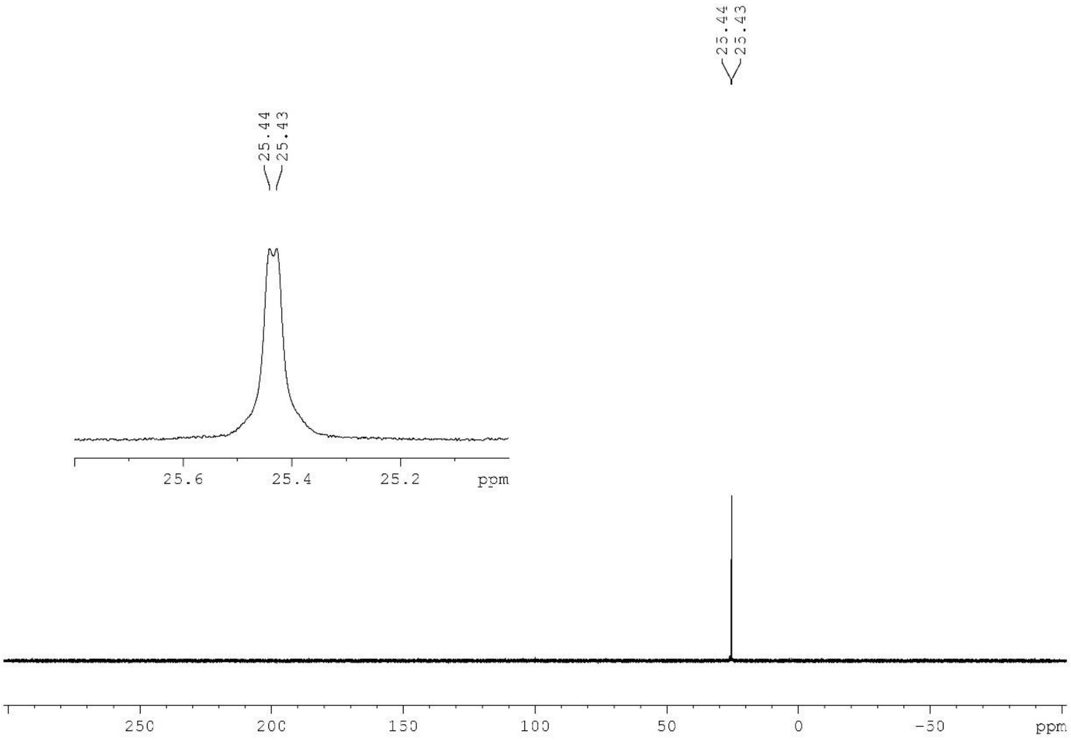

Figure S18: $^{31}P\{^1H\}$ NMR spectrum of **4** ($CDCl_3$, 121.5 MHz).

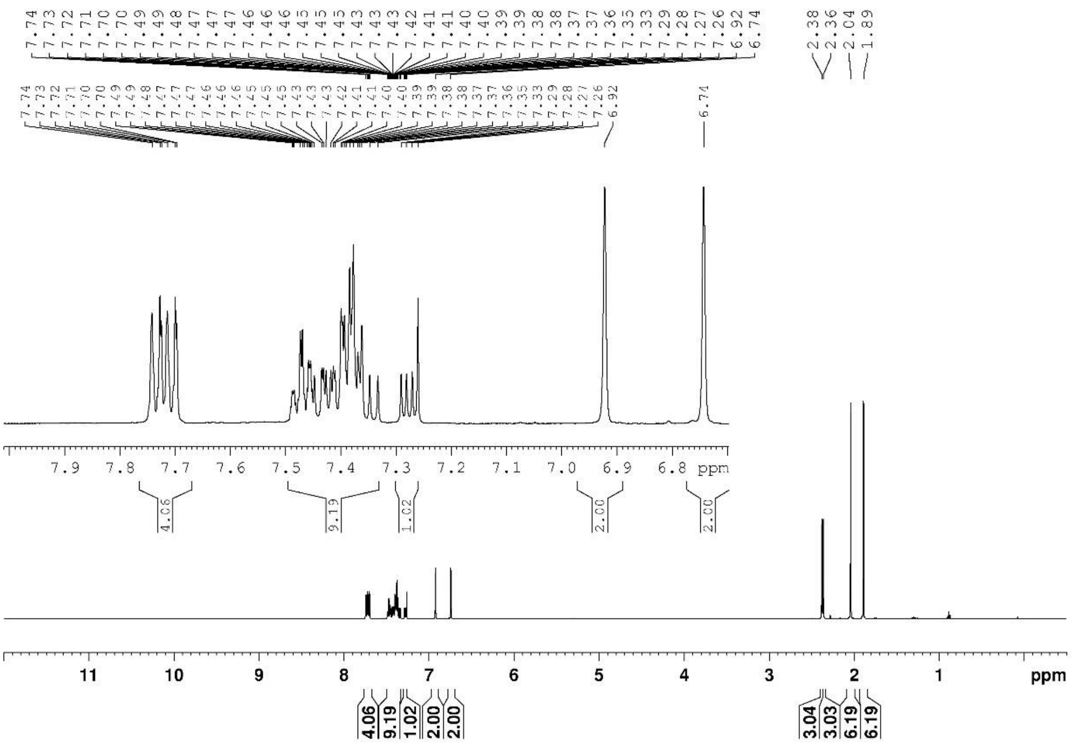

Figure S19: ^{1}H NMR spectrum of **5** (CDCl$_3$, 500.2 MHz).

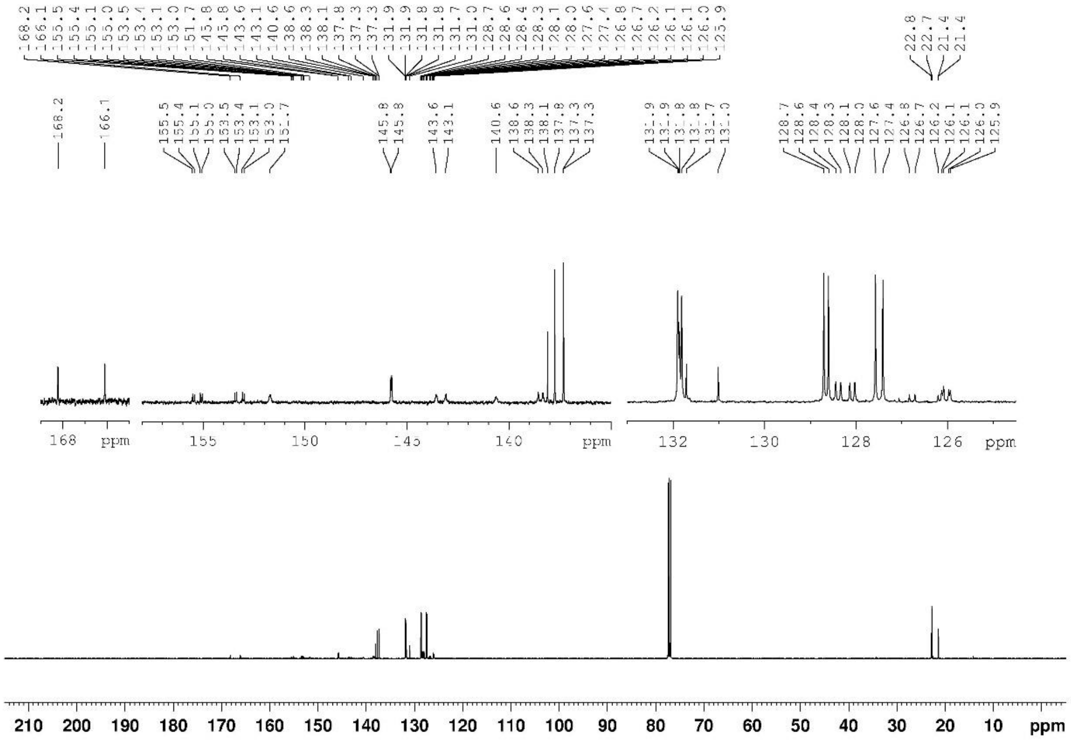

Figure S20: ^{13}C{^{1}H} NMR spectrum of **5** (CDCl$_3$, 125.8 MHz).

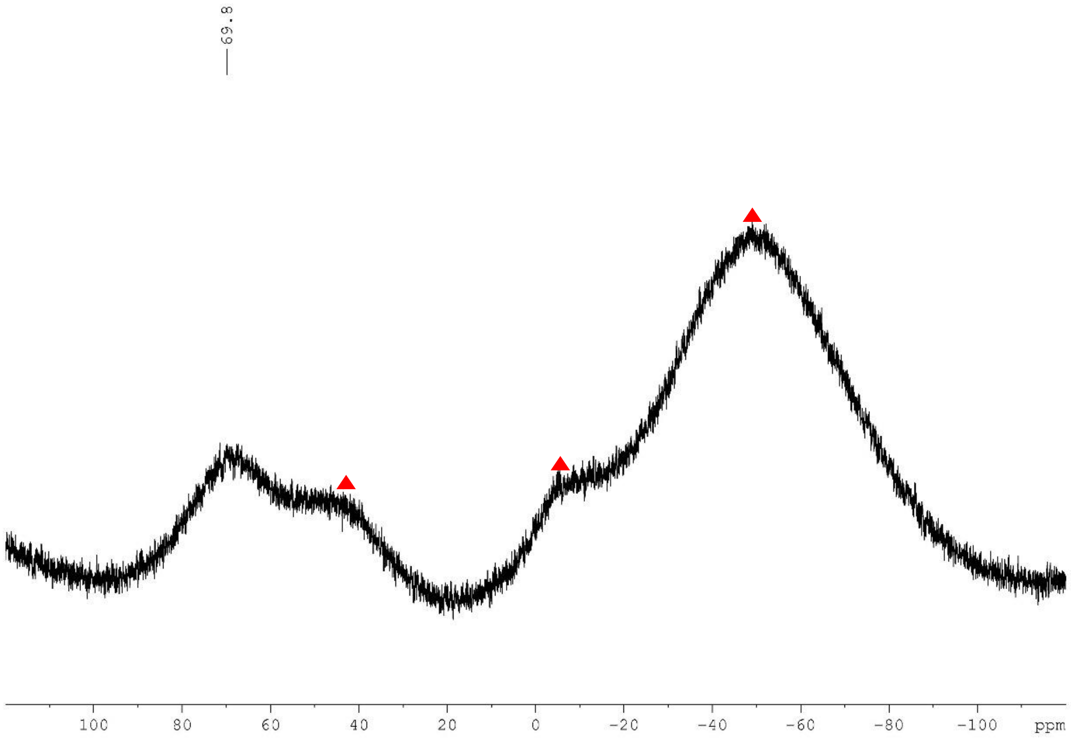

Figure S21: ^{11}B NMR spectrum of **5** (CDCl$_3$, 96.3 MHz; ▲: borosilicate glass resonance).

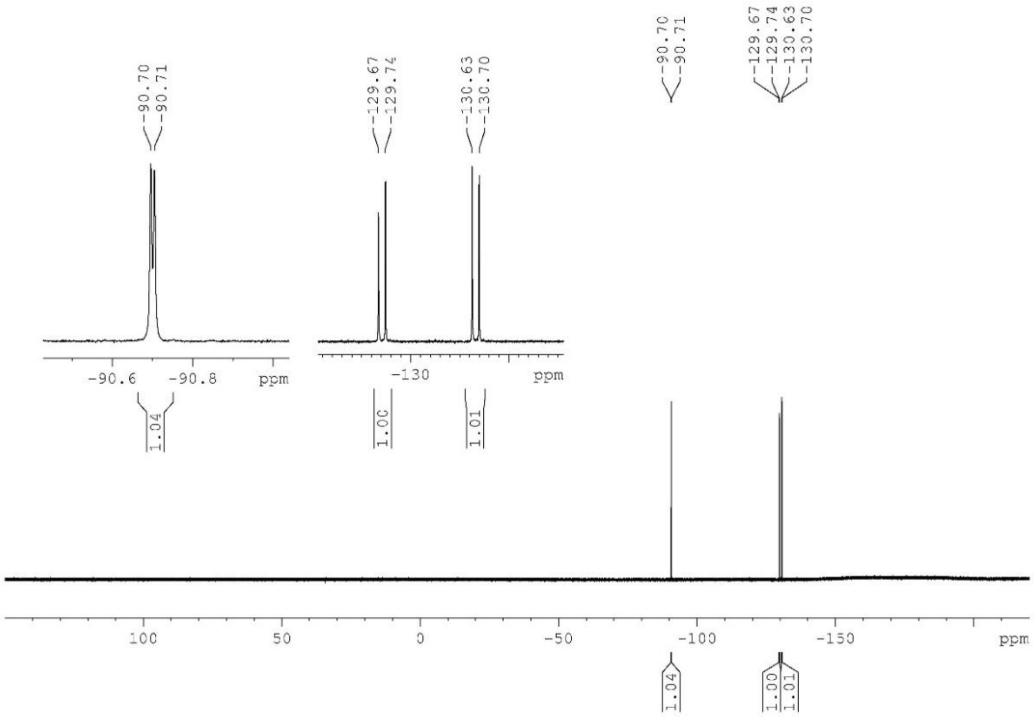

Figure S22: ^{19}F{^{1}H} NMR spectrum of **5** (CDCl$_3$, 282.3 MHz).

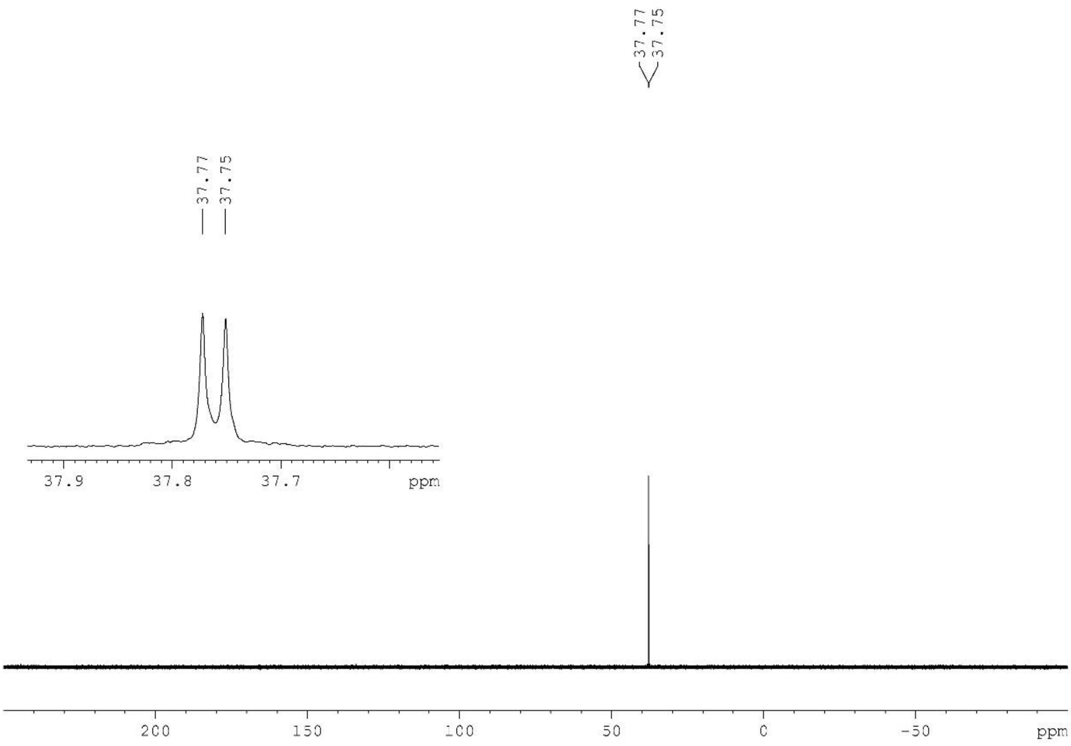

Figure S23: $^{31}P\{^{1}H\}$ NMR spectrum of **5** ($CDCl_3$, 121.5 MHz).

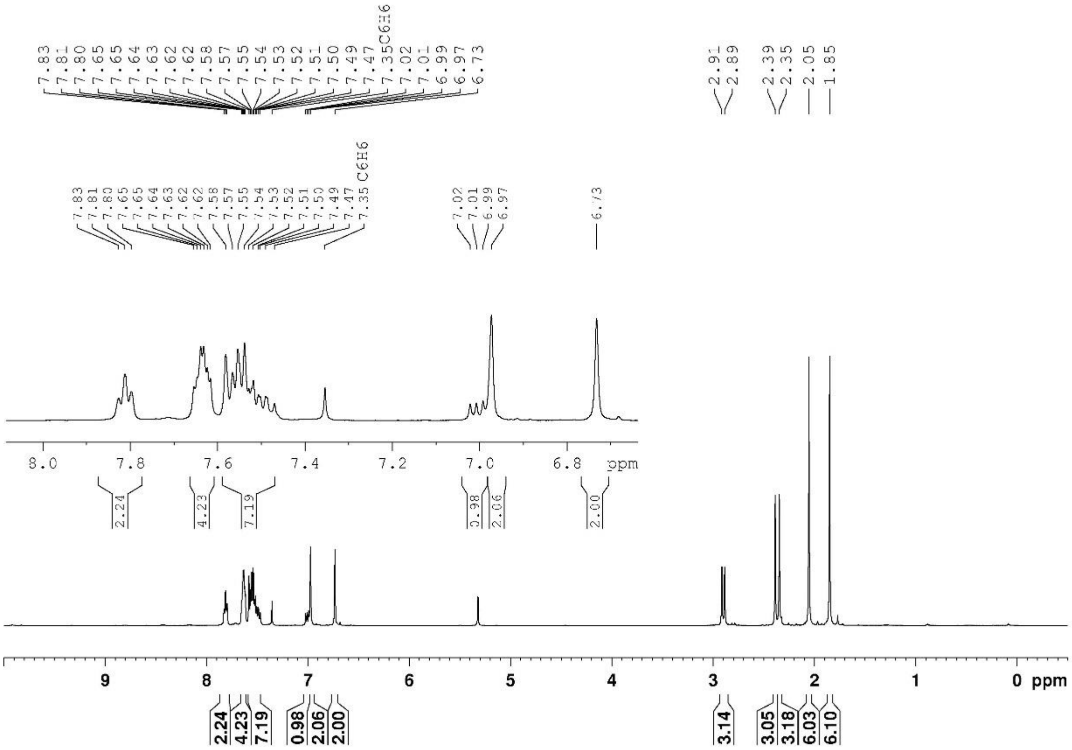

Figure S24: ^{1}H NMR spectrum of [**6**]OTf (CD_2Cl_2, 500.2 MHz).

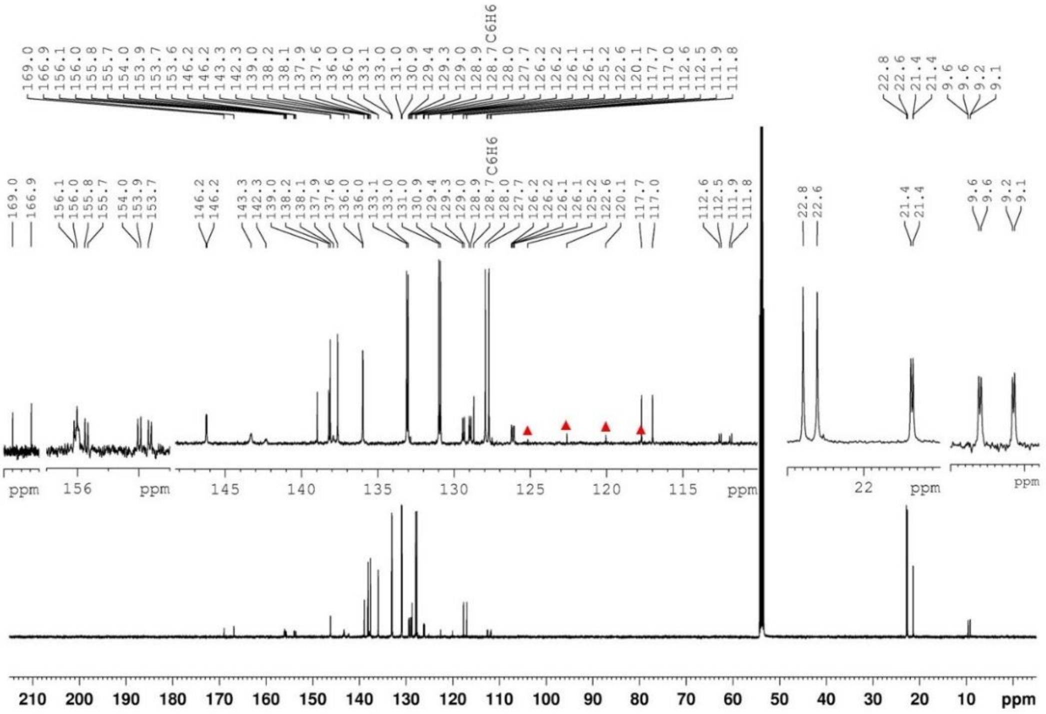

Figure S25: $^{13}C\{^{1}H\}$ NMR spectrum of [**6**]OTf (CD_2Cl_2, 125.8 MHz; ▲: CF_3 resonance).

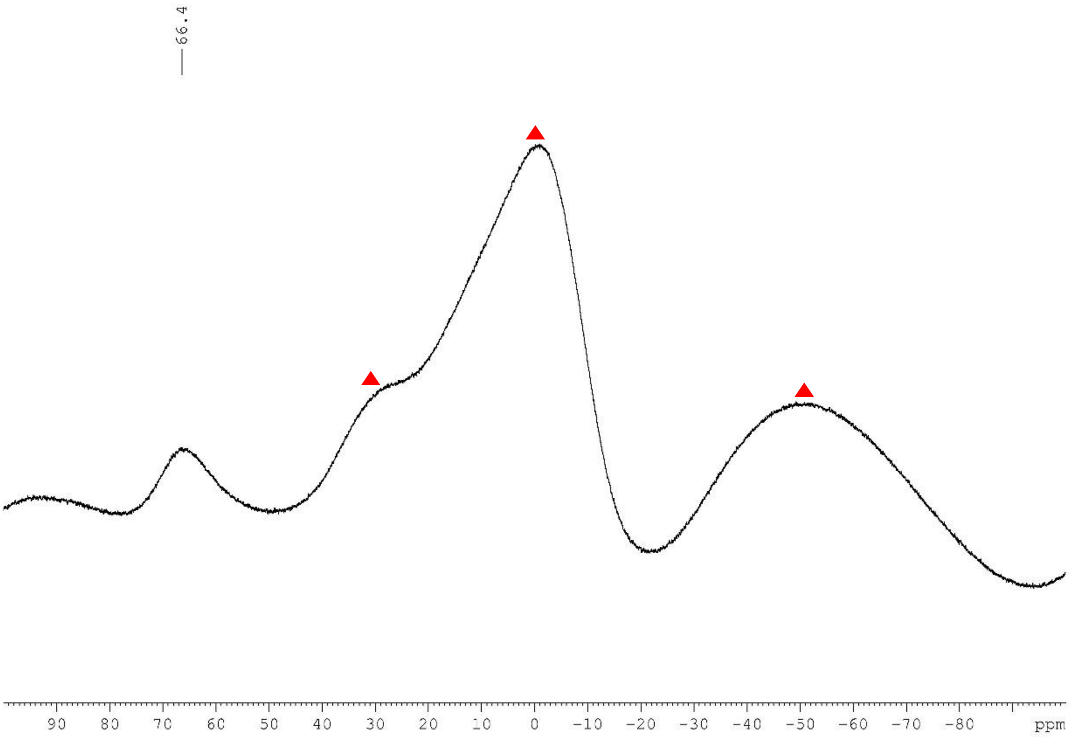

Figure S26: ^{11}B NMR spectrum of [**6**]OTf (CD_2Cl_2, 160.5 MHz; ▲: borosilicate glass resonance).

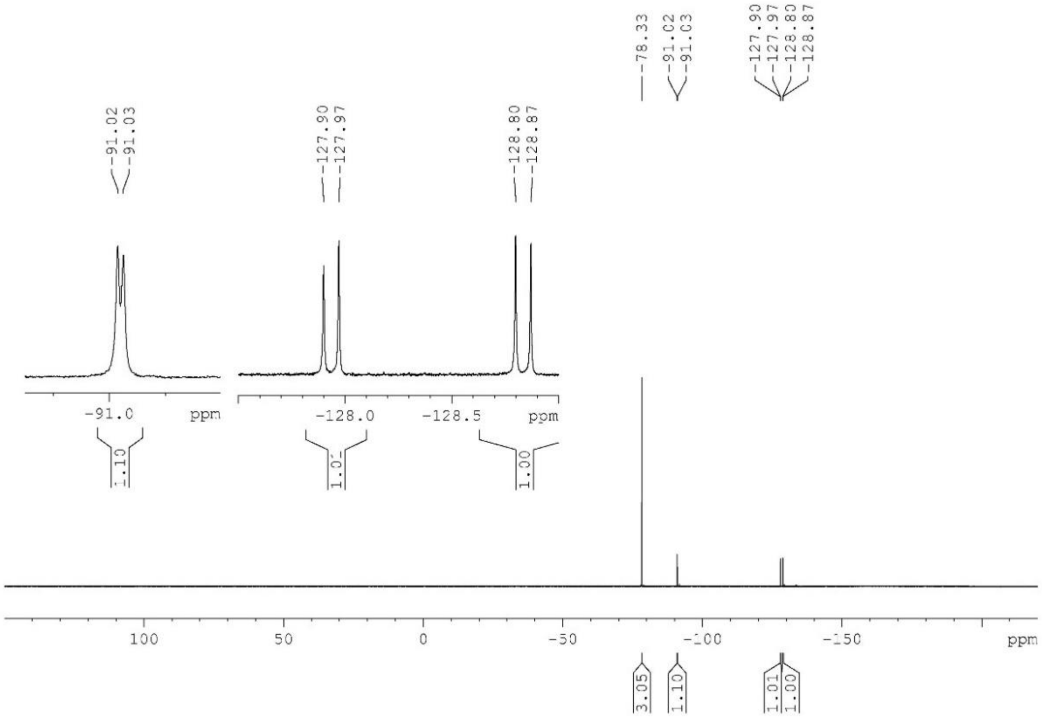

Figure S27: ^{19}F{^{1}H} NMR spectrum of [**6**]OTf (CD_2Cl_2, 282.3 MHz).

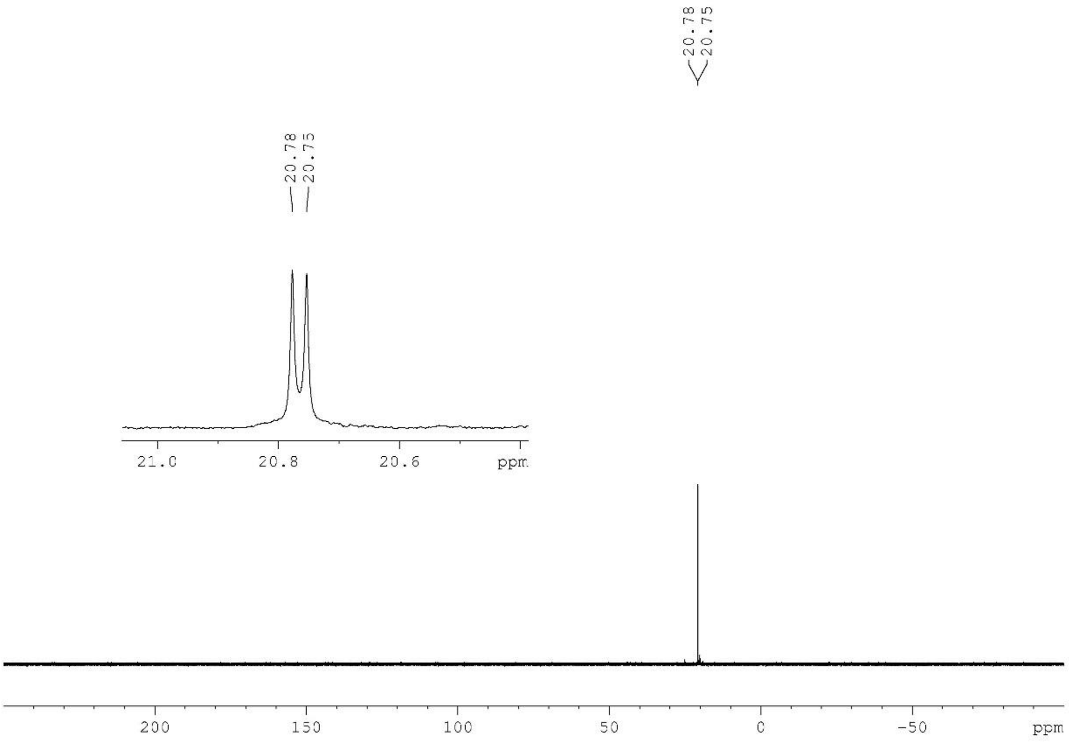

Figure S28: $^{31}P\{^{1}H\}$ NMR spectrum of [**6**]OTf (CD_2Cl_2, 121.5 MHz).

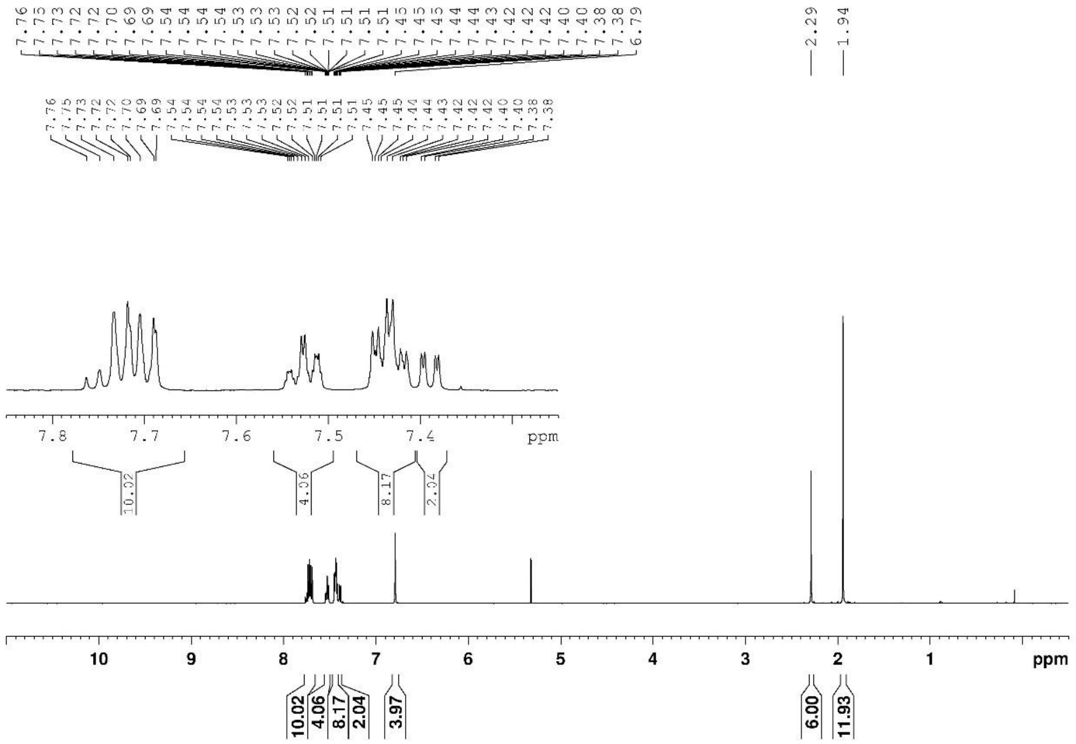

Figure S29: ^{1}H NMR spectrum of **7** (CD_2Cl_2, 500.2 MHz).

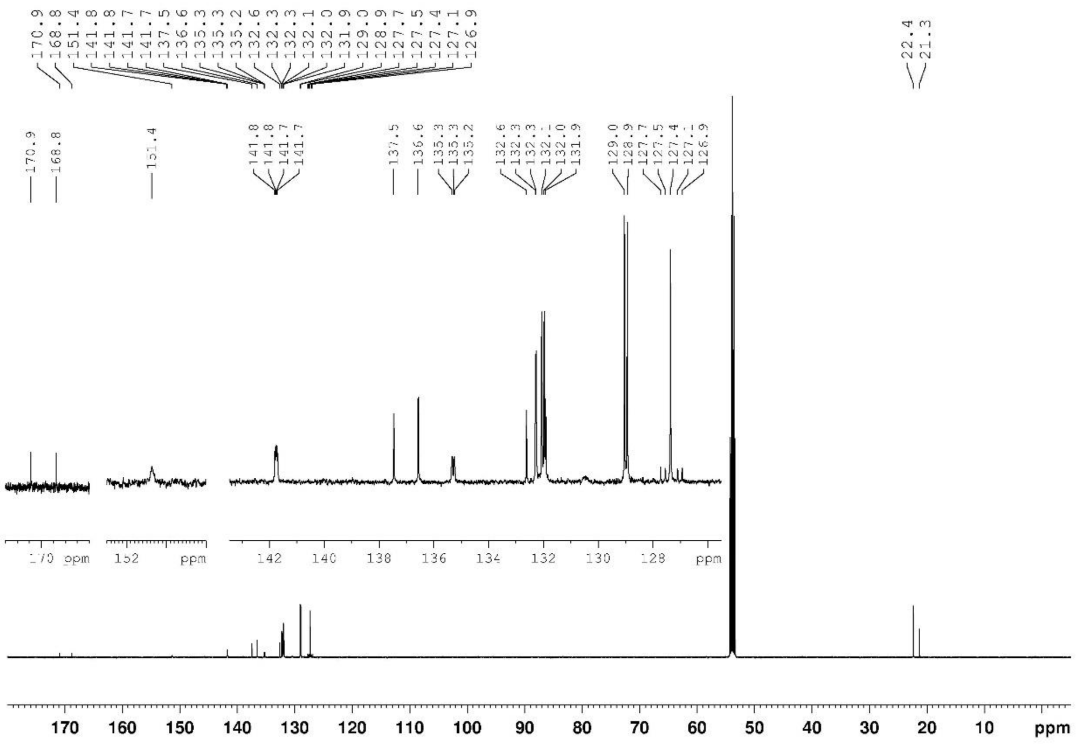

Figure S30: $^{13}C\{^1H\}$ NMR spectrum of **7** (CD_2Cl_2, 125.8 MHz).

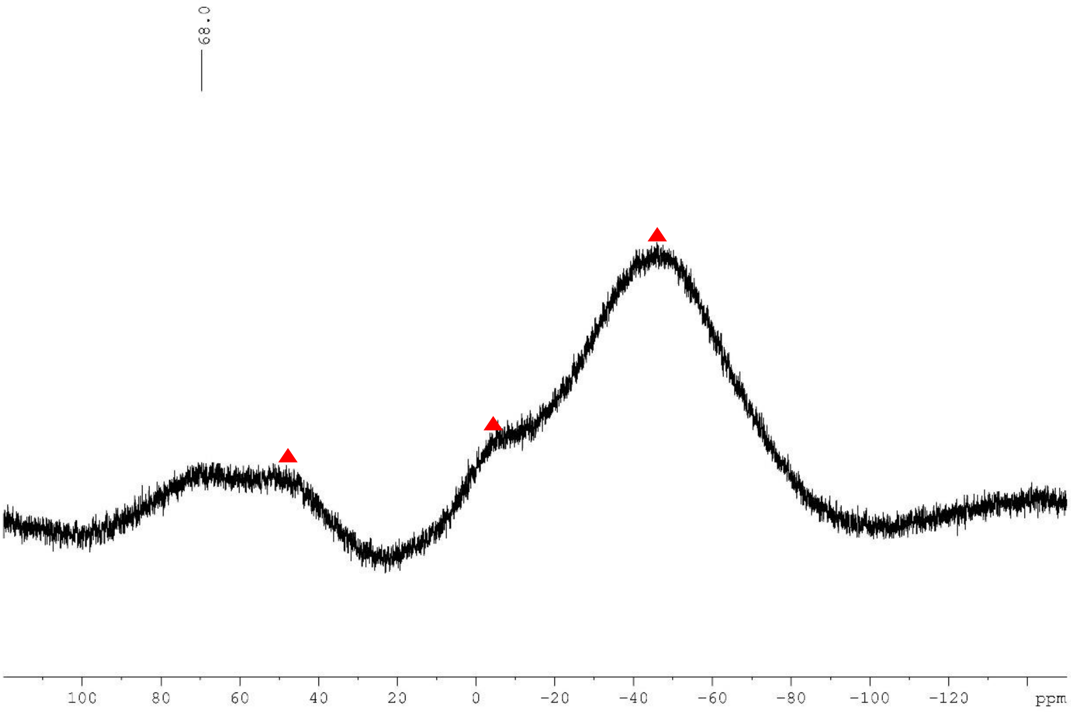

Figure S31: ^{11}B NMR spectrum of **7** (CD_2Cl_2, 96.3 MHz; ▲: borosilicate glass resonance).

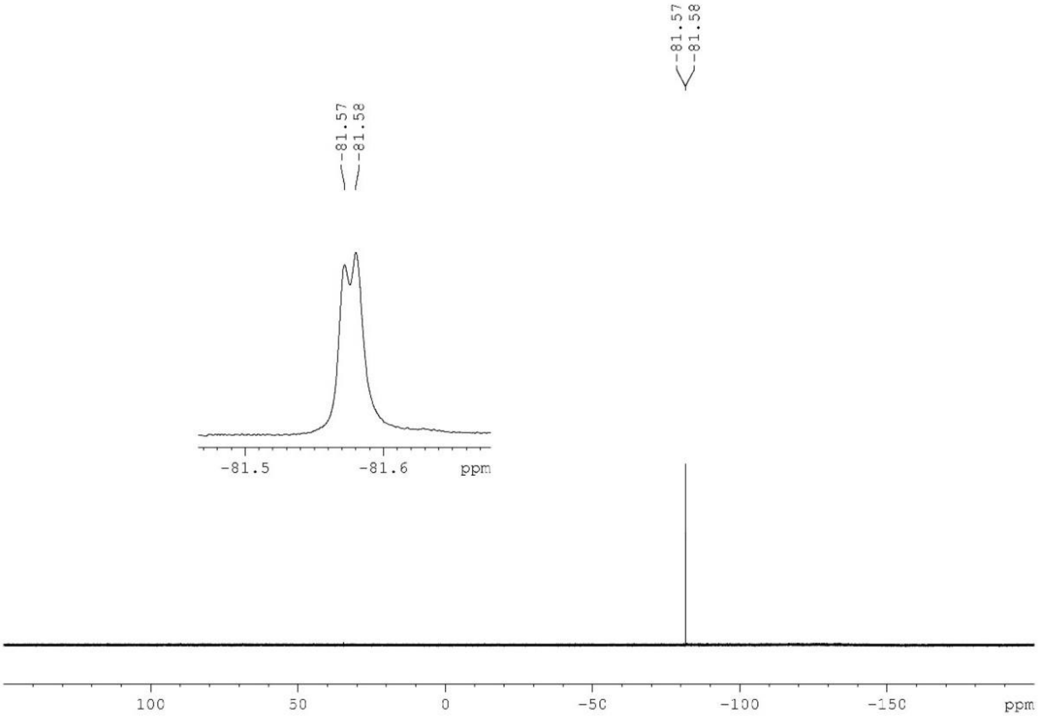

Figure S32: ^{19}F{^{1}H} NMR spectrum of **7** (CD_2Cl_2, 282.3 MHz).

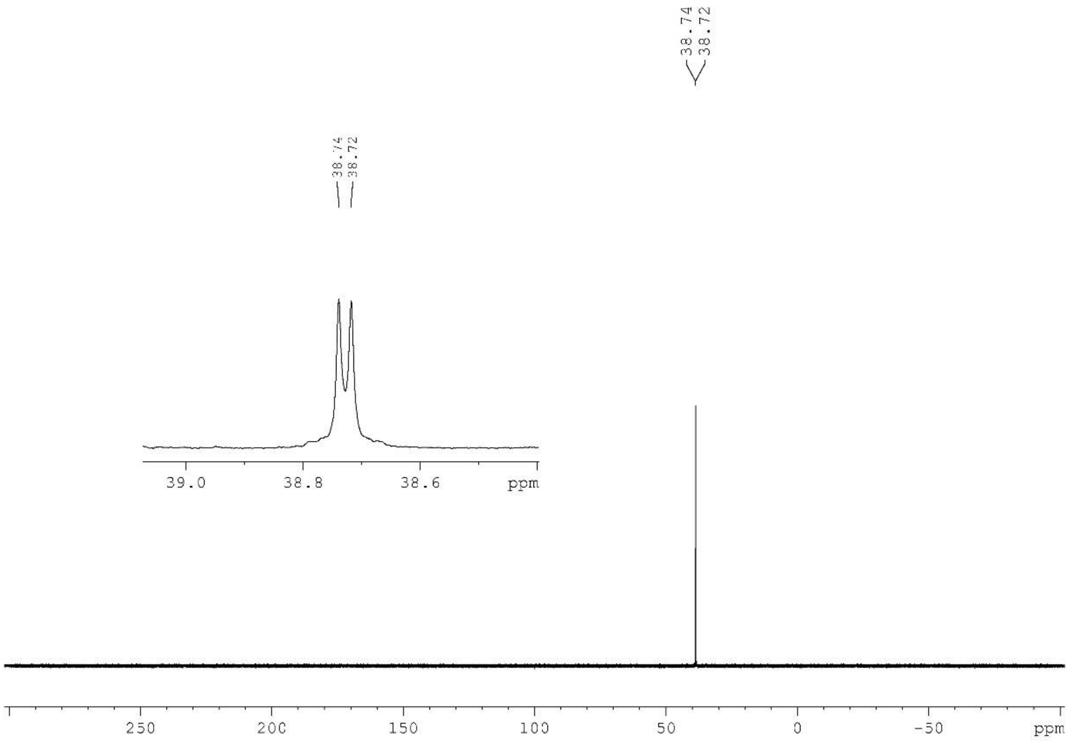

Figure S33: $^{31}P\{^1H\}$ NMR spectrum of **7** (CD_2Cl_2, 121.5 MHz).

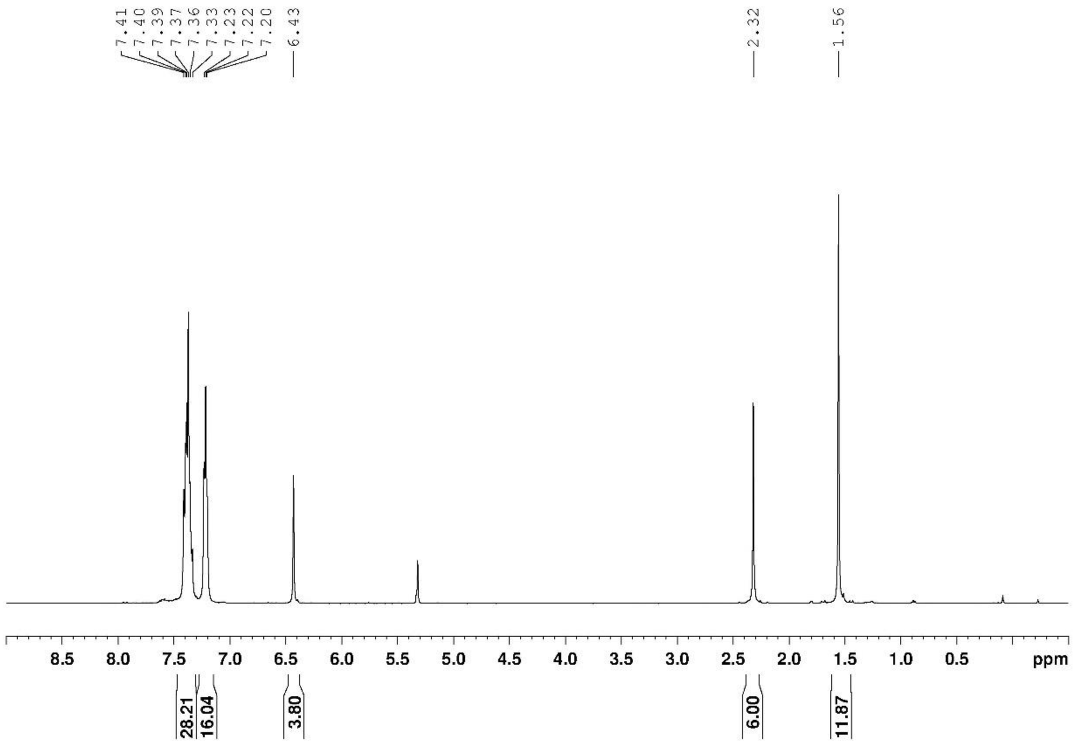

Figure S34: ^{1}H NMR spectrum of **8** (CD_2Cl_2, 500.2 MHz).

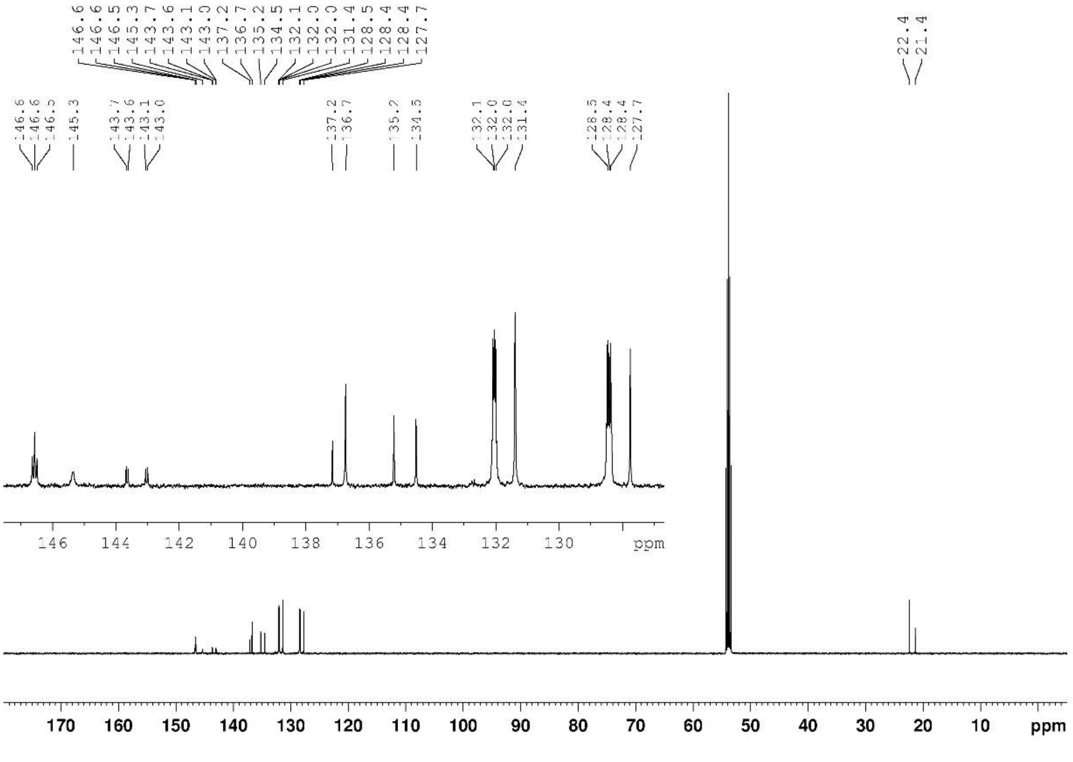

Figure S35: $^{13}C\{^1H\}$ NMR spectrum of **8** (CD_2Cl_2, 125.8 MHz).

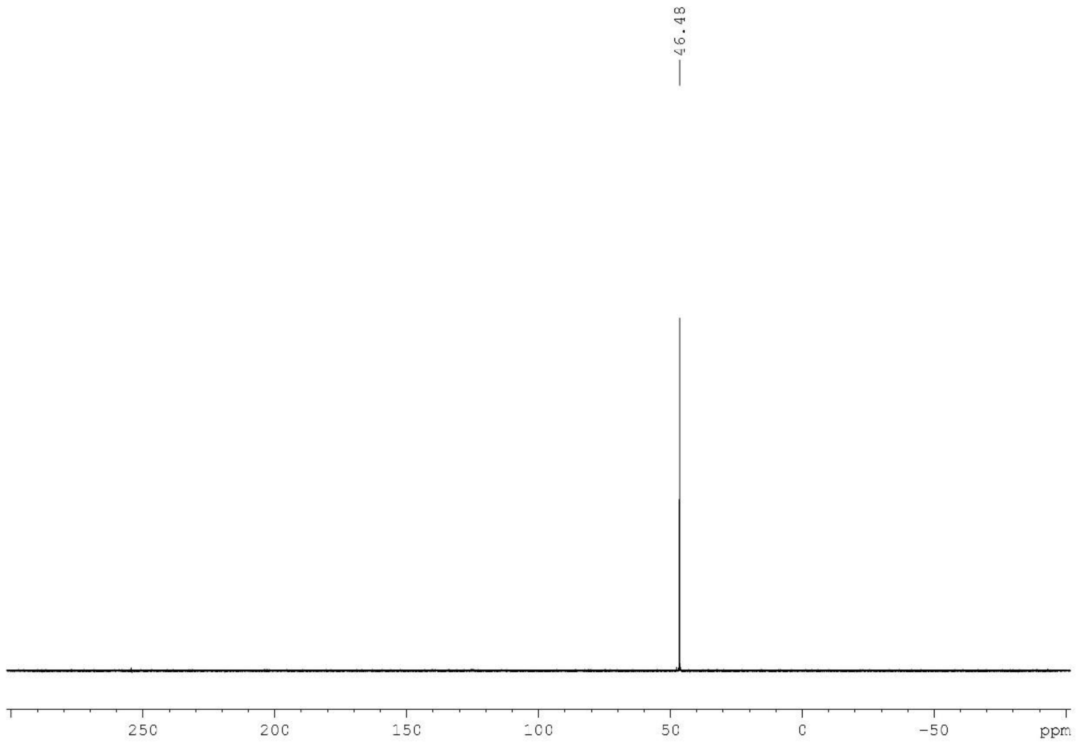

Figure S36: $^{31}P\{^{1}H\}$ NMR spectrum of **8** (CD_2Cl_2, 121.5 MHz).

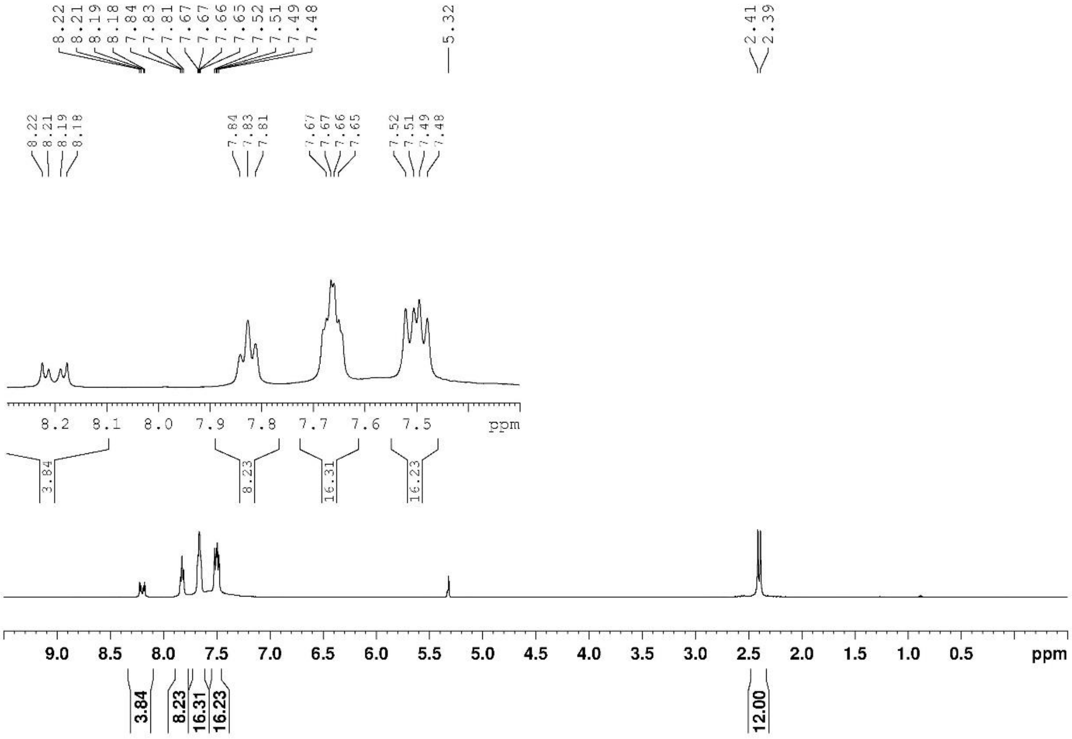

Figure S37: ^{1}H NMR spectrum of [**10**](OTf)$_2$ (CD$_2$Cl$_2$, 500.2 MHz).

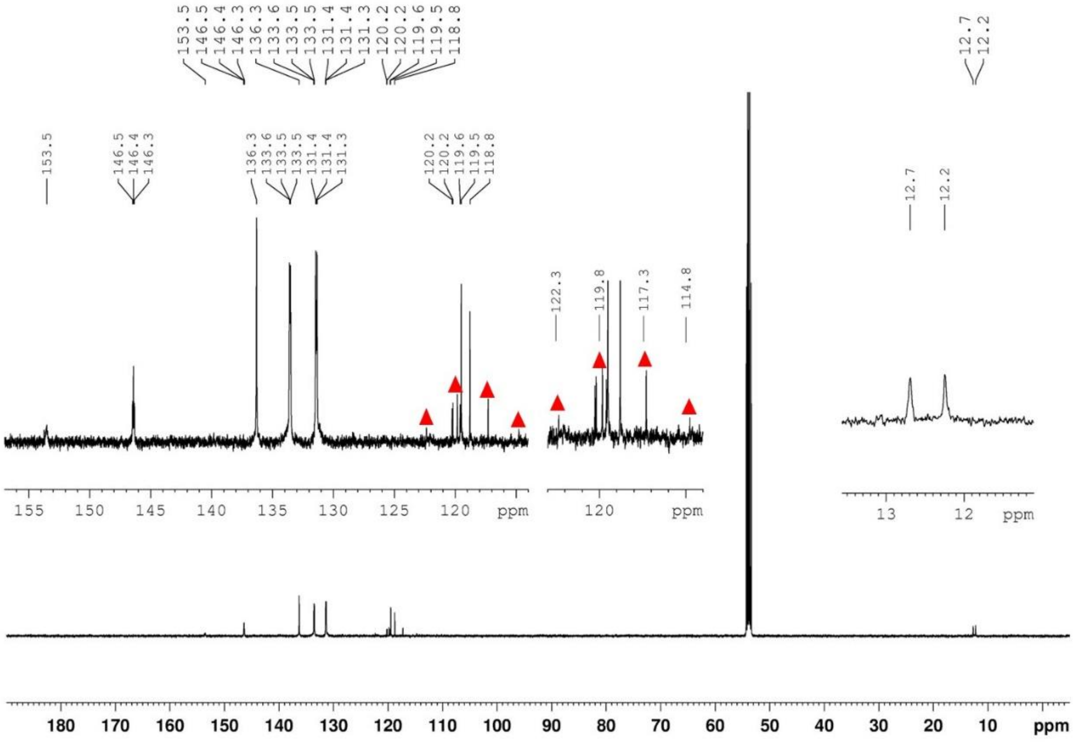

Figure S38: ^{13}C{^{1}H} NMR spectrum of [**10**](OTf)$_2$ (CD$_2$Cl$_2$, 125.8 MHz; ▲: CF$_3$ resonance).

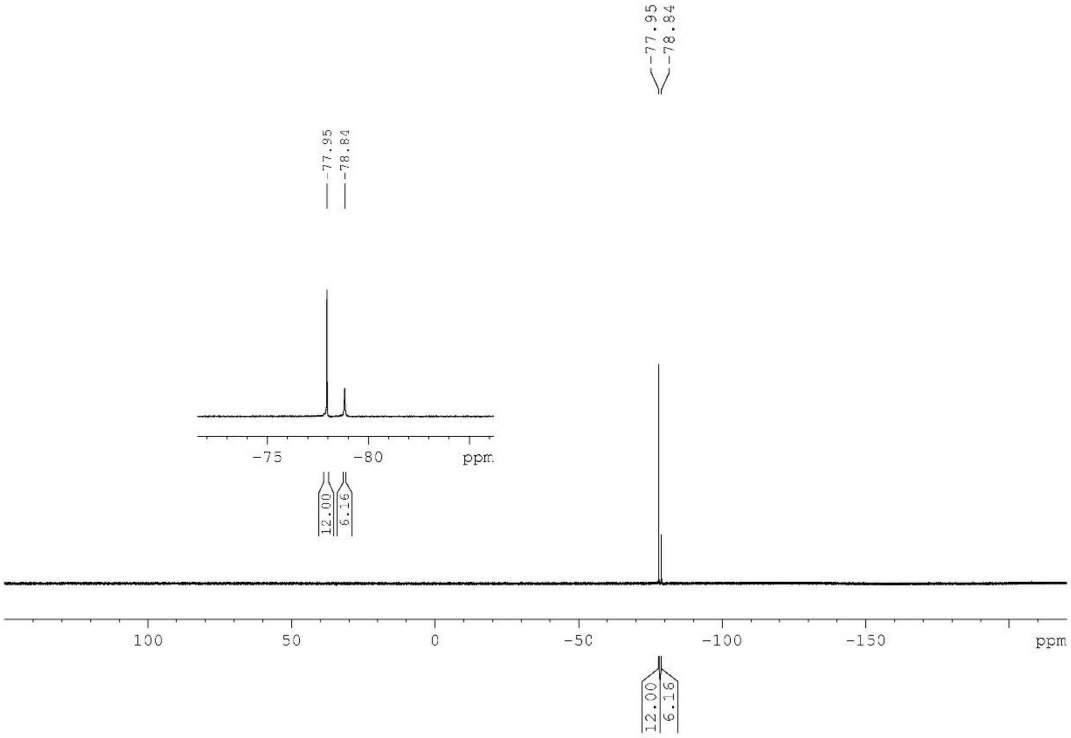

Figure S39: $^{19}F\{^1H\}$ NMR spectrum of [**10**](OTf)$_2$ (CD_2Cl_2, 282.3 MHz).

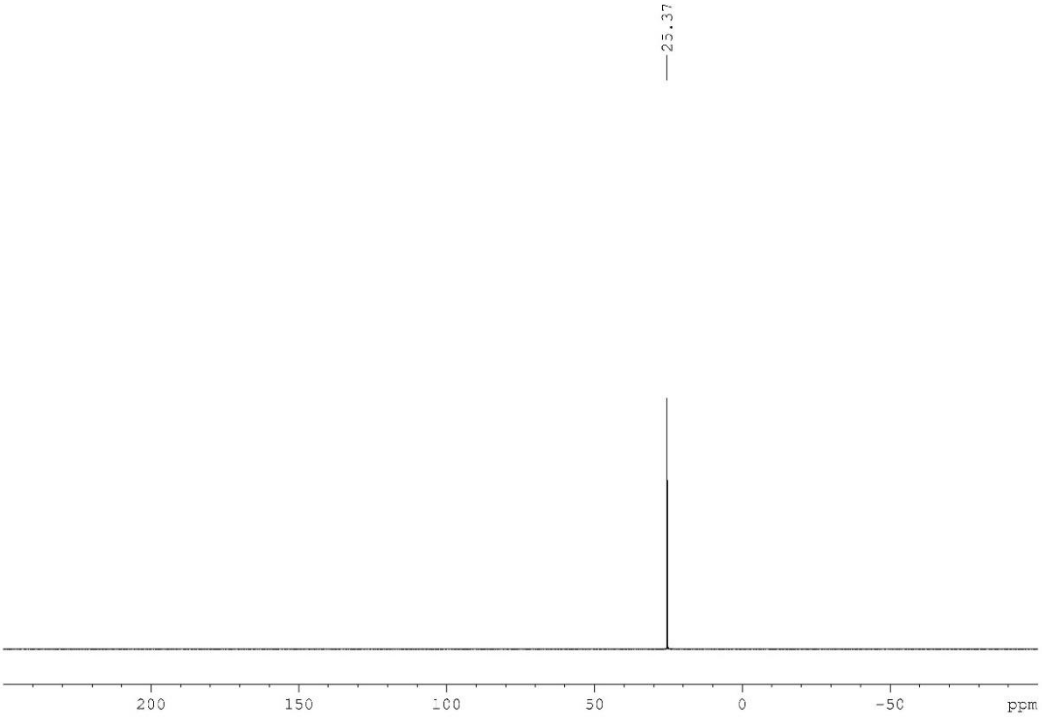

Figure S40: $^{31}P\{^1H\}$ NMR spectrum of [**10**](OTf)$_2$ (CD_2Cl_2, 202.5 MHz).

5. NMR spectra of the methylation reaction of 2.

An NMR-tube was charged with **2** (10 mg, 12 µmol) and CD_2Cl_2 (0.6 mL). Neat MeOTf (4.0 mg, 24 µmol) was added at room temperature via syringe. The NMR-tube was flame sealed under vacuum and an orange solution was obtained after the sample had been stored for 1 h at room temperature. Afterwards, the NMR measurement of the sample was performed to characterize [**9**][OTf]$_2$ (Figure S41-43).

^{1}H NMR (400.2 MHz, CD_2Cl_2): δ = 7.85-7.81 (m, 4H), 7.69-7.64 (m, 10H), 7.59-7.53 (m, 8H), 7.05-6.98 (m, 2H), 6.73 (s, 4H; Mes-C*H*-*m*), 2.74 (d, ^2J(H,P) = 13.7 Hz, 6H; PC*H*$_3$) 2.23 (s, 6H; Mes-C*H*$_3$-*p*), 2.03 (s, 12H; Mes-C*H*$_3$-*o*).

^{31}P{^{1}H} NMR (162.0 MHz, CD_2Cl_2): δ = 20.1 (d, ^3J(P,F) = 6.0 Hz).

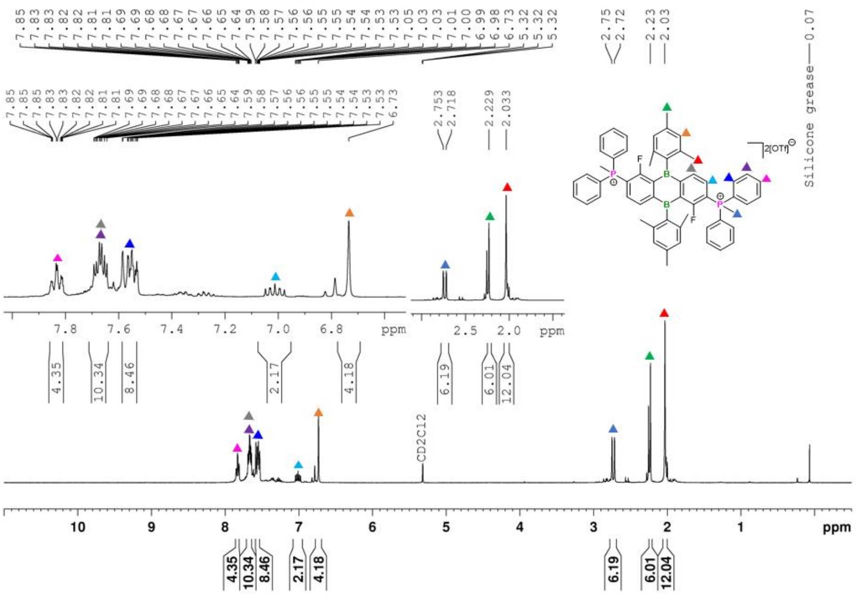

Figure S41: ^{1}H NMR spectrum (without purification) of [**9**][OTf]$_2$ (CD_2Cl_2, 400.2 MHz).

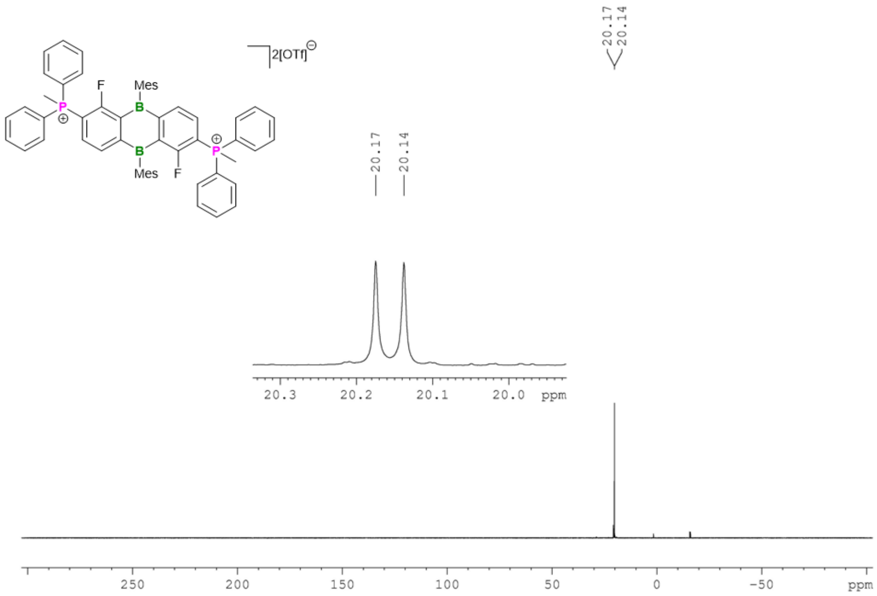

Figure S42: ^{31}P{^{1}H} NMR spectrum (without purification) of [**9**][OTf]$_2$ (CD_2Cl_2, 162.0 MHz).

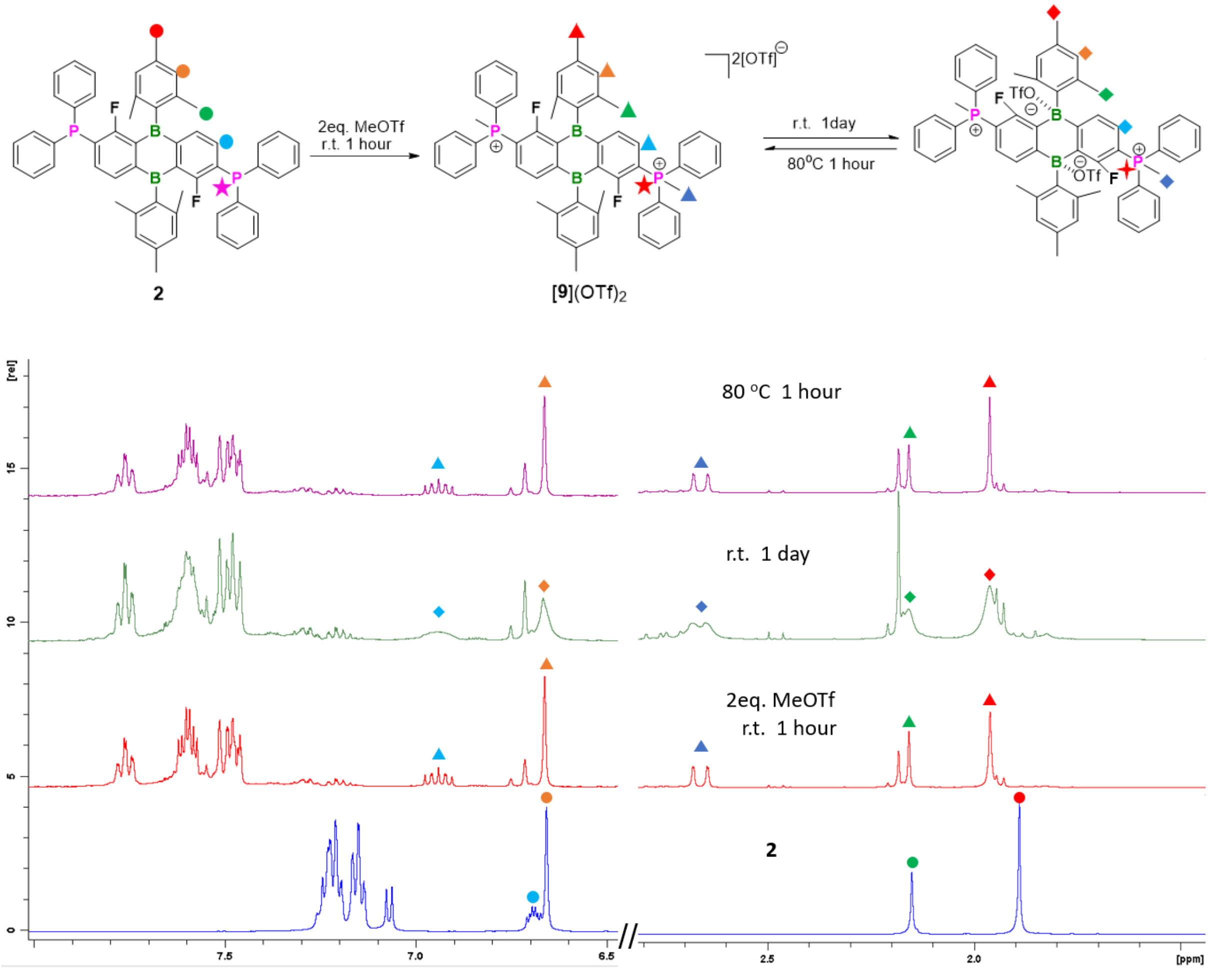

Figure S43: ^{1}H NMR spectroscopic monitoring of the methylation reaction of 2 under various conditions (CD_2Cl_2, 400.2 MHz).

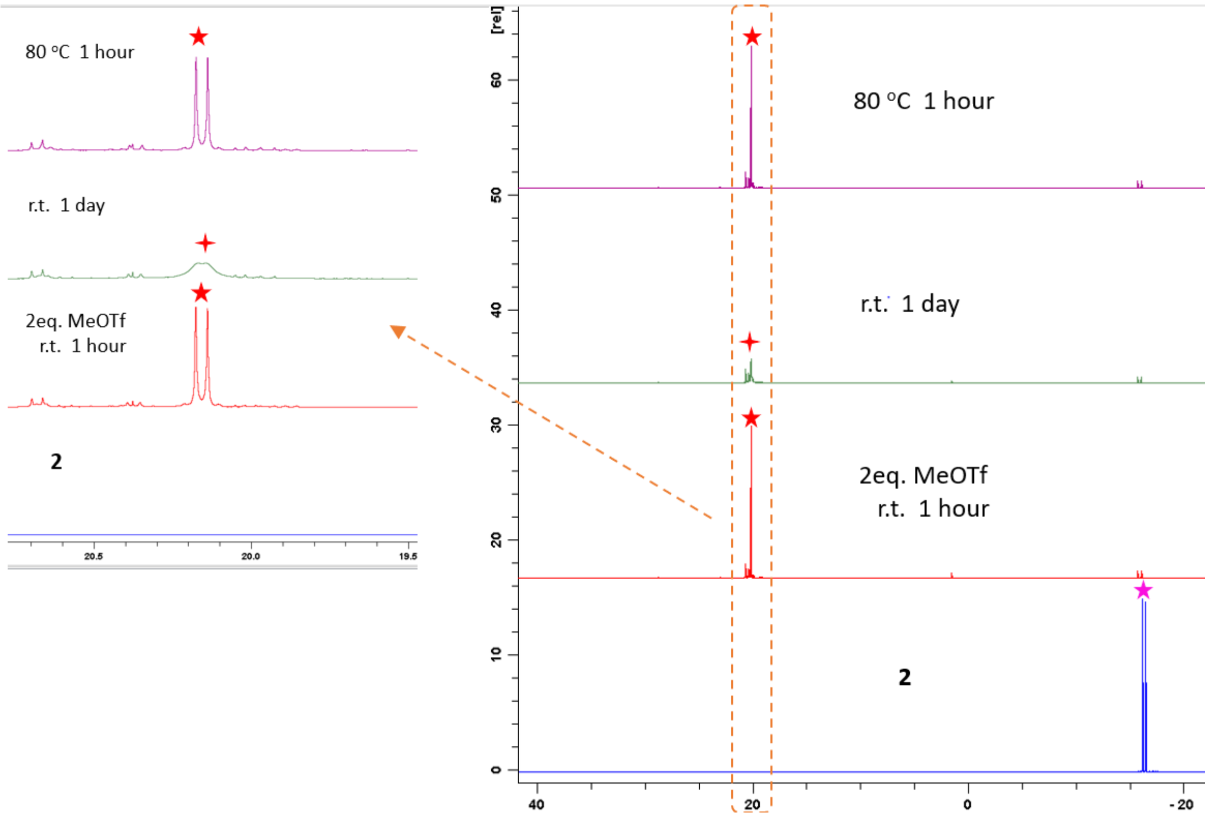

Figure S44: $^{31}P\{^{1}H\}$ NMR-spectroscopic monitoring of the methylation reaction of **2** under various conditions (CD_2Cl_2, 162.0 MHz).

6. HRMS of the mixture of di-, tri-, and tetraphosphanyl derivatives obtained after treatment of B with 1 eq. of Ph_2PSiMe_3.

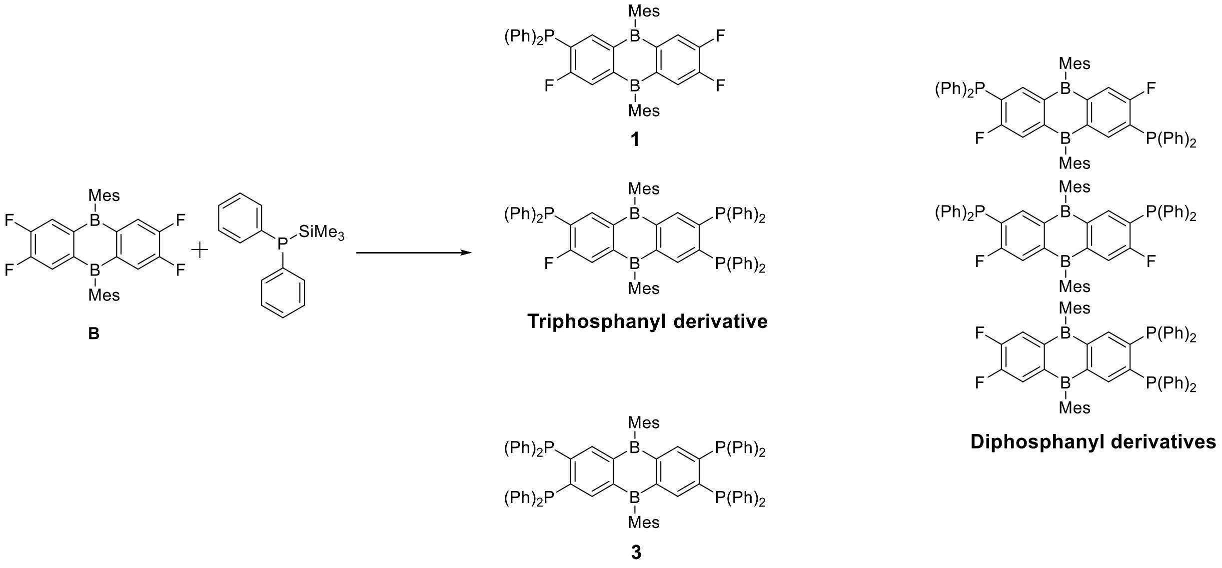

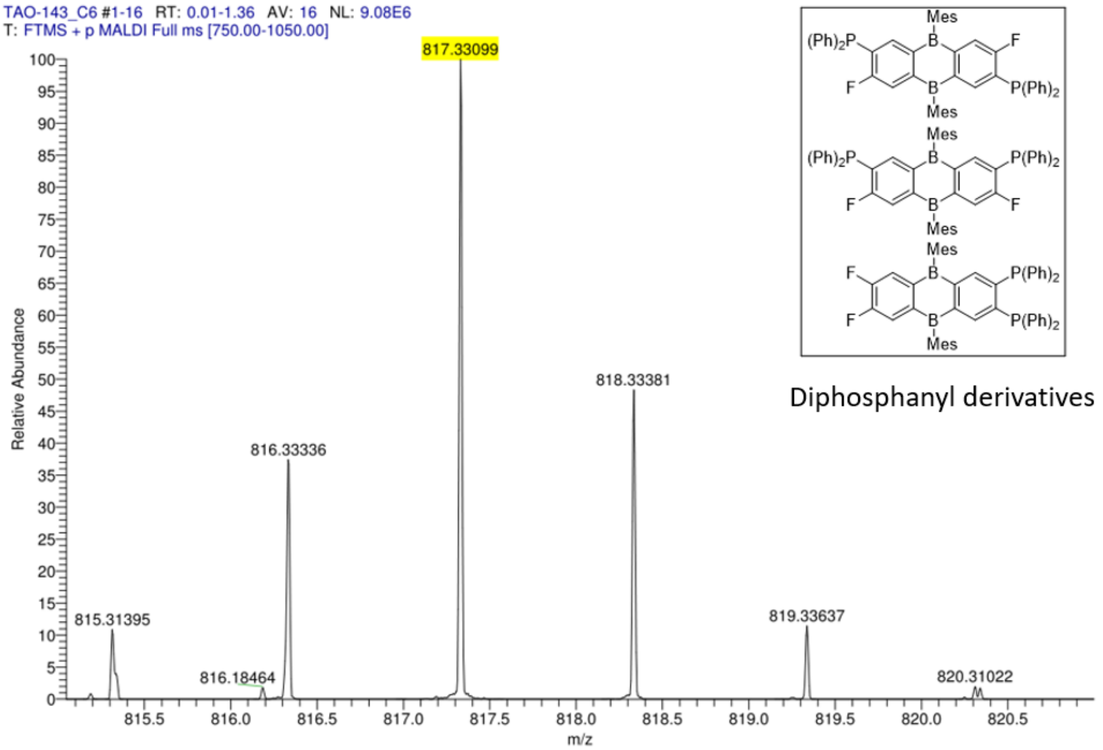

Figure S45: HRMS of the diphosphanyl derivatives (Calculated *m/z* for $[C_{54}H_{46}B_2F_2P_2+H]^+$: 817.33017, found: 817.33099).

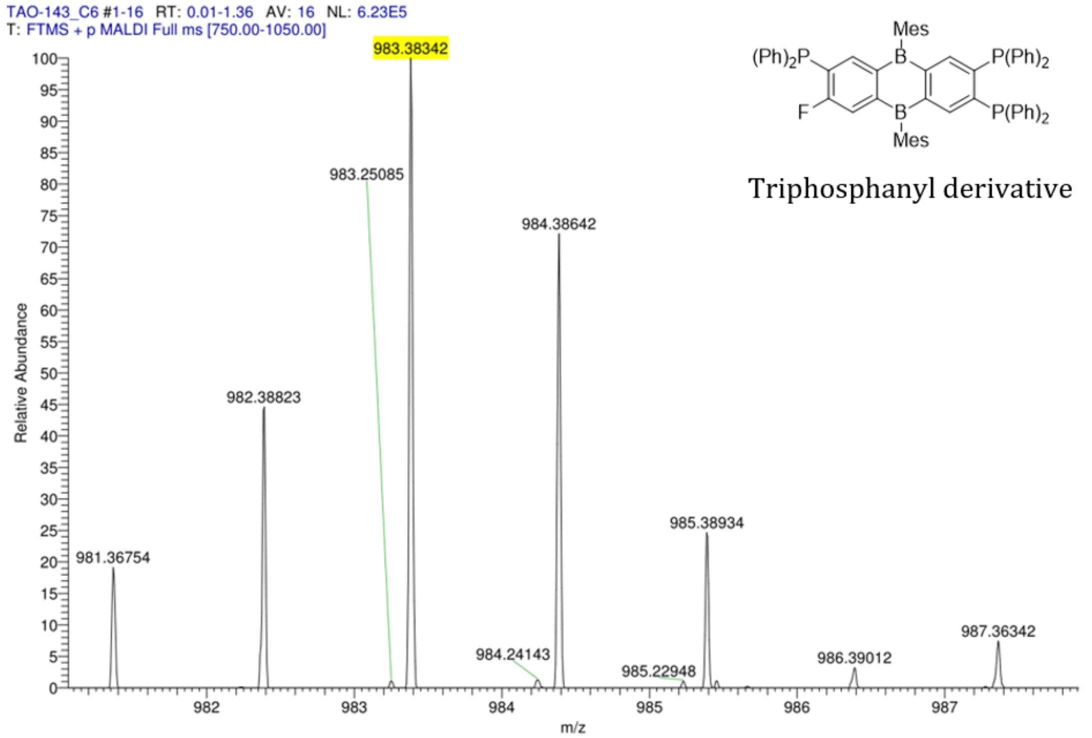

Figure S46: HRMS of the triphosphanyl derivative (Calculated *m/z* for $[C_{66}H_{57}B_2F_1P_3+H]^+$: 983.38378, found: 983.38342).

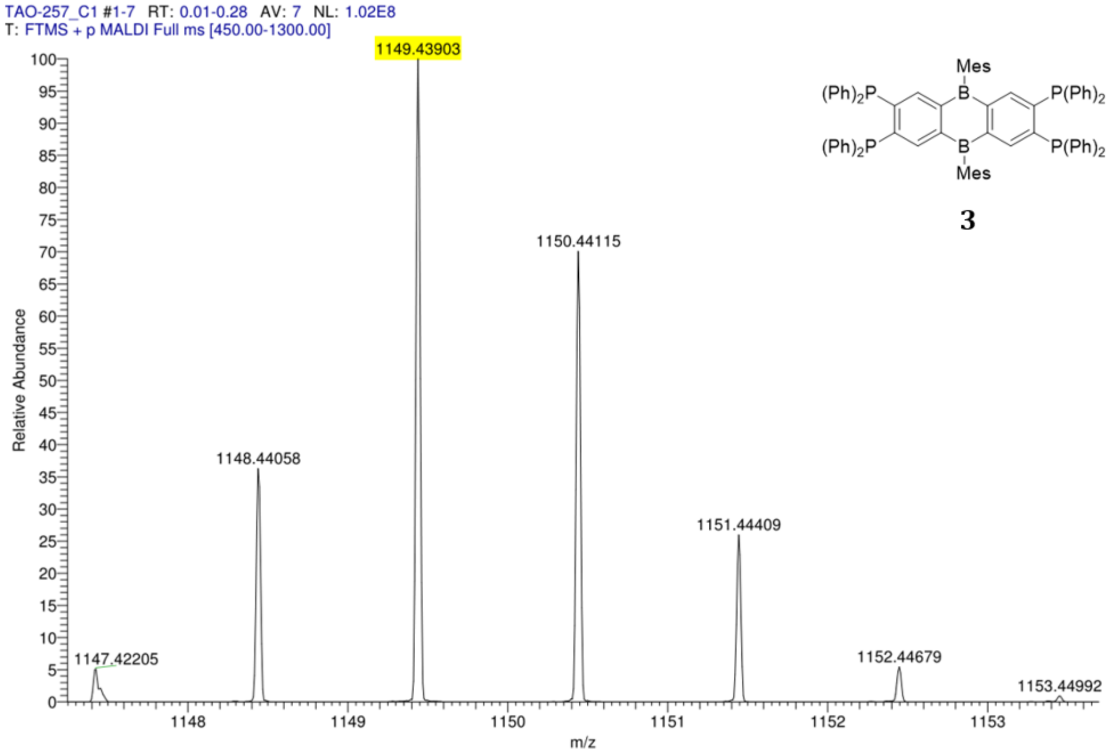

Figure S47: HRMS of the tetraphosphanyl derivative (**3**) (Calculated *m/z* for $[C_{78}H_{66}B_2P_4+H]^+$: 1149.43739, found: 1149.43903).

7. Photophysical and electrochemical data.

Table S1: Photophysical and electrochemical data of the compounds **1-8.** Optical measurements and electrochemical measurements were performed in CH_2Cl_2.

	λ_{abs} [nm][a] (ε [M^{-1} cm^{-1}])	λ_{abs} (tail) [nm][b]	λ_{ex} [nm]	λ_{em} [nm]	Φ_{PL} [%][c]	E_{LUMO} [eV][d]	$E_{1/2}$ [V]
1	257 (42700) 274 (sh) 360 (5700)	480	-	-	-	−3.17	−1.63
2	247 (43200) 290 (37500) 395 (16100)	480	-	-	-	−3.22	−1.58
3	258 (77600) 293 (78100) 330 (sh) 381 (sh)	525	-	-	-	−3.10	−1.70
4	266 (86000) 328 (sh) 338 (6800)	430	265 340[e] 340[f]	528 516[e] 543[f]	46 37[e] 18[f]	−3.28	−1.52
5	265 (89300) 343 (8200)	445	-	-	-	−3.37	−1.43
[**6**]OTf	267 (49100) 338 (4400)	480	267 267[g]	574 560[g]	11 7[g]	−3.56	−1.24
7	260 (58900) 374 (16200)	500	-	-	-	−3.47	−1.33
8	262 (121000) 298 (sh) 371 (19000)	520	-	-	-	−3.57	−1.23

[a] Resolved vibrational fine structure. [b] The approximate wavelength at the end of the tail of the absorption. [c] Quantum yields were determined by using a calibrated integrating sphere. [d] E_{LUMO} = −4.8 eV−$E_{1/2}^{Red}$ (FcH/FcH^{+} = −4.8 eV vs vacuum level). [e] Measurements were performed in C_6H_6. [f] Measurements were performed in THF. [g] Measurements were performed in $CHCl_3$. sh = shoulder.

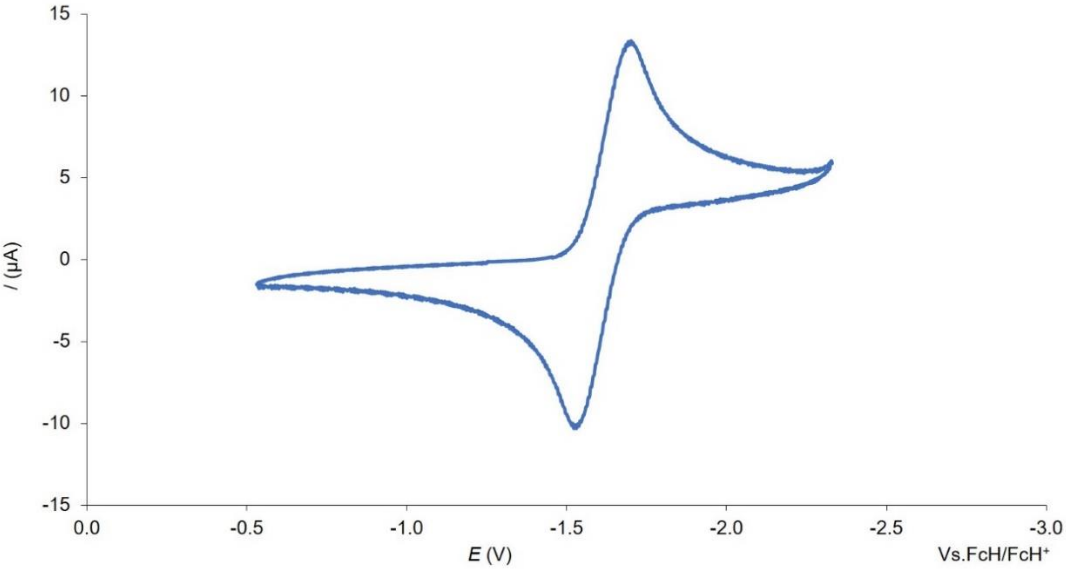

Figure S48: Cyclic voltammogram of **1** (cathodic part only; switching potentials: –0.5 to –2.4 V) in CH_2Cl_2 (room temperature, supporting electrolyte: $[n\mathrm{Bu}_4\mathrm{N}][\mathrm{PF}_6]$ (0.1 M), scan rate: 200 mV s^{-1}).

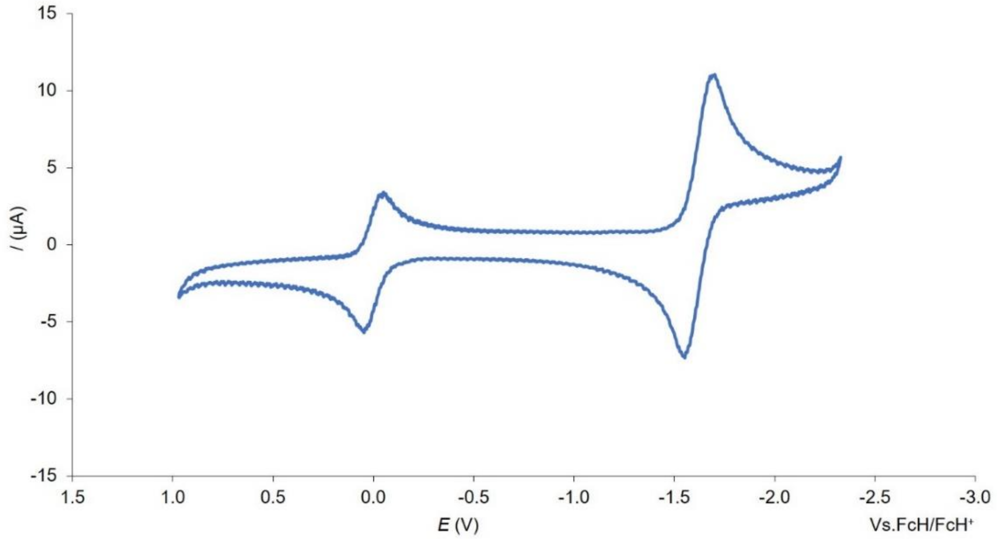

Figure S49: Cyclic voltammogram of **1** in CH_2Cl_2 (room temperature, supporting electrolyte: $[n\mathrm{Bu}_4\mathrm{N}][\mathrm{PF}_6]$ (0.1 M), scan rate: 200 mV s^{-1}).

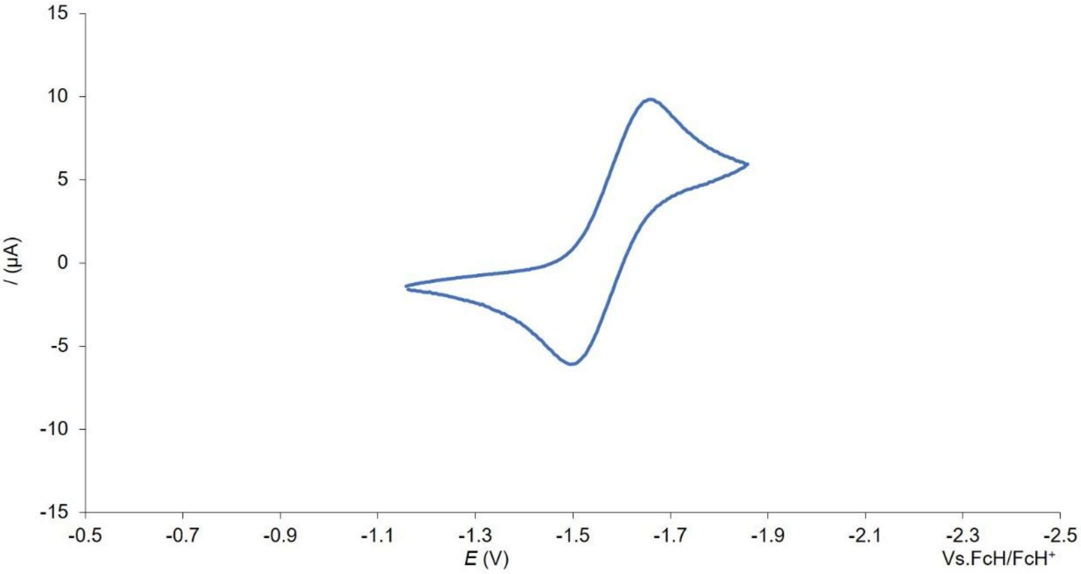

Figure S50: Cyclic voltammogram of **2** (cathodic part only; switching potentials: −1.1 to −1.9 V) in CH_2Cl_2 (room temperature, supporting electrolyte: $[n\text{Bu}_4\text{N}][\text{PF}_6]$ (0.1 M), scan rate: 200 mV s^{-1}).

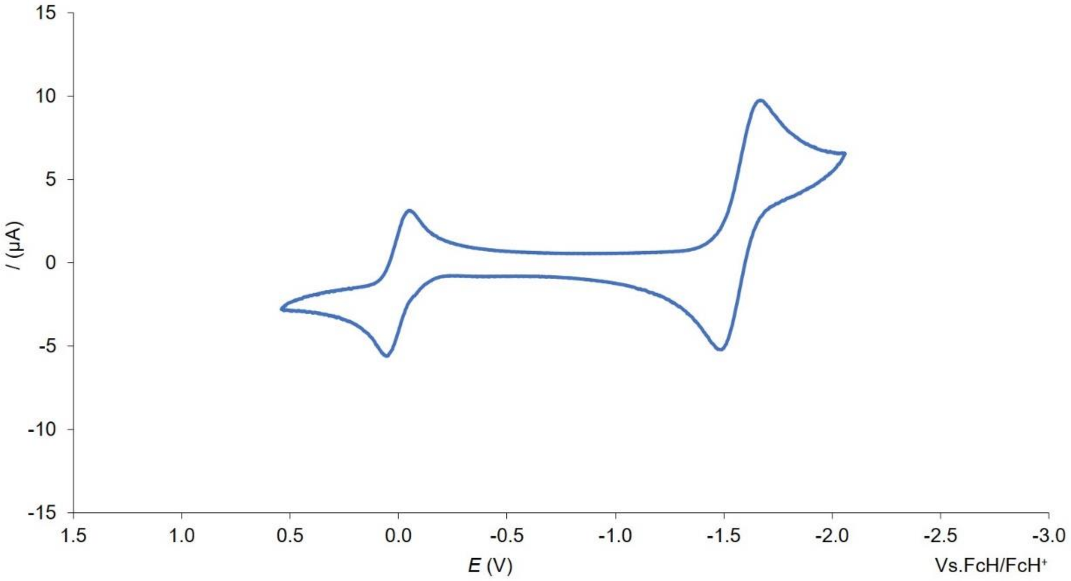

Figure S51: Cyclic voltammogram of **2** in CH_2Cl_2 (room temperature, supporting electrolyte: $[n\text{Bu}_4\text{N}][\text{PF}_6]$ (0.1 M), scan rate: 200 mV s^{-1}).

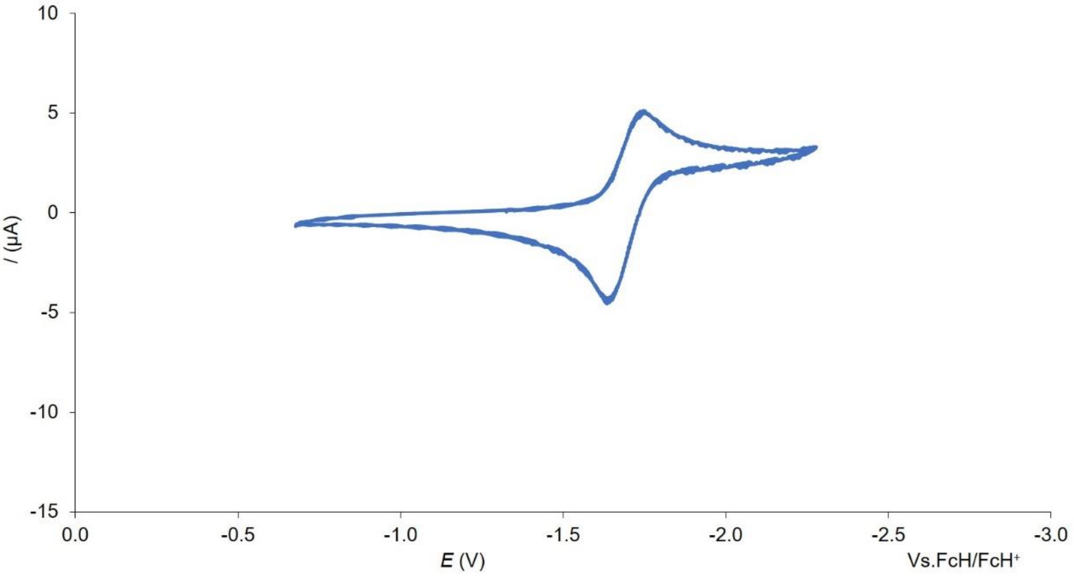

Figure S52: Cyclic voltammogram of **3** (cathodic part only; switching potentials: −0.7 to −2.3 V) in CH_2Cl_2 (room temperature, supporting electrolyte: [*n*Bu_4N][PF_6] (0.1 M), scan rate: 200 mV s^{-1}).

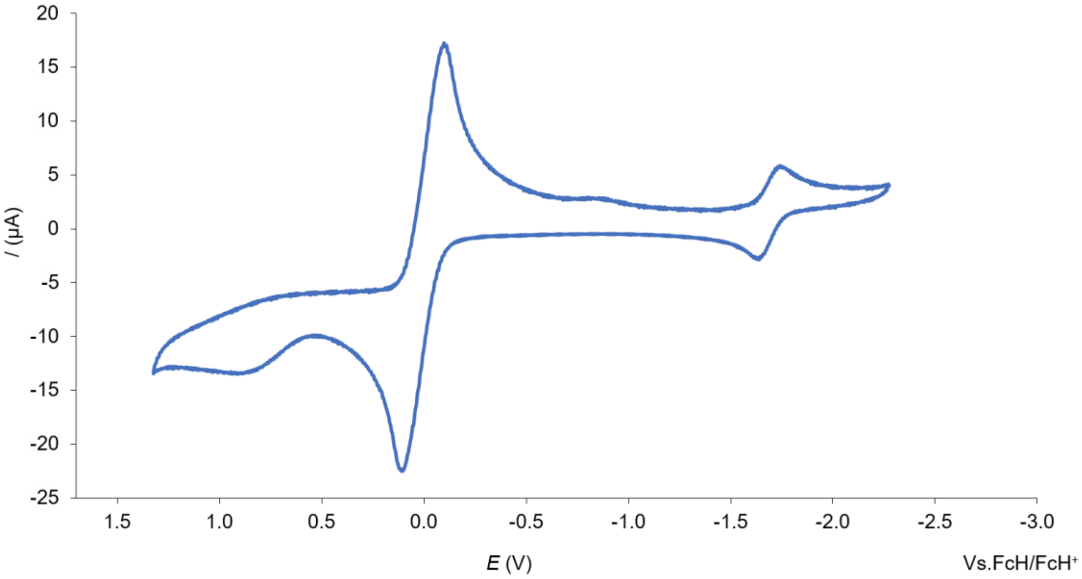

Figure S53: Cyclic voltammogram of **3** in CH_2Cl_2 (room temperature, supporting electrolyte: [*n*Bu_4N][PF_6] (0.1 M), scan rate: 200 mV s^{-1}).

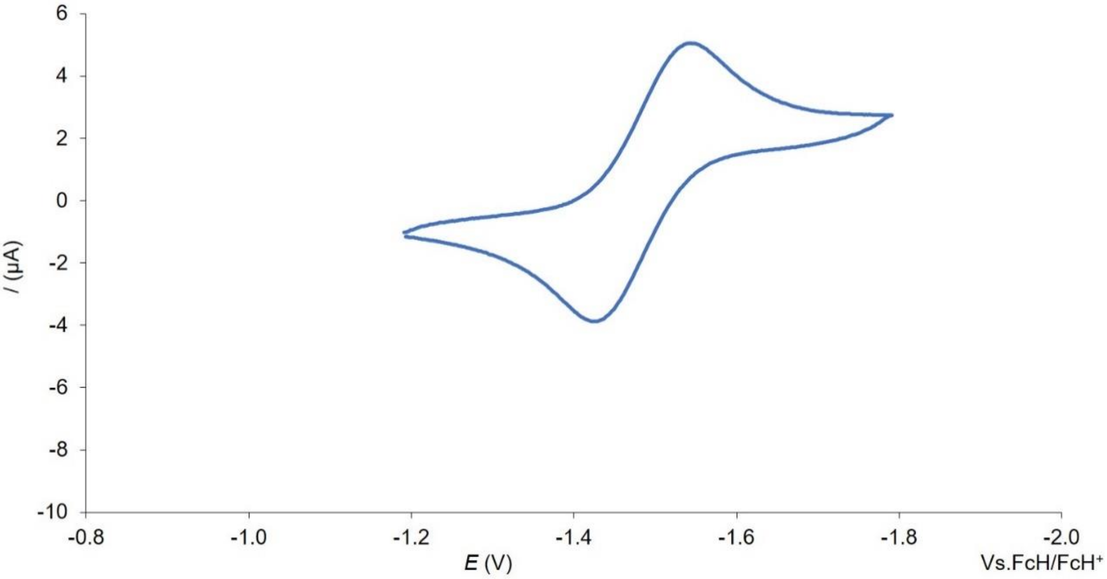

Figure S54: Cyclic voltammogram of **4** (cathodic part only; switching potentials: −1.2 to −1.8 V) in CH_2Cl_2 (room temperature, supporting electrolyte: [*n*Bu_4N][PF_6] (0.1 M), scan rate: 200 mV s^{-1}).

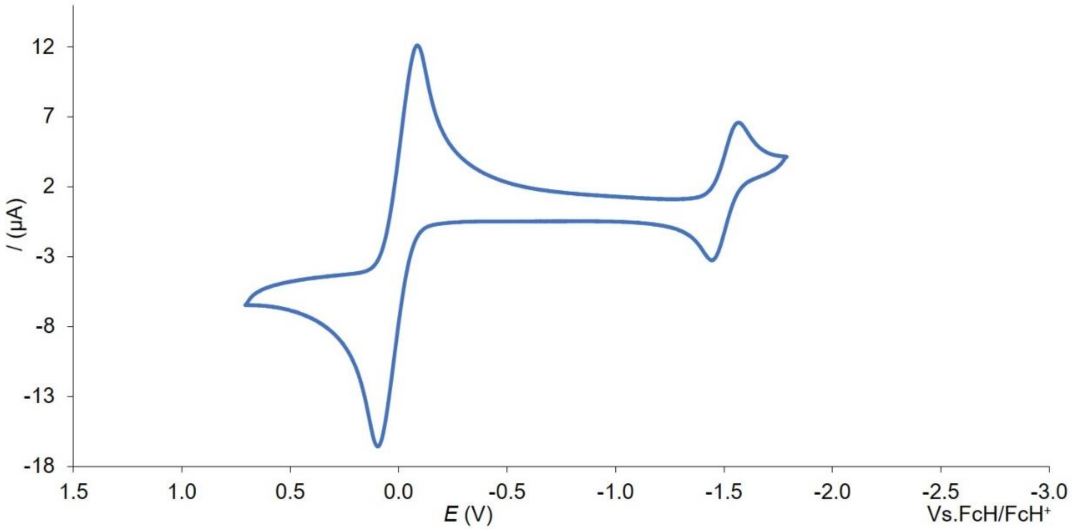

Figure S55: Cyclic voltammogram of **4** in CH_2Cl_2 (room temperature, supporting electrolyte: [*n*Bu_4N][PF_6] (0.1 M), scan rate: 200 mV s^{-1}).

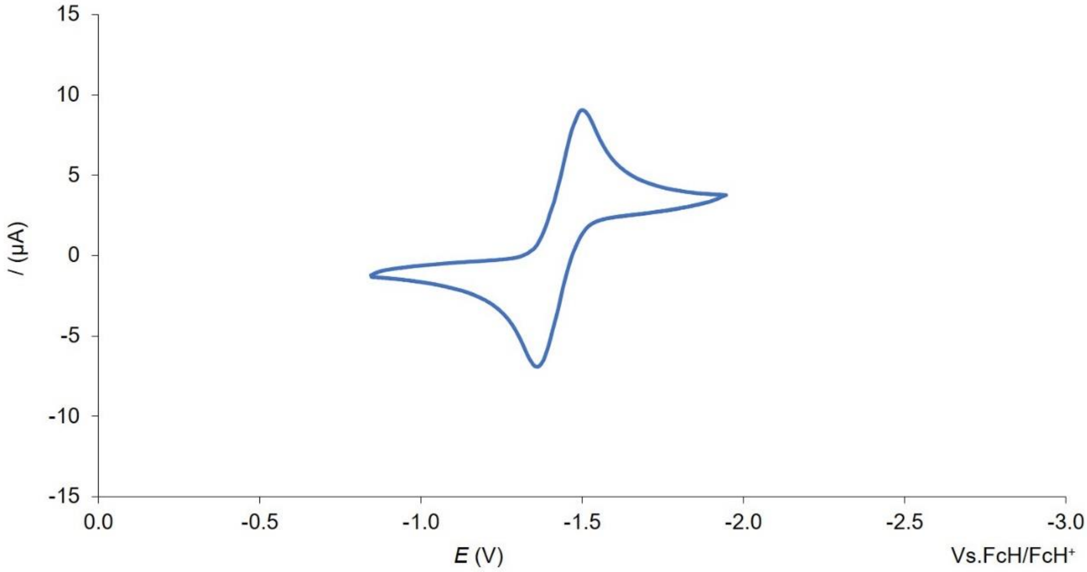

Figure S56: Cyclic voltammogram of **5** (cathodic part only; switching potentials: –0.8 to –1.9 V) in CH_2Cl_2 (room temperature, supporting electrolyte: [*n*Bu_4N][PF_6] (0.1 M), scan rate: 200 mV s^{-1}).

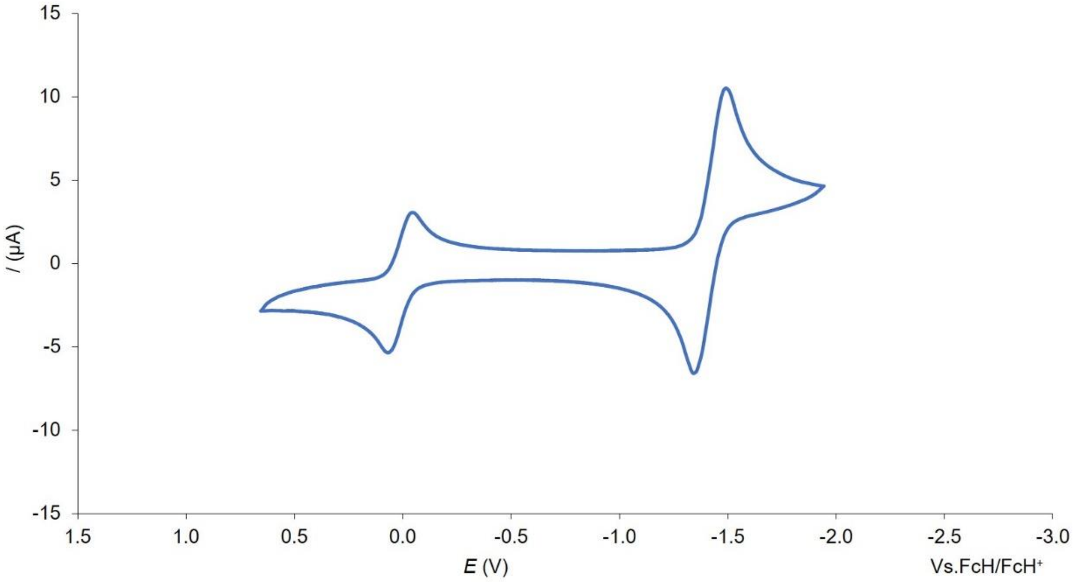

Figure S57: Cyclic voltammogram of **5** in CH_2Cl_2 (room temperature, supporting electrolyte: [*n*Bu_4N][PF_6] (0.1 M), scan rate: 200 mV s^{-1}).

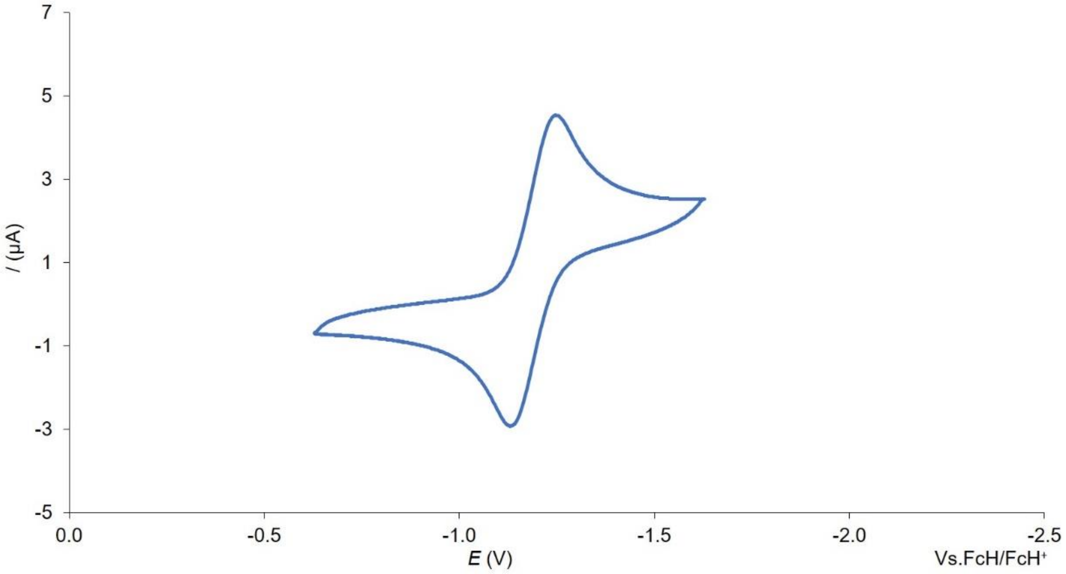

Figure S58: Cyclic voltammogram of [**6**]OTf (cathodic part only; switching potentials: −0.6 to −1.6 V) in CH_2Cl_2 (room temperature, supporting electrolyte: [*n*Bu_4N][PF_6] (0.1 M), scan rate: 200 mV s^{-1}).

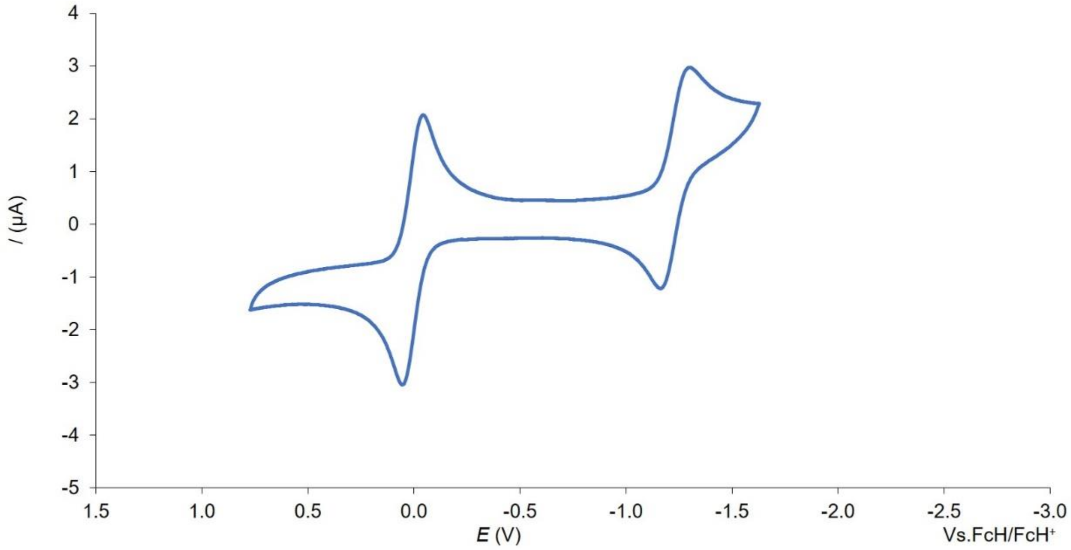

Figure S59: Cyclic voltammogram of [**6**]OTf in CH_2Cl_2 (room temperature, supporting electrolyte: [*n*Bu_4N][PF_6] (0.1 M), scan rate: 200 mV s^{-1}).

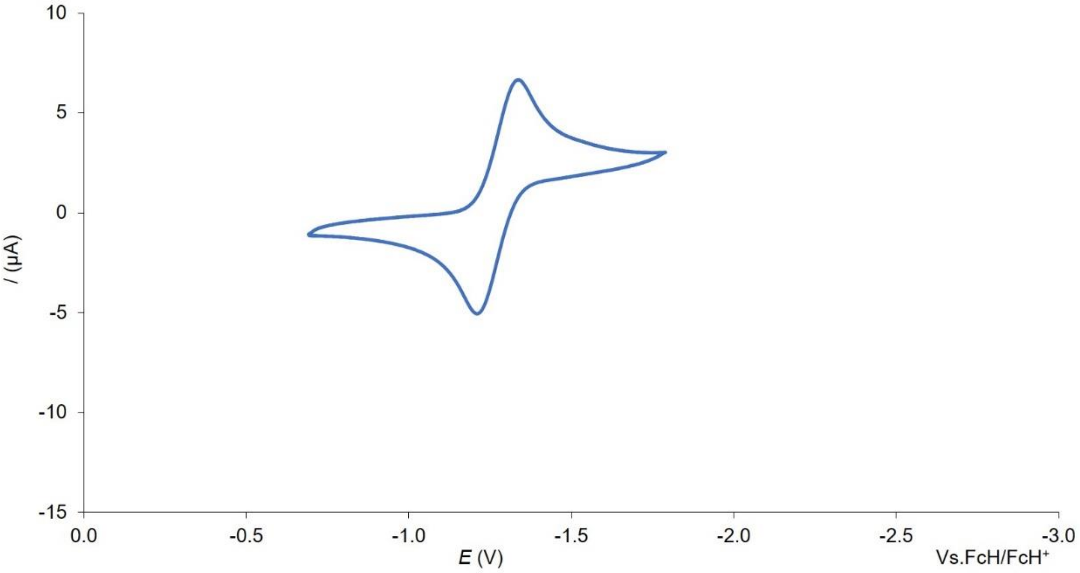

Figure S60: Cyclic voltammogram of **7** (cathodic part only; switching potential: −0.7 to −1.8 V) in CH_2Cl_2 (room temperature, supporting electrolyte: $[n\mathrm{Bu}_4\mathrm{N}][\mathrm{PF}_6]$ (0.1 M), scan rate: 200 mV s^{-1}).

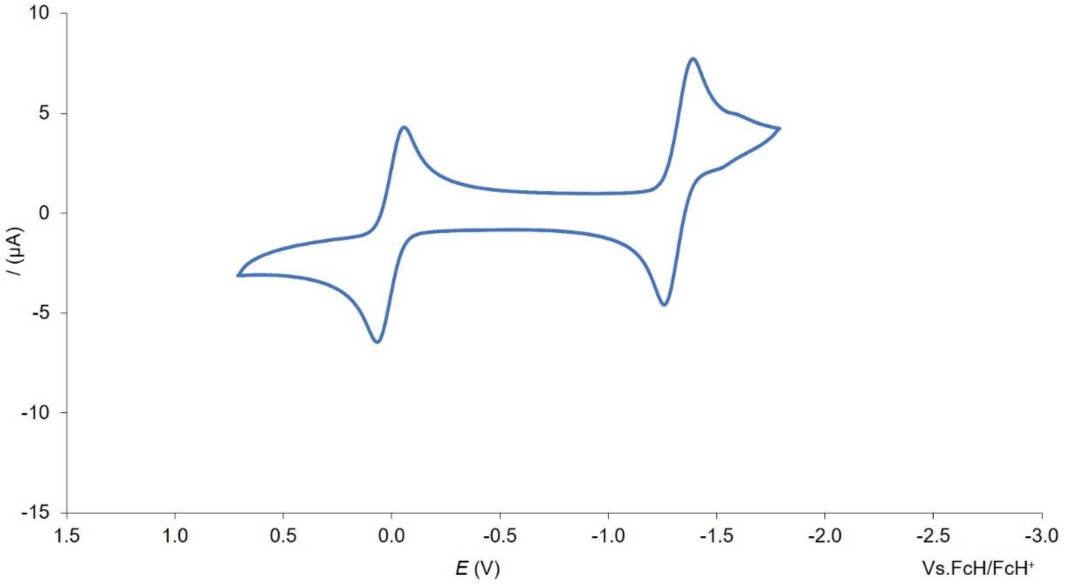

Figure S61: Cyclic voltammogram of **7** in CH_2Cl_2 (room temperature, supporting electrolyte: $[n\mathrm{Bu}_4\mathrm{N}][\mathrm{PF}_6]$ (0.1 M), scan rate: 200 mV s^{-1}).

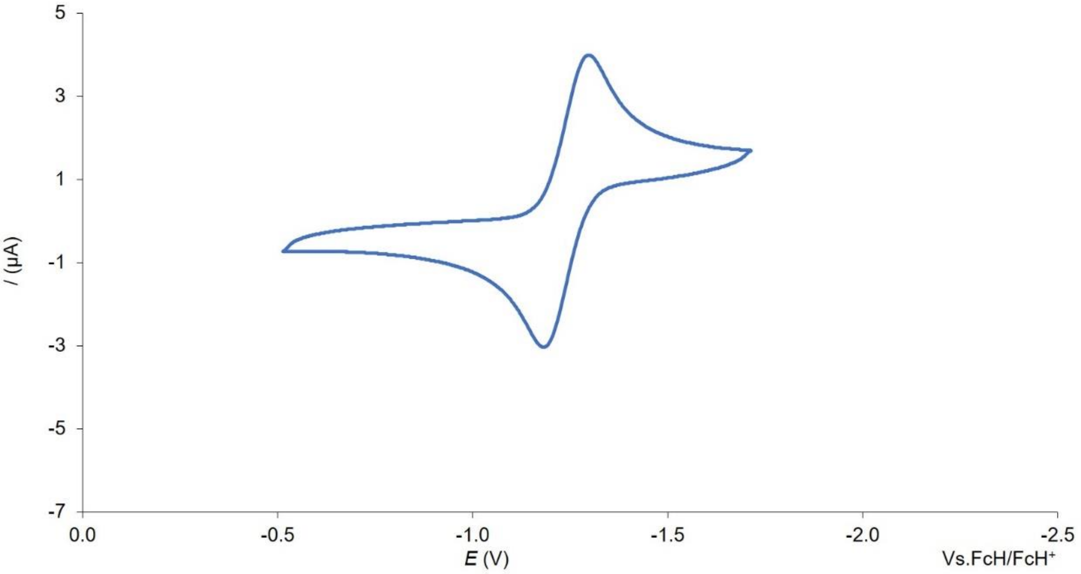

Figure S62: Cyclic voltammogram of **8** (cathodic part only; switching potentials: −0.5 to −1.7 V) in CH_2Cl_2 (room temperature, supporting electrolyte: [*n*Bu_4N][PF_6] (0.1 M), scan rate: 200 mV s^{-1}).

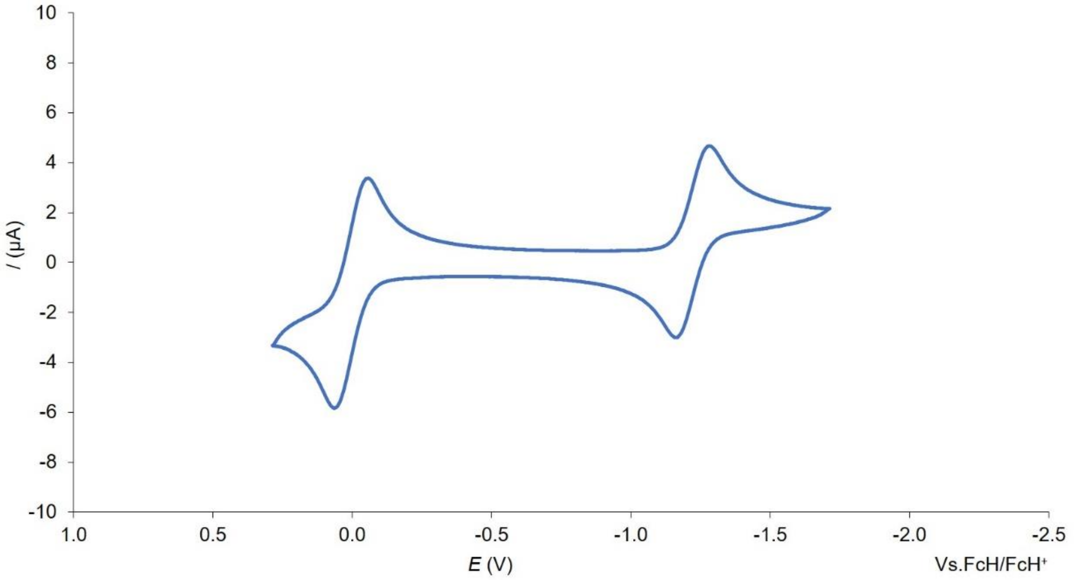

Figure S63: Cyclic voltammogram of **8** in CH_2Cl_2 (room temperature, supporting electrolyte: [*n*Bu_4N][PF_6] (0.1 M), scan rate: 200 mV s^{-1}).

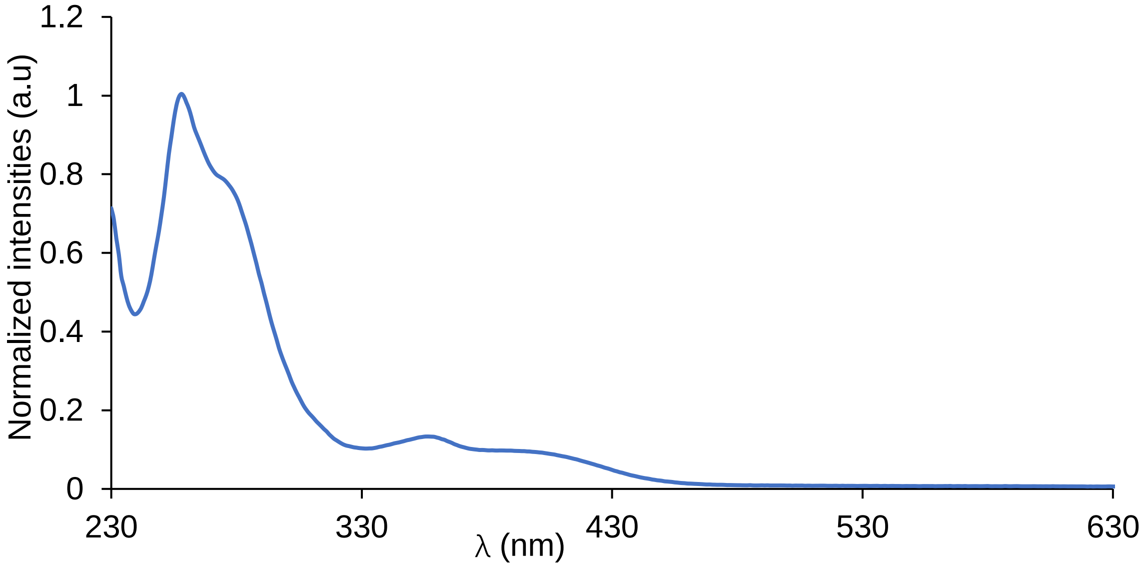

Figure S64: Normalized UV/Vis absorption spectrum of **1** in CH_2Cl_2.

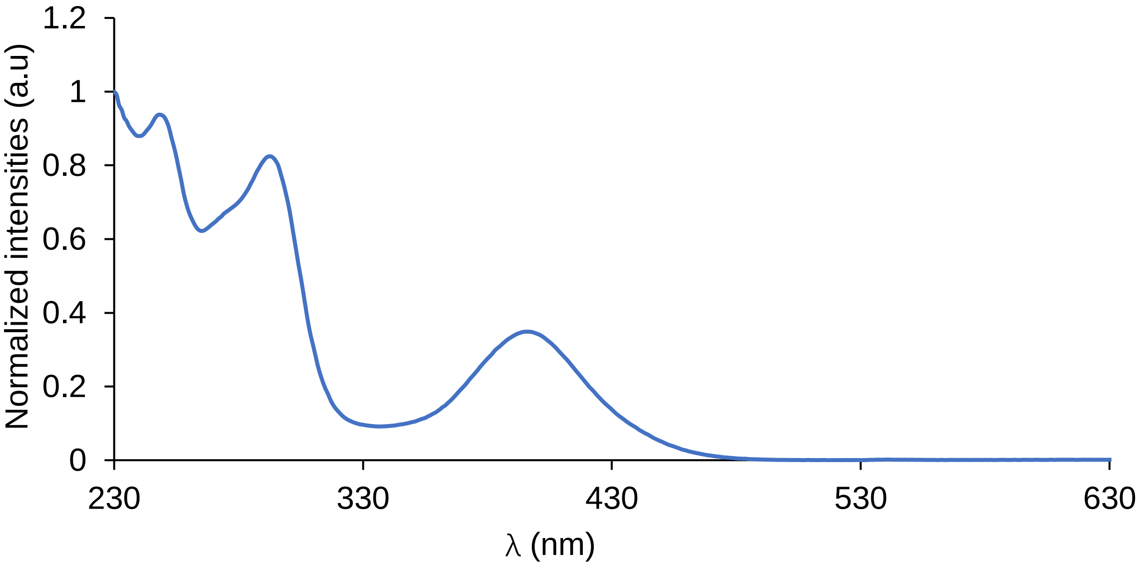

Figure S65: Normalized UV/Vis absorption spectrum of **2** in CH_2Cl_2.

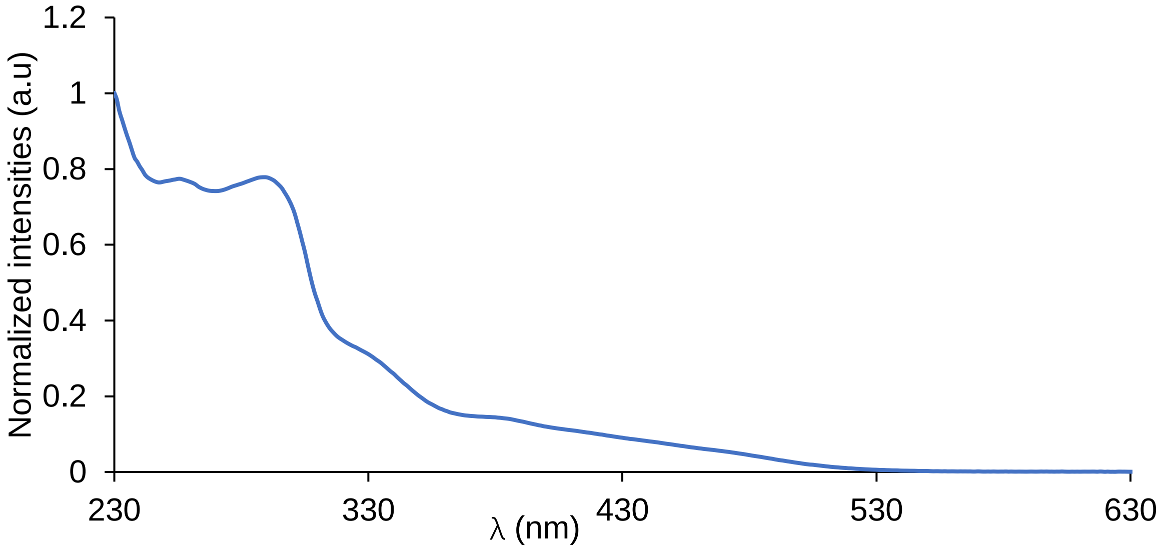

Figure S66: Normalized UV/Vis absorption spectrum of **3** in CH_2Cl_2.

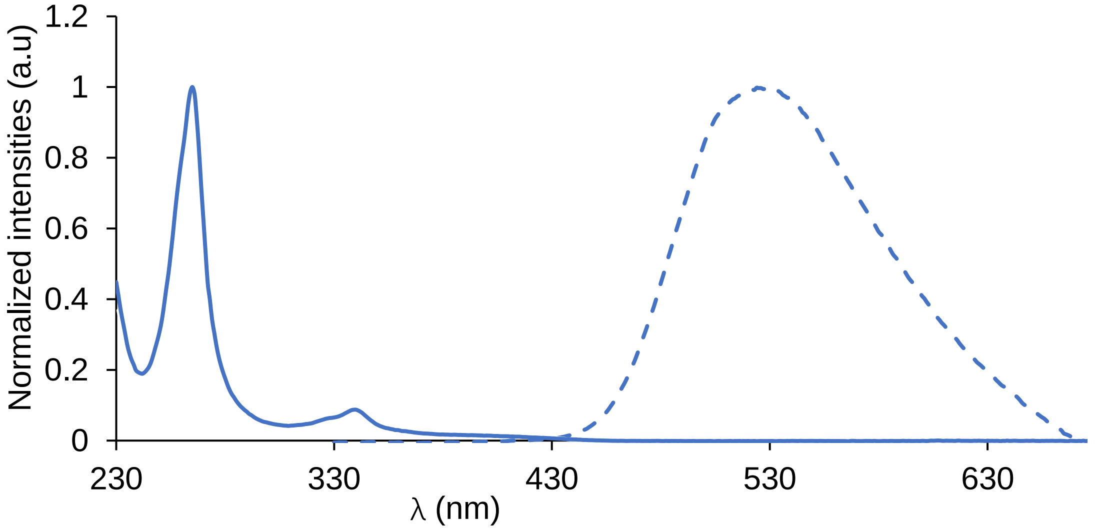

Figure S67: Normalized UV/Vis absorption and emission spectra of **4** in CH_2Cl_2.

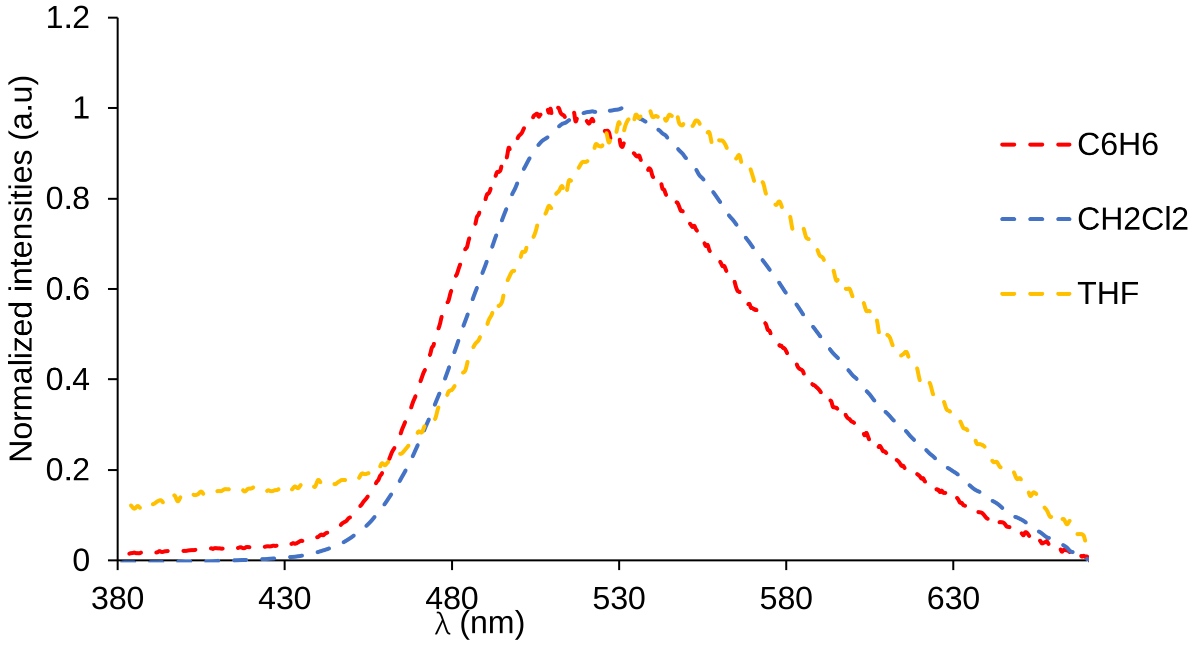

Figure S68: Normalized emission spectra of **4** in C_6H_6 (red curve; λ_{ex} = 340 nm), CH_2Cl_2 (blue curve; λ_{ex} = 265 nm), and THF (yellow curve; λ_{ex} = 340 nm).

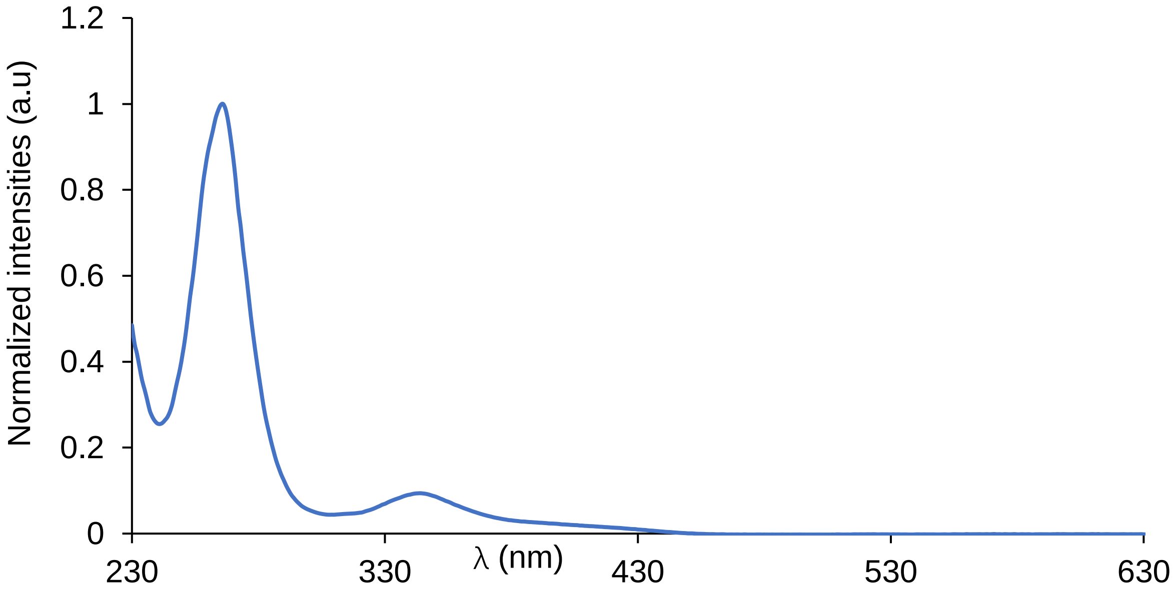

Figure S69: Normalized UV/Vis absorption spectrum of **5** in CH_2Cl_2.

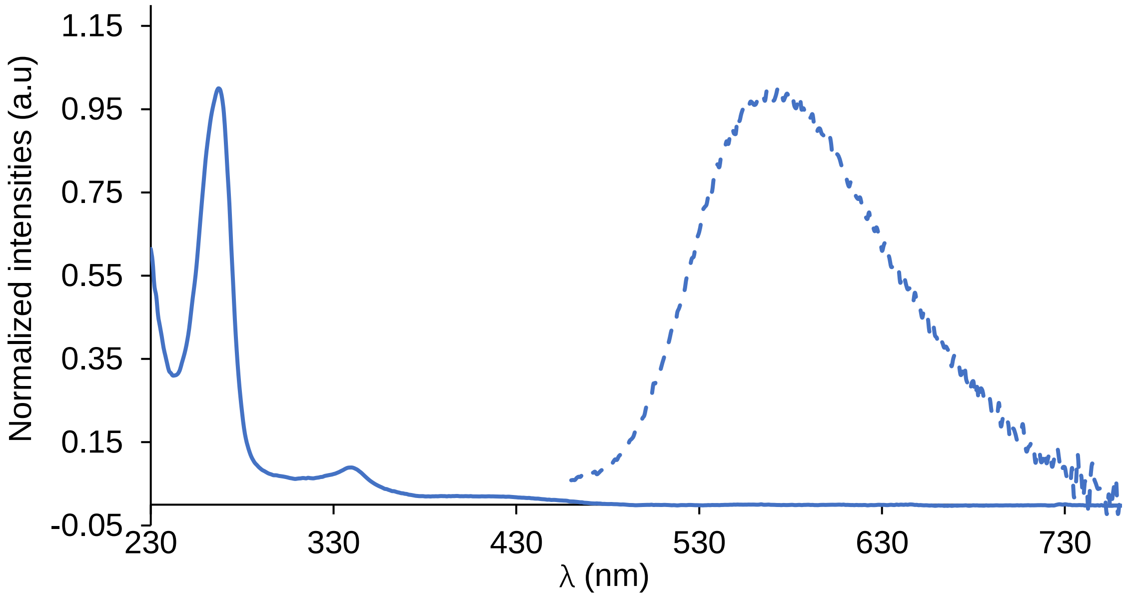

Figure S70: Normalized UV/Vis absorption and emission spectra of [**6**]OTf in CH_2Cl_2.

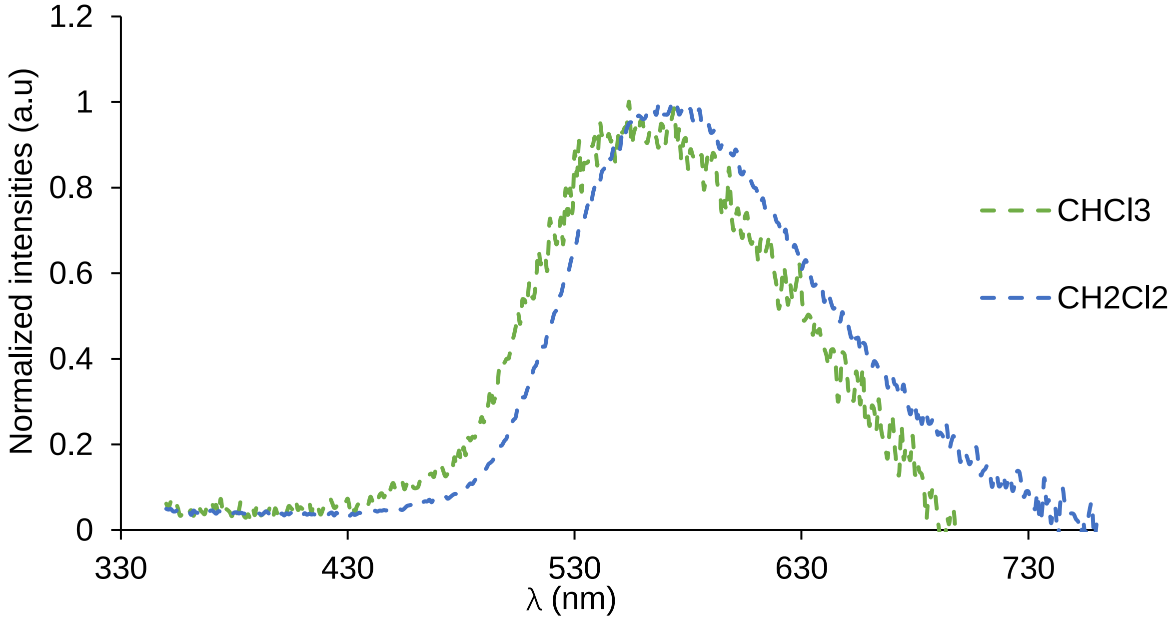

Figure S71: Normalized emission spectra of [**6**]OTf in $CHCl_3$ (green curve; λ_{ex} = 267 nm) and CH_2Cl_2 (blue curve; λ_{ex} = 267 nm).

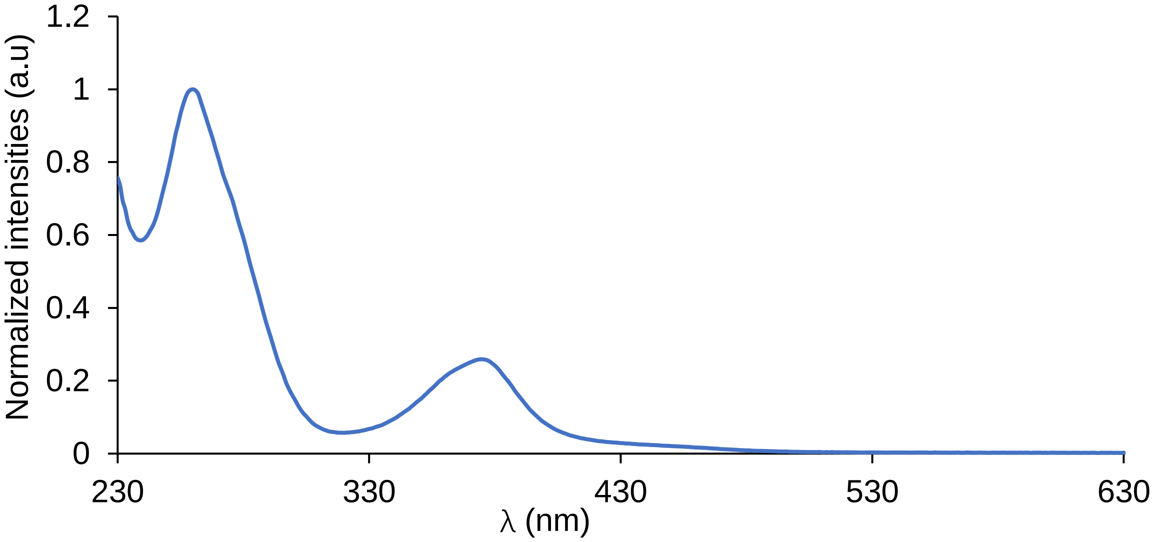

Figure S72: Normalized UV/Vis absorption spectrum of **7** in CH_2Cl_2.

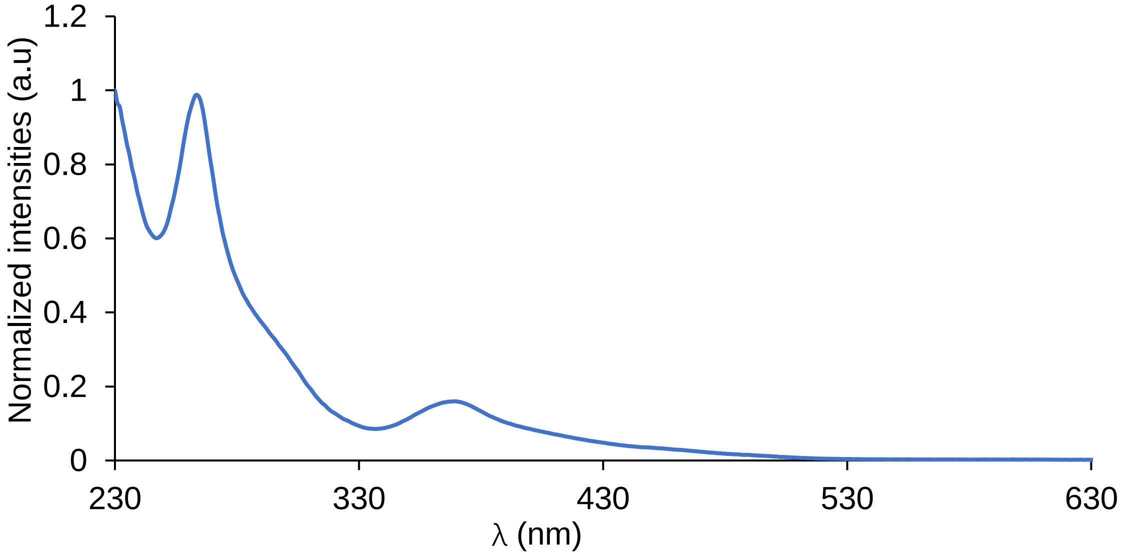

Figure S73: Normalized UV/Vis absorption spectrum of **8** in CH_2Cl_2.

8. X-ray crystal structure analyses

Crystal structure determinations. Data for all structures were collected on a STOE IPDS II two-circle diffractometer with a Genix Microfocus tube with mirror optics using MoK_α radiation (λ = 0.71073 Å). The data were scaled using the frame scaling procedure in the *X-AREA* program system (Stoe & Cie, 2002). The structures were solved by direct methods using the program *SHELXS* (Sheldrick, 2008) and refined against F^2 with full-matrix least-squares techniques using the program *SHELXL* (Sheldrick, 2008).[S7,S8]

In **1 (CCDC 2176264)**, the H atoms of one methyl group are disordered over two equally occupied positions.

2 (CCDC 2176266) crystallizes with half a molecule (located on a center of inversion) and one molecule of dichloromethane in the asymmetric unit.

3 (CCDC 2176265) crystallizes with half a molecule (located on a center of inversion) in the asymmetric unit.

For **8 (CCDC 2176267)**, no further remarks are necessary.

The cation of [**10**](OTf)$_2$ **(CCDC 2176268)** is located on a center of inversion.

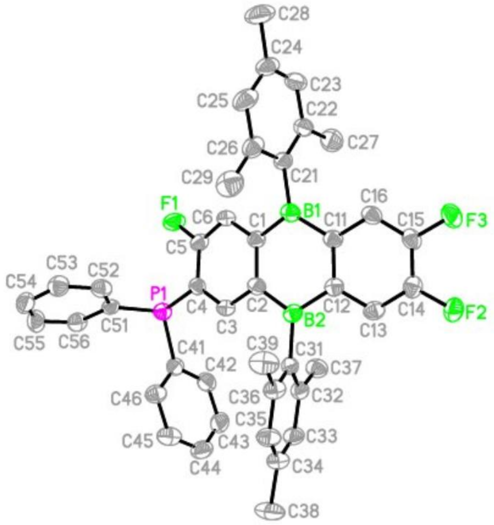

Figure S74: (CCDC 2176264): Molecular structure of **1** in the solid state. Displacement ellipsoids are drawn at the 50 % probability level; hydrogen atoms are omitted to clarity. Selected bond lengths (Å) and bond angles (°): B(1)-C(1) = 1.563(5), B(1)-C(11) = 1.572(5), B(1)-C(21) = 1.576(5), B(2)-C(2) = 1.555(5), B(2)-C(12) = 1.561(5), B(2)-C(31) = 1.572(5), F(1)-C(5) = 1.358(3), F(2)-C(14) = 1.351(4), F(3)-C(15) = 1.358(4), P(1)-C(4) = 1.841(3), P(1)-C(41) = 1.837(3), P(1)-C(51) = 1.831(3); C(1)-B(1)-C(11) = 118.1(3), C(1)-B(1)-C(21) = 120.9(3), C(11)-B(1)-C(21) = 121.0(3), C(2)-B(2)-C(12) = 118.2(3), C(2)-B(2)-C(31) = 120.5(3), C(12)-B(2)-C(31) = 121.3(3), F(1)-C(5)-C(4) = 117.3(3), F(1)-C(5)-C(6) = 118.4(3), F(2)-C(14)-C(13) = 121.0(3), F(2)-C(14)-C(15) = 118.6(3), F(3)-C(15)-C(16) = 120.4(3), F(3)-C(15)-C(14) = 118.6(3), C(4)-P(1)-C(41) = 100.2(2), C(4)-P(1)-C(51) = 101.8 (2), C(41)-P(1)-C(51) = 102.1(2).

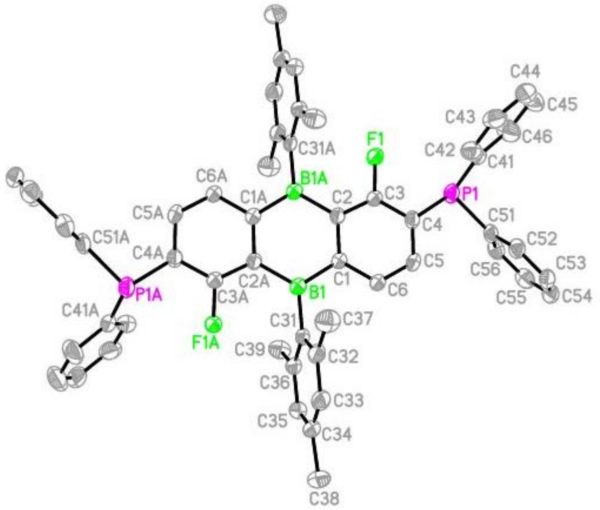

Figure S75: (CCDC 2176266): Molecular structure of **2** in the solid state. Displacement ellipsoids are drawn at the 50 % probability level; hydrogen atoms are omitted to clarity. Selected bond lengths (Å) and bond angles (°): B(1)-C(1) = 1.569(4), B(1)-C(2A) = 1.565(4), B(1)-C(31) = 1.582(4), F(1)-C(3) = 1.365(3), P(1)-C(4) = 1.841(3), P(1)-C(41) = 1.831(4), P(1)-C(51) = 1.834(3); C(1)-B(1)-C(2A) = 118.3(2), C(1)-B(1)-C(31) = 118.9(2), C(2A)-B(1)-C(31) = 122.8(2), F(1)-C(3)-C(2) = 119.0(2), F(1)-C(3)-C(4) = 114.8(2), C(4)-P(1)-C(41) = 103.9(2), C(4)-P(1)-C(51) = 101.6(2), C(41)-P(1)-C(51) = 101.3(2). Symmetry transformations used to generate equivalent atoms: A, –x+1/2, –y+3/2, –z+1.

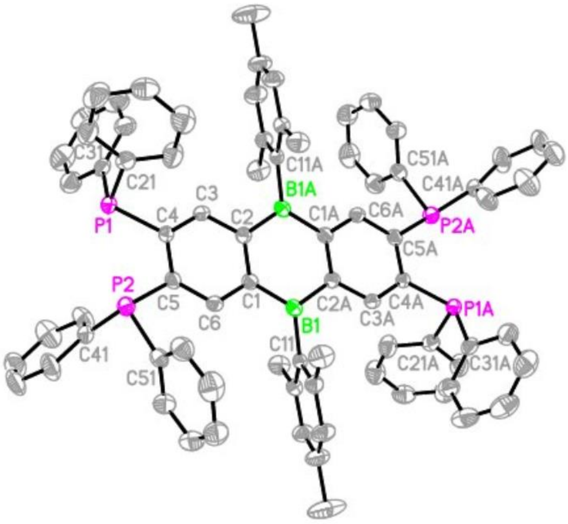

Figure S76: (CCDC 2176265): Molecular structure of **3** in the solid state. Displacement ellipsoids are drawn at the 50 % probability level; hydrogen atoms are omitted to clarity. Selected bond lengths (Å) and bond angles (°): B(1)-C(1) = 1.561(3), B(1)-C(2A) = 1.575(3), B(1)-C(11) = 1.572(3), P(1)-C(4) = 1.850(2), P(1)-C(21) = 1.831(2), P(1)-C(31) = 1.840(2), P(2)-C(5) = 1.854(2), P(2)-C(41) = 1.837(3), P(2)-C(51) = 1.832(2); C(1)-B(1)-C(2A) = 118.6(2), C(1)-B(1)-C(11) = 123.0(2), C(2A)-B(1)-C(1) = 118.6(2), C(4)-P(1)-C(21) = 101.5(1), C(4)-P(1)-C(31) = 102.8 (1), C(21)-P(1)-C(31) = 102.2(2), C(5)-P(2)-C(41) = 102.7(2), C(5)-P(2)-C(51) = 101.7(1), C(41)-P(2)-C(51) = 104.8(2). Symmetry transformations used to generate equivalent atoms:

A, –x+2, –y+1, –z+1.

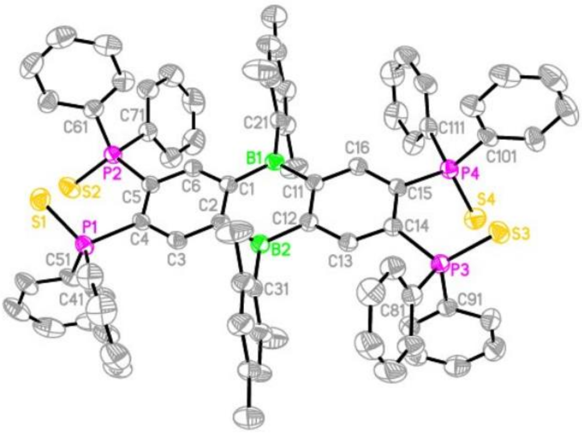

Figure S77: (CCDC 2176267): Molecular structure of **8** in the solid state. Displacement ellipsoids are drawn at the 50 % probability level; hydrogen atoms are omitted to clarity. Selected bond lengths (Å) and bond angles (°): B(1)-C(1) = 1.569(4), B(1)-C(11) = 1.560(3), B(1)-C(21) = 1.566(3), B(2)-C(2) = 1.560(3), B(2)-C(12) = 1.572(3), B(2)-C(31) = 1.573(3), P(1)-C(4) = 1.852(2), P(1)-C(41) = 1.826(3), P(1)-C(51) = 1.820(3), P(1)-S(1) = 1.940(1), P(2)-C(5) = 1.845(2), P(2)-C(61) = 1.818(3), P(2)-C(71) = 1.824(2), P(2)-S(2) = 1.938(1), P(3)-C(14) = 1.847(2), P(3)-C(81) = 1.828(2), P(3)-C(91) = 1.819(3), P(3)-S(3) = 1.942(1), P(4)-C(15) = 1.850(2), P(4)-C(101) = 1.815(3), P(4)-C(111) = 1.826(2), P(4)-S(4) = 1.946(1); C(1)-B(1)-C(11) = 117.1(2), C(1)-B(1)-C(21) = 118.7(2), C(11)-B(1)-C(21) = 124.2(2), C(2)-B(2)-C(12) = 117.4(2), C(2)-B(2)-C(31) = 123.3(2), C(12)-B(2)-C(31) = 119.3(2), C(4)-P(1)-C(41) = 103.4(2), C(4)-P(1)-C(51) = 108.2 (2), C(41)-P(1)-C(51) = 103.0(2), C(5)-P(2)-C(61) = 103.6(2), C(5)-P(2)-C(71) = 103.7(2), C(61)-P(2)-C(71) = 105.4(2), C(14)-P(3)-C(81) = 103.2(2), C(14)-P(3)-C(91) = 104.2(2), C(81)-P(3)-C(91) = 104.9(2), C(15)-P(4)-C(101) = 111.7(2), C(15)-P(4)-C(111) = 103.1(2), C(101)-P(4)-C(111) = 103.1(2), S(1)-P(1)-C(4) = 112.3(1), S(1)-P(1)-C(41) = 111.8(1), S(1)-P(1)-C(51) = 116.9(1), S(2)-P(2)-C(5) = 116.8(1), S(2)-P(2)-C(61) = 116.1(1), S(2)-P(2)-C(71) = 110.0(1), S(3)-P(3)-C(14) = 116.7(1), S(3)-P(3)-C(81) = 111.0(1), S(3)-P(3)-C(91) = 115.5(1), S(4)-P(4)-C(15) = 110.1(1), S(4)-P(4)-C(101) = 115.9(1), S(4)-P(4)-C(111) = 112.1(1).

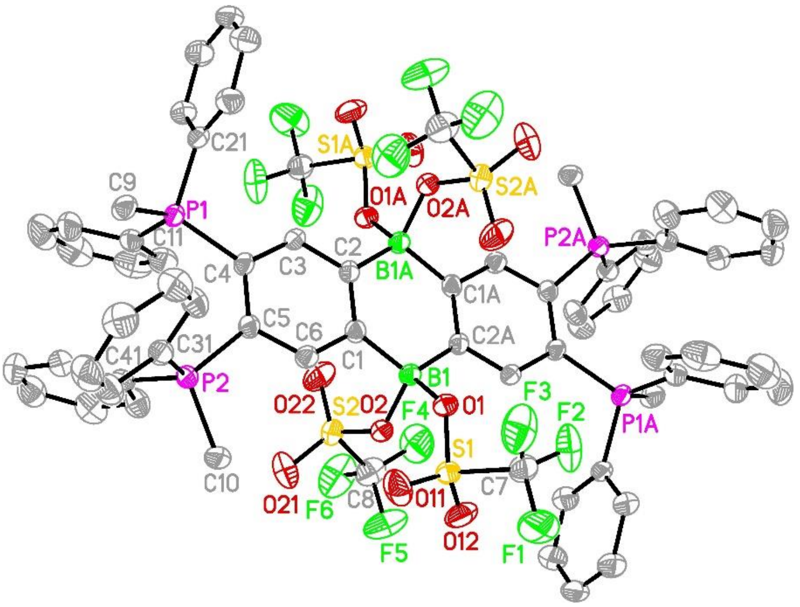

Figure S78: (CCDC 2176268): Molecular structure of $[\mathbf{10}](\mathrm{OTf})_2$ in the solid state. Displacement ellipsoids are drawn at the 50% probability level; hydrogen atoms are omitted for clarity. Selected bond lengths (Å) and bond angles (°): B(1)-C(1) = 1.603(5), B(1)-C(2A) = 1.601(5), B(1)-O(1) = 1.544(4), B(1)-O(2) = 1.558(4), P(1)-C(4) = 1.25(3), P(1)-C(9) = 1.791(3), P(1)-C(11) = 1.784(4), P(1)-C(21) = 1.806(3), P(2)-C(5) = 1.18(3), P(2)-C(10) = 1.800(3), P(2)-C(31) = 1.798(4), P(2)-C(41) = 1.792(4); C(1)-B(1)-C(2A) = 116.3(3), C(1)-B(1)-O(1) = 110.9(3), C(1)-B(1)-O(2) = 108.3(2), C(2A)-B(1)-O(1) = 107.8(3), C(2A)-B(1)-O(2) = 111.0(3), C(4)-P(1)-C(9) = 114.9(1), C(4)-P(1)-C(11) = 109.9(3), C(4)-P(1)-C(21) = 108.5(1), C(9)-P(1)-C(11) = 111.9(1), C(9)-P(1)-C(21) = 105.1(3), C(5)-P(2)-C(10) = 109.2(3), C(5)-P(2)-C(31) = 112.7(7), C(5)-P(2)-C(41) = 109.9(3), C(10)-P(2)-C(31) = 105.8(2), C(10)-P(2)-C(41) = 109.9(3). Symmetry transformations used to generate equivalent atoms: A, -x+1, -y+1, -z+1

Table S2: Crystal data and structure refinement for **1.**

CCDC	2176264	
Empirical formula	$C_{42} H_{36} B_2 F_3 P$	
Formula weight	650.30	
Temperature	173(2) K	
Wavelength	0.71073 Å	
Crystal system	Monoclinic	
Space group	$P\,2_1/n$	
Unit cell dimensions	a = 10.6718(5) Å	α= 90°.
	b = 17.6291(9) Å	β= 105.422(4)°.
	c = 19.0191(9) Å	γ = 90°.
Volume	3449.3(3) $Å^3$	
Z	4	
Density (calculated)	1.252 Mg/m^3	
Absorption coefficient	0.126 mm^{-1}	
F(000)	1360	
Crystal color, shape	yellow plate	
Crystal size	0.310 x 0.200 x 0.110 mm^3	
Theta range for data collection	3.395 to 25.630°.	
Index ranges	-12<=h<=12, -21<=k<=21, -23<=l<=23	
Reflections collected	32564	
Independent reflections	6461 [R(int) = 0.0547]	
Completeness to theta = 25.000°	99.8 %	
Absorption correction	Semi-empirical from equivalents	
Max. and min. transmission	1.000 and 0.487	
Refinement method	Full-matrix least-squares on F^2	
Data / restraints / parameters	6461 / 0 / 439	
Goodness-of-fit on F^2	1.246	
Final R indices [I>2sigma(I)]	R1 = 0.0775, wR2 = 0.1202	
R indices (all data)	R1 = 0.1113, wR2 = 0.1305	
Largest diff. peak and hole	0.238 and -0.229 e.$Å^{-3}$	

Table S3: Crystal data and structure refinement for **2**.

CCDC	2176266	
Empirical formula	$C_{56} H_{50} B_2 Cl_4 F_2 P_2$	
Formula weight	986.32	
Temperature	173(2) K	
Wavelength	0.71073 Å	
Crystal system	Monoclinic	
Space group	*C* 2/*c*	
Unit cell dimensions	a = 25.3221(10) Å	α= 90°.
	b = 9.3948(3) Å	β= 92.156(3)°.
	c = 21.2159(9) Å	γ = 90°.
Volume	5043.6(3) $Å^3$	
Z	4	
Density (calculated)	1.299 Mg/m^3	
Absorption coefficient	0.343 mm^{-1}	
F(000)	2048	
Crystal color, shape	yellow block	
Crystal size	0.220 x 0.190 x 0.140 mm^3	
Theta range for data collection	1.921 to 25.501°.	
Index ranges	-30<=h<=30, -11<=k<=11, -25<=l<=25	
Reflections collected	20614	
Independent reflections	4640 [R(int) = 0.0291]	
Completeness to theta = 25.000°	99.7 %	
Absorption correction	Semi-empirical from equivalents	
Max. and min. transmission	1.000 and 0.593	
Refinement method	Full-matrix least-squares on F^2	
Data / restraints / parameters	4640 / 0 / 301	
Goodness-of-fit on F^2	1.100	
Final R indices [I>2sigma(I)]	R1 = 0.0672, wR2 = 0.1810	
R indices (all data)	R1 = 0.0756, wR2 = 0.1893	
Largest diff. peak and hole	0.460 and -0.920 e.$Å^{-3}$	

Table S4: Crystal data and structure refinement for **3**.

CCDC	2176265	
Empirical formula	$C_{78} H_{66} B_2 P_4$	
Formula weight	1148.80	
Temperature	173(2) K	
Wavelength	0.71073 Å	
Crystal system	Monoclinic	
Space group	*P* 2_1/*c*	
Unit cell dimensions	a = 14.3549(8) Å	α= 90°.
	b = 15.3536(6) Å	β= 111.512(4)°.
	c = 15.4112(8) Å	γ = 90°.
Volume	3160.0(3) $Å^3$	
Z	2	
Density (calculated)	1.207 Mg/m^3	
Absorption coefficient	0.164 mm^{-1}	
F(000)	1208	
Crystal color, shape	red orange plate	
Crystal size	0.190 x 0.160 x 0.030 mm^3	
Theta range for data collection	2.653 to 25.476°.	
Index ranges	-17<=h<=17, -18<=k<=18, -18<=l<=18	
Reflections collected	23140	
Independent reflections	5796 [R(int) = 0.0550]	
Completeness to theta = 25.000°	99.9 %	
Absorption correction	Semi-empirical from equivalents	
Max. and min. transmission	1.000 and 0.322	
Refinement method	Full-matrix least-squares on F^2	
Data / restraints / parameters	5796 / 0 / 382	
Goodness-of-fit on F^2	1.044	
Final R indices [I>2sigma(I)]	R1 = 0.0544, wR2 = 0.1312	
R indices (all data)	R1 = 0.0702, wR2 = 0.1391	
Largest diff. peak and hole	0.320 and -0.269 e.$Å^{-3}$	

Table S5: Crystal data and structure refinement for **8**.

CCDC	2176267	
Empirical formula	$C_{78} H_{66} B_2 P_4 S_4$	
Formula weight	1277.04	
Temperature	173(2) K	
Wavelength	0.71073 Å	
Crystal system	Monoclinic	
Space group	$P\ 2_1/c$	
Unit cell dimensions	a = 18.3036(8) Å	α= 90°.
	b = 16.6651(5) Å	β= 108.330(3)°.
	c = 23.4589(10) Å	γ = 90°.
Volume	6792.6(5) Å^3	
Z	4	
Density (calculated)	1.249 Mg/m^3	
Absorption coefficient	0.278 mm^{-1}	
F(000)	2672	
Crystal colour, shape	orange block	
Crystal size	0.220 x 0.140 x 0.130 mm^3	
Theta range for data collection	2.200 to 26.158°.	
Index ranges	-22<=h<=22, -20<=k<=20, -28<=l<=28	
Reflections collected	86330	
Independent reflections	13271 [R(int) = 0.0809]	
Completeness to theta = 25.000°	99.9 %	
Absorption correction	Semi-empirical from equivalents	
Max. and min. transmission	1.000 and 0.389	
Refinement method	Full-matrix least-squares on F^2	
Data / restraints / parameters	13271 / 0 / 799	
Goodness-of-fit on F^2	1.030	
Final R indices [I>2sigma(I)]	R1 = 0.0546, wR2 = 0.1441	
R indices (all data)	R1 = 0.0724, wR2 = 0.1613	
Largest diff. peak and hole	0.519 and -0.424 e.Å^{-3}	

Table S6: Crystal data and structure refinement for [**10**](OTf)$_2$.

CCDC	2176268	
Empirical formula	$C_{70} H_{56} B_2 F_{18} O_{18} P_4 S_6$	
Formula weight	1865.00	
Temperature	173(2) K	
Wavelength	0.71073 Å	
Crystal system	Triclinic	
Space group	*P* -1	
Unit cell dimensions	a = 10.1731(6) Å	α= 70.995(4)°.
	b = 11.8017(7) Å	β= 80.089(4)°.
	c = 17.1337(9) Å	γ = 88.822(5)°.
Volume	1914.5(2) Å^3	
Z	1	
Density (calculated)	1.618 Mg/m^3	
Absorption coefficient	0.376 mm^{-1}	
F(000)	948	
Crystal colour, shape	colourless block	
Crystal size	0.180 x 0.160 x 0.110 mm^3	
Theta range for data collection	3.439 to 25.689°.	
Index ranges	-12<=h<=10, -14<=k<=14, -20<=l<=20	
Reflections collected	17711	
Independent reflections	7161 [R(int) = 0.0299]	
Completeness to theta = 25.000°	99.7 %	
Absorption correction	Semi-empirical from equivalents	
Max. and min. transmission	1.000 and 0.715	
Refinement method	Full-matrix least-squares on F^2	
Data / restraints / parameters	7161 / 0 / 532	
Goodness-of-fit on F^2	1.266	
Final R indices [I>2sigma(I)]	R1 = 0.0592, wR2 = 0.1196	
R indices (all data)	R1 = 0.0730, wR2 = 0.1255	
Largest diff. peak and hole	0.393 and -0.342 e.Å^{-3}	

9. References

[S1] S.-E. Tunney and J. K. Stille, *J. Org. Chem.*, 1987, **52**, 748

[S2] S. Brend'amour, J. Gilmer, M. Bolte, H.-W. Lerner and M. Wagner, *Chem.–Eur. J.*, 2018, **24**, 16910–16918.

[S3] A. John, M. Bolte, H.-W. Lerner, G. Meng, S. Wang, T. Peng and M. Wagner, *J. Mater. Chem. C*, 2018, **6**, 10881–10887.

[S3] X.-R. Zhou, Z. Jiang, L.-X. Xue, P. Lu and Y.-G. Wang, *Eur. J. Org. Chem.,* 2015, **51**, 5789-5797.

[S4] K. Suzuki, A. Kobayashi, S. Kaneko, K. Takehira, T. Yoshihara, H. Ishida, Y. Shiina, S. Oishi and S. Tobita, *Phys. Chem. Chem. Phys.,* 2009, **11,** 9850–9860.

[S5] A.-M. Brouwer, *Pure Appl. Chem.,* 2011, **83**, 2213–2228.

[S6] T.-S. Ahn, R. O. Al-Kaysi, A.-M. Müller, K.-M. Wentz and C.-J. Bardeen, *Rev. Sci. Instrum.,* 2007, **78**, 2005–2008.

[S7] Stoe & Cie, *X-AREA*. Diffractometer control program system. Stoe & Cie, Darmstadt, Germany, 2002.

[S8] G. M. Sheldrick, *Acta Crystallogr. Sect. A*, 2008, **64**, 112–122.